Evaluation of Polymeric Membranes for Gas Separation Processes: Poly(ether-*b*-amide) (PEBAX®2533) Block Copolymer

by

Jennifer Chih-Yi Chen

A thesis

presented to the University of Waterloo

in fulfilment of the

thesis requirement for the degree of

Master of Applied Science

in

Chemical Engineering

Waterloo, Ontario, Canada, 2002

I hereby declare that I am the sole author of this thesis. This is a true copy of the thesis, including any required final revisions, as accepted by my examiners.

I understand that my thesis may be made electronically available to the public.

Abstract

The development of polymeric membranes for gas separations has provided an alternative to traditional energy-intensive processes, especially for hydrocarbon separations. Material studies of the membrane can provide insights to its formation and modification. Gas permeation behaviour through two types of polymeric membrane material is investigated herein. Though the main objective of our investigation was to determine the hydrocarbon gas permeation properties of poly(ether-*b*-amide) PEBAX®2533 copolymer membranes over a range of operating temperatures and pressures, we first tested a poly(ethylene oxide) (PEO) membrane for permeability of ethane and ethylene. The screening results from the tests of PEO membranes containing silver salts, indicate that although PEO membranes may possess high olefin/paraffin selectivity through facilitated transport, difficult membrane preparation and unstable structure remain major obstacles to their commercial use. However, the knowledge acquired on preparation technique and permeability testing from these trials was carried over to our study of PEBAX®2533 membranes. Permeability coefficients were determined at temperatures ranging from 25^{o}C to 75^{o}C, and pressures from 25 psig to 200 psig for ethane, ethylene, nitrogen, propane, propylene, and carbon dioxide. The PEBAX®2533 membranes showed high organic gas permeabilities. Plasticization effects on the membrane were pronounced with propane and propylene at elevated pressure (100 psig). Activation energies of permeation (E_p) were determined. E_p of nitrogen is nearly constant and is the highest among gases tested in the pressure range. E_p shows a linear decreasing trend as pressure increases for hydrocarbons. Relatively high selectivities (12 to 26) were observed for the polar and non-polar gas pair CO_2/N_2. As temperature increased, the selectivity of CO_2/N_2 decreased. This study provides the groundwork for the use of PEO and PEBAX®2533 membranes for hydrocarbon separations.

Acknowledgements

I would like to take this opportunity to thank a group of people who have given me the greatest support during my masters study at the University of Waterloo.

I am most grateful to my supervisor Dr. Alex Penlidis for giving me an opportunity to pursue a masters degree. Many times, his patience and constant encouragement has steered me to the right direction. To Dr. Xianshe Feng for introducing me to membranes and his diligent guidance throughout the project. To Dr. Tom Duever for his careful review on my thesis.

To my friend Ying Huang, for her motivational energy and challenging mind. Many nights of expresso coffee beans have finally paid off. To Beth Lee for her kind, understanding, and warm heart. To Alex Gunz for being there whenever I need a shoulder and a perfect sentence.

To my officemates Matthew Scorah, Brian Barclay, and other members in the polymer group. It is not easy to calm me down and they did it. Also to Yujing, Dr. Li Liu, and Pinghai, for dealing with my endless questions about separations and experiments.

To Tony and Claude-Guy for their help in LaTeX. To Shane, Craig, Kalok, Stan, and Nadar for keeping my life busy and interesting. To Tracy for making me feel that my family is nearby.

At last and most importantly, I would like to thank my family for their open-mindedness and endless support. They are always close to my heart.

Contents

List of Tables

List of Figures

Chapter 1

Introduction

Gas separations have always been one of the key processes in the field of chemical engineering. With industry's demand on lowering operating costs and increasing separation efficiency, more research is being conducted on process improvements. Gas separation is usually achieved by physical or physicochemical phenomena. Over the past two decades, gas separation using polymeric membranes has drawn a great deal of interest from researchers due to many advantages such as low energy costs and high selectivities. This is especially true for hydrocarbon separations performed by the petrochemical industry.

In particular, olefin/paraffin separations incur a heavy cost to petrochemical companies. With a growing awareness of the importance of conserving natural resources, companies are enthusiastic about finding ways to reduce energy consumption and to recycle purge or waste streams. Traditionally, cryogenic distillation at elevated pressures in trayed fractionators is used to separate olefins and paraffins. This distillation system is expensive to build and operate, and is currently only economically attractive for streams containing high quality of olefins. Other available separation technologies include extractive distillation, physical or chemical adsorption, physical or chemical absorption, and more recently, membrane separation. A more thorough description of

different separation technologies can be found in the review written by Eldridge (1993).

1.1 Thesis Outline

The objective of this research is to develop an advanced membrane that exhibits high gas permeability and selectivity, particulary for olefins and paraffins. More specifically, it is to gain knowledge on both the preparation and the gas permeation properties of the new poly(ether-*b*-amide) copolymer membrane, PEBAX®2533.

To provide a basic understanding of the membrane separation process, an introduction to the transport mechanism through polymeric membranes used for gas separations is covered in Chapter 2. Transport models and equations are described and factors affecting gas permeation are discussed. Chapter 3 presents procedures for membrane preparation and permeability testing along with a description of the testing apparatus. Chapter 4 describes a screening study based on olefin/paraffin separation using poly(ethylene oxide) membranes containing silver nitrate. More background is given for this process that makes use of active facilitated transport via silver nitrate. Experimental methods are detailed and results from the study are presented and discussed. Our study of polyether-*b*-amide copolymer membrane, PEBAX® 2533 is covered in Chapter 5, and a brief review of recent investigations of PEBAX® membranes used for separation. Flat film membranes were made from PEBAX® resin and permeability tests were conducted to evaluate its gas separating performance against N_2, CO_2, and several hydrocarbon gases. Interactions between gas and membrane material over a range of temperatures and pressures were tested and discussed. Sample calculations from both PEO and PEBAX studies are included in Appendix C. Finally, based on the results from the experimental investigation of the two polymeric membranes, concluding remarks are presented in Chapter 6, along with recommendations for further work.

Chapter 2

Background and Literature Review

Membrane separation technology is currently one of the most innovative and rapidly growing fields across science and engineering. Many different separation processes are widely used in industry in liquid-liquid and liquid-solid systems. Several books have been published to detail the fundamental principles and applications of membrane technology (Bitter, 1991; Mulder, 1991; Noble and Stern, 1995), and some articles have provided overviews to membrane structure and formation (Kesting, 1985; Pinnau and Freeman, 2000).

The most attractive features of membrane separation systems are cost effectiveness, environmental friendliness, versatility, and simplicity. Membrane processes are classified according to the driving force by which they achieve separation. Table 2.1 lists commonly known means of separation along with their primary driving force and type of mechanism. Types of membranes used today include nonporous (dense) and porous polymers, ceramic and metal films with symmetric or asymmetric structures, liquid films with selective carrier components, and electrically charged barriers (Strathmann, 2001). The performance of a membrane is determined by several key properties: high selectivity and permeability; excellent chemical, thermal, and mechanical stability under the process operating conditions; low maintenance; good space efficiency; and

defect-free production.

Table 2.1: Various membrane separation processes and the corresponding driving forces

Process	Driving Force	Transport Mode
microfiltration	Δp	convection
ultrafiltration	Δp	convection
reverse osmosis	ΔC($\Delta\mu_i$)	diffusion
dialysis	ΔC(Δa)	diffusion
gas separation	Δp(Δf$_i$)	diffusion
pervaporation	Δp$_i$(Δf$_i$)	diffusion
electrodialysis	$\Delta\varphi$	migration

(p-hydrostatic pressure, μ-chemical potential, C-contentration a-activity, p_i-partial pressure, f_i-fugacity, φ-electrical potential)

In the last two decades, the membrane industry has extended its interests to gas and vapor separations. Combined with advances in polymeric materials, membrane-based separations have become an important chemical unit operation which successfully competes with other well-established industrial gas separation processes such as cryogenic distillation, absorption, and pressure swing adsorption (Spillman, 1989).

Commercially, the most widely practiced separations using membranes include the separation of oxygen and nitrogen; the recovery of hydrogen from mixtures with larger components such as nitrogen, methane and carbon dioxide; and the removal of carbon dioxide from natural gas mixtures. For these separations, membranes with adequately high fluxes of the more permeable components (oxygen, hydrogen, and carbon dioxide, respectively) and sufficient selectivity have been developed. The membrane materials used in these separations are glassy polymers, which derive high selectivity from their ability to separate gases based on differences in penetrant size (Freeman and Pinnau, 1997).

Membranes can be categorized according to their geometry, bulk structure, production method,

separation regime, and application (Pinnau and Freeman, 2000). The basic scheme for membrane classification is shown in Figure 2.1. Hollow-fiber membranes are used commonly by industries due to their high surface area and compactness. Flat-sheet membranes are easy to produce and are used in laboratory experiments. In terms of structure, membranes can be separated into two groups; asymmetric and symmetric. This simply refers to the types of pores that can be found within the membrane. Symmetric membranes have pores which do not change in diameter significantly through the sheet. On the other hand, asymmetric membranes contain pores which increase in size from one side of the sheet to the other. The new membrane composites are good example of asymmetric membranes. They are made with a thin polymer film deposited onto a porous backing material. The separation is determined by the properties of the thin film while the mass transport or rate is dependent upon the porosity of the backing.

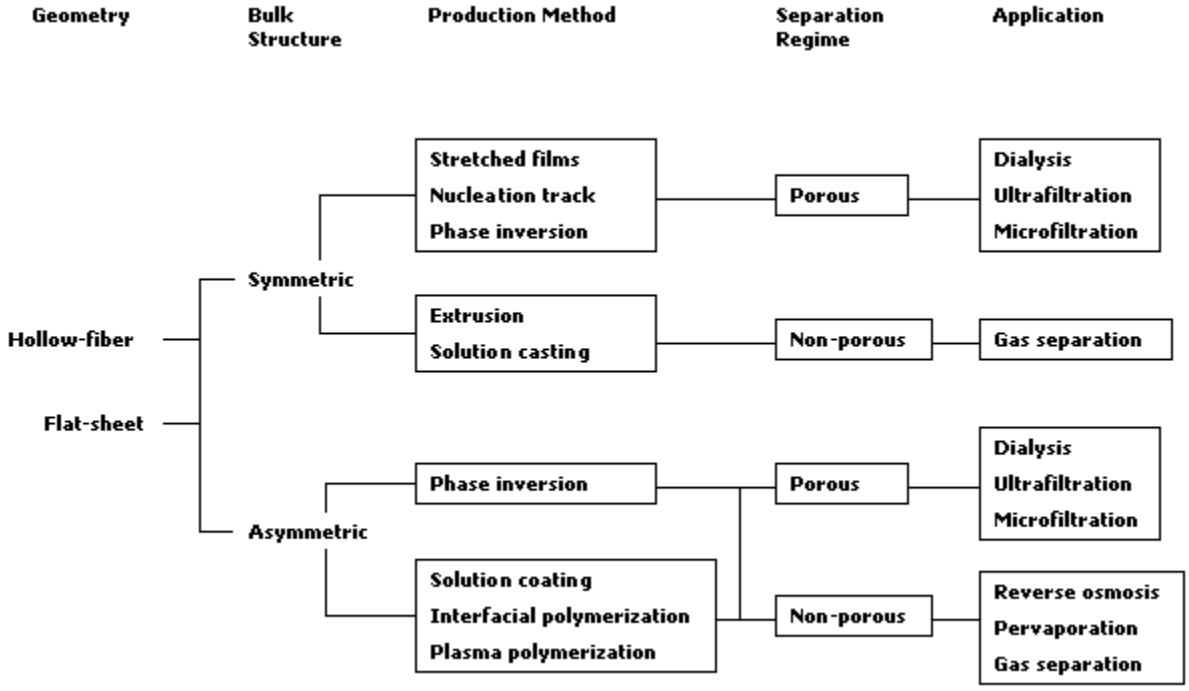

Figure 2.1: Classification scheme of synthetic membranes

Different production methods can result in membranes with unique characteristics. Membranes are the result of pressing a powder into a porous film and then sintering, stretching an extruded polymer into a sheet, irradiating a thin film with nuclear particles and then etching in a bath (nucleation track), dissolving a polymer in a solvent and spreading into a film followed by precipitation (solution casting), contacting two monomers in two immiscible liquids (interfacial polymerization), or condensing gaseous monomers on a substrate layer through a stimulated plasma (plasma polymerization).

2.1 Types of Gas Separation Membranes and Applications

Most gas separation membranes are made of amorphous (noncrystalline) polymers which are in either the glassy or the rubbery state. In the glassy state, polymers are rigid and often brittle. There is low level of molecular movement and the rate of diffusion of large molecules is small. In the rubbery state, polymers tend to be soft and more flexible. What separates the two states is the glass transition temperature, T_g, of the polymer. Properties that change around T_g include density, specific heat, dielectric coefficient, rates of gas/liquid diffusion through the polymer, and conductivity or charge mobility.

The majority of industrial membrane processes for gas separations utilize glassy polymeric membranes because of their high gas selectivity and good mechanical properties. Glassy polymers like polyimides are used for CO_2/CH_4 separation; polysulfones are used in H_2 separations, and cellulose acetate membranes are used for the removal of CO_2 and H_2S from natural gas. In the area of rubbery polymers, polyurethanes possess high permeability and are being applied in O_2/N_2 separation. Silicon polymers, particularly polydimethylsiloxanes (PDMS), are widely studied due to their large free volume, high permeability, and low selectivity. Stern (1994) has presented a thorough review on the structure/permeability/selectivity relationship on selected

rubbery and glassy polymers.

In view of their physical properties, including sorption and gas transport, rubbery polymers are considered equilibrium materials. Glassy polymers go through a physical aging process to attempt to reach equilibrium in the course of time. Details of the sorption and diffusion behaviours in both rubbery and glassy polymers can be found in reviews by Ghosal and Freeman (1993), and George and Thomas (2001). Through modifications, such as copolymerization and sol-gel process, polymer properties can be adjusted and enhanced to achieve desirable separation performance and mechanical strength.

2.2 Fundamentals

Three general transport mechanisms are commonly used to describe gas separations using membranes, as illustrated in Figure 2.2 (Koros and Fleming, 1993). They are Knudsen diffusion, molecular sieving, and solution-diffusion. As the name implies, the first type of separation is based on Knudsen diffusion and separation is achieved when the mean free paths of the molecules are large relative to the membrane pore radius. The separation factor from Knudsen diffusion is based on the inverse square root ratio of two molecular weights, assuming the gas mixture consists of only the two types of molecules. The process is limited to systems with large values for the molecular weight ratio, such as is found in H_2 separation. Due to their low selectivities, Knudsen diffusion membranes are not commercially attractive.

The molecular sieving mechanism describes the ideal condition for the separation of vapour compounds of different molecular sizes through a porous membrane. Smaller molecules have the highest diffusion rates. This process can happen only with sufficient driving force. In other words, the upstream partial pressure of the ”faster” gas should be higher than the downsteam

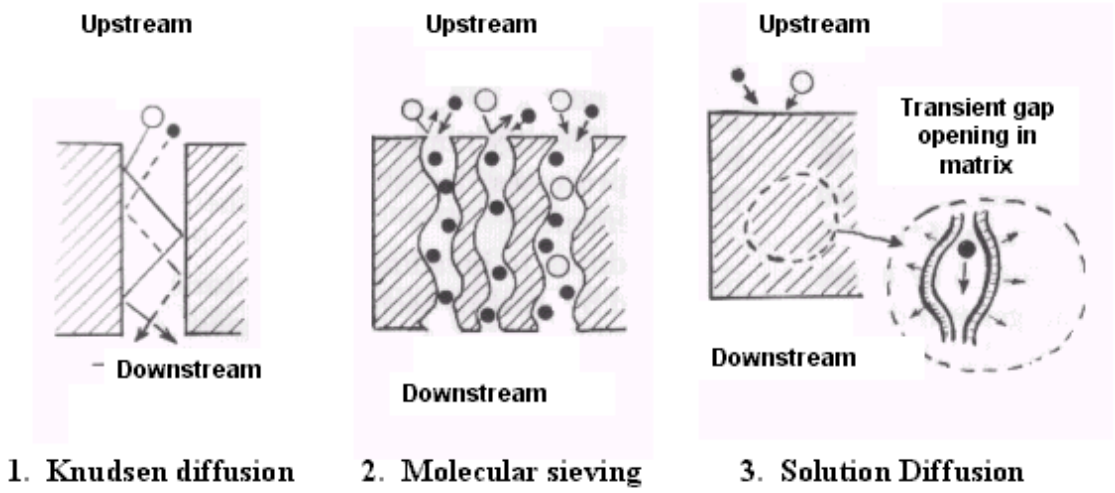

Figure 2.2: General transport mechanisms for gas separations using membranes

partial pressure. The main limitation is that condensible gases cause fouling, and alter the structure of the membrane; therefore, it is only feasible commercially in robust systems, such as those that use ultramicroporous carbon or hollow fibre glass membranes.

Solution-diffusion separation is based on both solubility and mobility factors. It is the most commonly used model in describing gas transport in non-porous membranes and it is applied in our studies. The details of this solution-diffusion model are given in the next section.

2.2.1 Solution-Diffusion Model and Permeability Equations

Gas permeation can be seen as a three-stage process in the solution-diffusion model:

1. adsorption and dissolution of gas at the polymer membrane interface.
2. diffusion of the gas in and through the bulk polymer.
3. desorption of gas into the external phase.

Permeation is used to describe the overall mass transport process, and diffusion refers only to the movement of gas molecules inside the polymer membrane. The model assumes that the pressure within a membrane is uniform and the chemical potential gradient across the membrane is expressed only as a concentration gradient. Koros et al. (1988) gave a thorough review on polymeric membranes for solution-diffusion based permeation separations. The review covered membranes for not only gas separations, but also for pervaporation, reverse osmosis, and liquid separation.

Koros and Fleming (1993) suggest that solution-diffusion is achieved via penetrant species undergoing random jumps in the polymer matrix due to a concentration difference between membrane upstream and downstream, resulting in a diffusion flux travelling downstream. Varying the chemical nature of the polymer allows control of the relative extent of solution and diffusion of different gases through the polymer matrix.

Figure 2.3 shows a schematic of gas transport across a membrane. The upstream gas, which has a pressure of p_1, comes in contact with the membrane interface. With a driving force (e.g., chemical potential, concentration gradient, etc.), the permeate gas forms a concentration profile across the membrane with respect to membrane thickness, l. The normalized flux is gas flow rate divided by the membrane surface area and it is denoted as N_A. Separation of the gas mixture is achieved when one of the components interacts more strongly with the membrane material or, in other words, diffuses faster through the membrane.

Among the three solution-diffusion stages, the diffusion step is the slowest; hence, it is the rate-determining step in permeation. In general, the relationship between the linear flux, J and the driving force is:

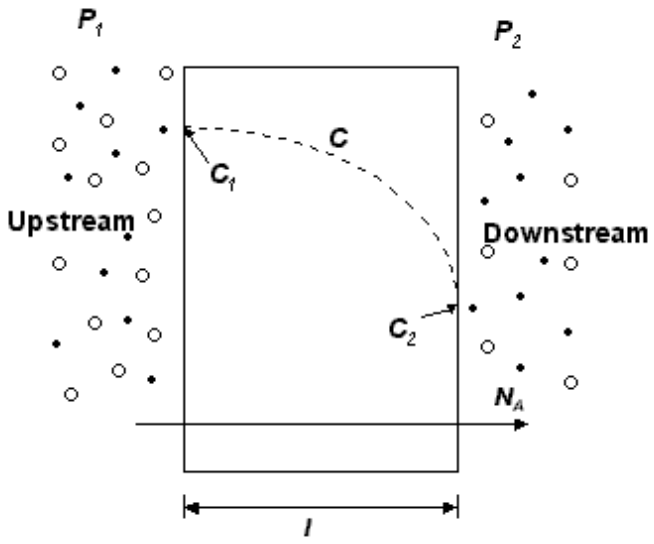

Figure 2.3: Gas transport across a membrane

$$J = -A\frac{dX}{dx} \tag{2.1}$$

where *A* is some phenomenological coefficient, *X* is a potential, and *x* denotes the space coordinate measured normal to the section. To describe gas diffusion in the membrane, Equation 2.1 can be written as:

$$J = -D\frac{dC}{dx} \tag{2.2}$$

where *D* is the diffusion coefficient, and *X* in Equation 2.1 now defines concentration and is denoted as *C*. Equation 2.2 is commonly known as Fick's first law.

When the solubility of a penetrant gas in a polymer is sufficiently low, the concentration of the penetrant is proportional to the vapor pressure of penetrant in polymer. This relationship is expressed as Henry's law, Equation 2.3. *S* is the solubility coefficient and *p* is the vapour

pressure of the penetrant.

$$C = S * p \tag{2.3}$$

At steady state, the permeation of a pure gas A through a membrane of thickness *l* is characterized by a permeability coefficient P_A. P_A is generally defined as:

$$P_A = \frac{N_A}{(p_1 - p_2)/l} = \frac{N_A}{(\Delta p/l)} \tag{2.4}$$

where N_A is the normalized flux, p_1 and p_2 are the upstream and downstream pressures, respectively, and Δp is p_1-p_2. In a gas mixture, p_1 and p_2 refer to the partial pressures of penetrant A at the two sides of the membrane. The permeability coefficient of dense film materials is commonly expressed in units of Barrer.

$$1\ Barrer = 1 * 10^{-10} \frac{cm^3(STP)\,cm}{cm^2\,sec\,cmHg} \tag{2.5}$$

If Henry's law applies, then *S* is constant at a given temperature and so is *D*. The permeability coefficient, *P*, can also be defined as:

$$P = D * S \tag{2.6}$$

The diffusion coefficient, *D*, is a kinetic term governed by the amount of energy necessary for a particular penetrant to execute a diffusive jump through the polymer and the intrinsic degree of segmental packing in the matrix. The solubility coefficient, *S*, is a thermodynamic term that depends on factors such as condensibility of the penetrant, interactions between the polymer and penetrant, and the amount of penetrant-scale non-equilibrium excess volume in glassy polymers.

For a binary gas mixture permeating through a polymer membrane, the selectivity of a polymer membrane towards two different penetrant gases, A and B, is commonly expressed in terms of the ideal selectivity or ideal permselectivity, α_{AB}. When the downstream pressure is negligible relative to the upstream pressure, α_{AB} can be written as the ratio of permeabilities:

$$\alpha_{AB} = \frac{P_A}{P_B} \tag{2.7}$$

Expanding the permeability into diffusivity and solubility terms, the ideal selectivity can be expressed by Equation 2.8.

$$\alpha_{AB} = (\frac{D_A}{D_B})(\frac{S_A}{S_B}) \tag{2.8}$$

Here, D_A/D_B is the ratio of the concentration-averaged diffusion coefficients of penetrants A and B, and is referred to as the membrane's "diffusivity selectivity". S_A/S_B is the ratio of solubility coefficients of penetrants A and B, and is called the "solubility selectivity" (Ghosal and Freeman, 1993). In typical gas separation applications, the downstream pressure is not negligible; however, α_{AB} generally provides a convenient measure for assessing the relative ability of various polymers to separate gas mixtures. High permeability and high selectivity are the most important criteria in evaluating a membrane.

2.2.2 Facilitated Transport

The gas permeability of a membrane may be improved by facilitated transport. This is an active transport of permeant molecules across a membrane achieved by utilizing a carrier species. The carrier reacts with a permeant molecule to form a labile complex. Within the membrane, the carrier shuttles the permeant across the membrane boundaries, and hence the permeant is transported from the side with higher permeant concentration to the side with lower permeant

concentration. When a feed mixture only contains one species that the carrier will react with, only the transport of that species will be ”facilitated” across the membrane. The process of facilitated transport is illustrated in Figure 2.4. The driving force in facilitated transport is a concentration gradient of permeant-carrier complexes across the membrane.

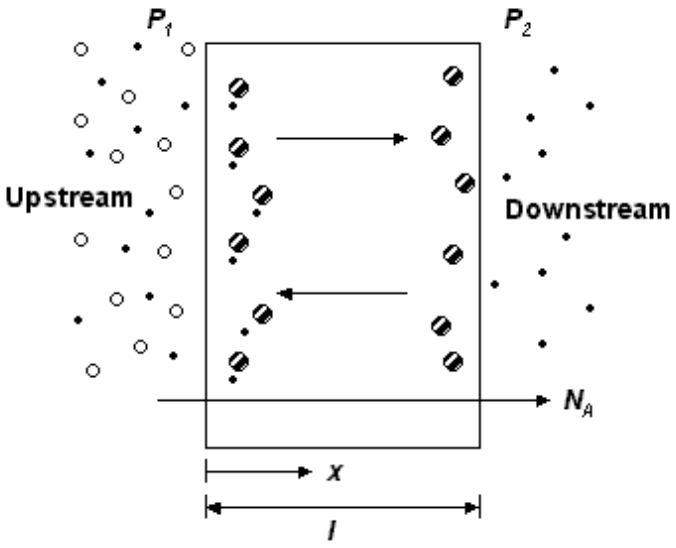

Figure 2.4: A schematic of facilitated transport mechanism across the membrane

It has been found that olefin transport can be facilitated by transition metals. Cuprous and silver ions are the mostly widely used in this type of research. The metal ions form a π-bond complexation with olefin molecules. More details will be given in Chapter 4.

Gas separation using facilitated transport is most commonly done with ”immobilized liquid” membranes, prepared by dissolving the carrier in an appropriate solvent and using this solution to impregnate an electrically uncharged, rigid microporous matrix. Once formed, surface tension forces serve to hold the carrier molecules inside the membrane. Another technique is to swell a gel membrane, such as porous cellulose.

2.3 Factors Affecting Gas Permeation in Membranes

2.3.1 Temperature

As mentioned in Section 2.2.1, gas diffusion through polymers is related to an activation energy, thus, the temperature dependence of *D*, *S*, and *P* can be described by the following Arrhenius relationships:

$$D = D_0 e^{-E_d/RT} \tag{2.9}$$

$$S = S_0 e^{-\Delta H_s/RT} \tag{2.10}$$

$$P = P_0 e^{-E_p/RT} \tag{2.11}$$

where E_d is the activation energy of diffusion; ΔH_s is the heat of sorption; and E_p is the activation energy of permeation, which is simply:

$$E_p = E_d + \Delta H_s \tag{2.12}$$

Values of E_p, E_d, and ΔH_s for many polymer and gas pairs can be found in the Polymer Handbook (Pauly et al., 1989).

Gas diffusion coefficients typically increase appreciably with increasing temperature when the polymer does not undergo thermally induced morphological rearrangements such as crystallization over the temperature range of interest (Ghosal and Freeman, 1993). Since both diffusivity and solubility coefficients are temperature dependent, the selectivity described by Equation 2.8 is also sensitive to changes in temperature.

The increased segmental motion at higher temperatures undermines the ability of polymer to

discriminate between penetrants of different physical dimensions, thereby resulting in a diffusivity selectivity loss. The temperature changes also affect the solubility selectivity, which is governed primarily by the chemical nature of the penetrant and polymer-penetrant interactions. For most gases, as temperature increases, the solubilities increase. The solubility selectivity, therefore, will vary depending on the extent of the temperature effect on each component in the gas mixture (Costello and Koros, 1994).

2.3.2 Pressure

Change in the pressure of penetrant contacting with the polymer may cause large permeability variations. Four typical patterns of response are observed in permeability versus pressure relationships (Koros and Chern, 1987), as seen in Figure 2.5.

(a) Linear, with slope close to 0. This represents the ideal case that satisfies the assumption of diffusion and solution being independent of gas pressure (i.e., low sorbing penetrants, such as He or N_2 in rubbery or glassy polymers).

(b) Nearly linear increase of permeability with increasing pressure. This often describes the permeability of an organic vapor into a rubbery polymer.

(c) A decreasing trend of permeability with increasing pressure. This is typically observed with highly soluble gases such as CO_2 in glassy polymers.

(d) Concave upwards. This can be perceived as a combination of (b) and (c), and is typical of a plasticizing penetrant such as organic vapor in a glassy polymer.

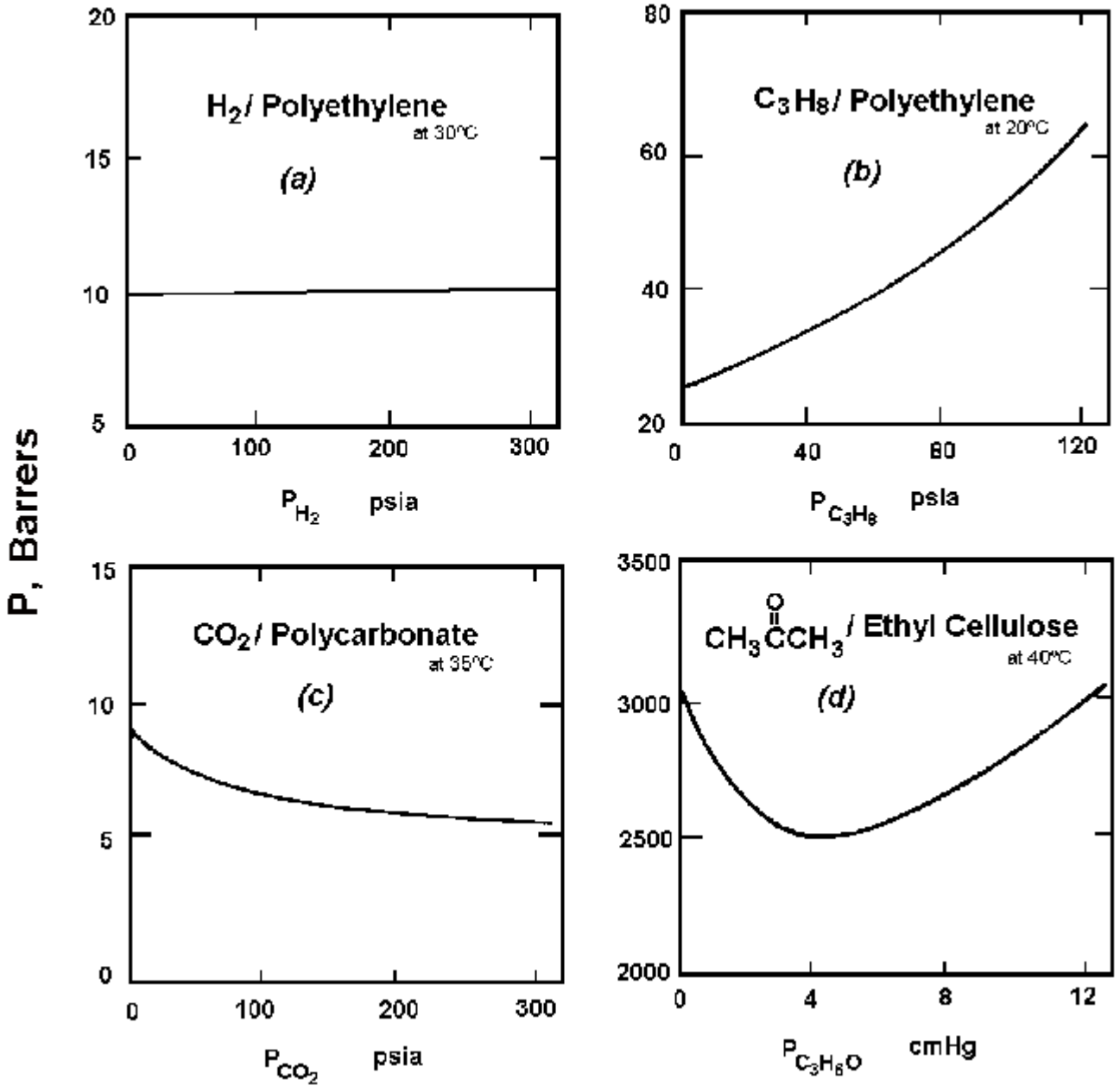

Figure 2.5: Pressure dependency of various penetrant-polymer systems

2.3.3 Plasticization

The pressure at which an increase in permeance occurs (i.e. the minimum in the permeance versus pressure plot, of a type (d) relationship mentioned in the previous section) is called the

plasticization pressure. At such feed pressure, the gas concentration in the polymer material disrupts the chain packing. The polymer matrix swells and the segmental mobility of the polymer chain increases. This results in an increase in gas diffusivity and induces permeability increases (Koros and Fleming, 1993). Therefore, when the polymer is highly plasticized by the penetrant, the diffusion coefficient may become a function of time and of history. This non-ideal behaviour is explained by free volume theory.

Free volume theory of diffusion suggests that molecules can only diffuse through free volume in a molecule matrix. Cohen and Turnbull (1959) have theorized that diffusion in a rubbery polymer is the result of redistribution of free volume within a matrix and migration of the penetrant among these volumes. Petropoulos (1994) has summarized the permeability equations derived based on the free volume approach to model the gas transport in plasticized polymer matrices. Studies have been done to suppress the plasticization effect on gas permeability and permselectivity by means of crosslinking, blending, or annealing of the polymer membranes (Ismail and Lorna, 2002; Krol et al., 2001; Bos et al., 2001; Petropoulos, 1992).

2.3.4 Other Factors

Apart from the operating conditions (i.e., temperature and pressure), factors such as composition in the gas mixture, penetrant condensibility, polymer-penetrant interactions, and polymer crystallinity may also affect the gas solubility. Furthermore, gas diffusivity is sensitive to properties such as penetrant size, polymer morphology, and polymer segmental dynamics.

In a binary or multi-component system, the case of $P = \sum P_i$, may be referred to as an ideal mixed gas transport system. It comes from the assumption that each single component behaves ideally, but the assumption will not hold when one of the permeants has a much higher perme-

ation flux than the other permeants. The non-ideality of this type of multi-component system must be accounted for to avoid invalid assumptions for permeability and permselectivity calculations. Models and descriptions of multi-component systems can be found in Petropoulos (1994), and Kamaruddin and Koros (1997).

In general, gas solubility in polymers increases with increasing gas condensibility. Condensibility can be measured as the gas critical temperature T_c, or the normal boiling point T_b. Diffusion coefficients of penetrants are found to decrease with increasing penetrant size. Diffusion coefficients in polymers are also sensitive to penetrant shape. Linear or oblong penetrant molecules like CO_2 exhibit higher diffusivities than those of spherical molecular shape of equivalent molecular volume such as CH_4. Specific interactions between gas and polymer molecules (i.e., polarity) also affect gas solubility. Gases such as CO_2, which has a quadrupole moment, are generally more soluble in polar polymers.

Crystallinity in polymers tends to reduce both penetrant solubility and diffusivity, thereby reducing permeability, which is generally undesirable. Polymer crosslinking reduces polymer segmental mobility; therefore, diffusion coefficients of the penetrant gas typically decrease with an increasing degree of crosslinking in the polymer. In lower molecular weight polymers, chains are more mobile and penetrant diffusivity decreases with increasing molecular weight. At higher molecular weights, when the concentration of chain ends is low, diffusivity is relatively independent of molecular weight as is solubility (Ghosal and Freeman, 1993).

Chapter 3

Experimental Apparatus and Methods

3.1 Membrane Preparation

Membranes are produced in various configurations including flat sheets, hollow fibres, capillaries, or tubes. Flat sheets are the most convenient for laboratory permeation tests. Dense flat sheet membranes are commonly made by melt extrusion or solution casting followed by solvent evaporation. Overviews of types of membrane formation have been done by Koros and Fleming (1993), and Pinnau and Freeman (2000).

In our studies, flat film membranes were prepared using the solution casting technique. The term ”casting” indicates a laying down process of a polymer solution (often on a support) during preparation. A homogeneous polymer solution was first made by dissolving polymer powder or pellets in an appropriate solvent with continuous mixing. After pouring the polymer solution onto a thin glass plate, a casting knife was applied to obtain even thickness of the membrane. The glass plate was then set in a fume hood to allow the membrane to dry. The weight of glass plate was measured until it did not change over time, indicating that the solvent has evaporated completely. Dried membranes with support material were cut into desired configurations and

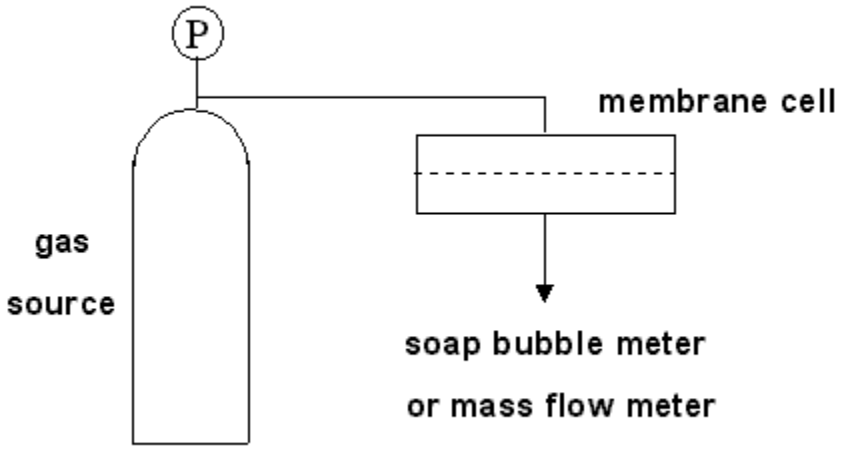

Figure 3.1: A schematic of gas permeation cell

placed in the membrane cell for permeation tests. Non-woven polyester fabric is used as our support material to obtain higher mechanical strength to the membranes during permeability tests. Gas permeation through the support fabric is neglected in our calculation since the gas resistance in the fabric is too small comparing to that in the membranes.

3.2 Membrane Module

Permeability measurements can be made using a simple experimental set-up. Figure 3.1 shows a schematic of a gas permeability testing apparatus (Mulder, 1991). It consists of an upstream gas source, a membrane cell, and a downstream device that measures the properties of the permeant. There are many types of apparatus used by researchers to measure permeabilities, but they are all based on two primary principles: constant pressure or constant volume. Constant volume/variable pressure and vacuum time-lag techniques are based on a constant volume principle whereas continuous flow techniques are based on a constant pressure principle.

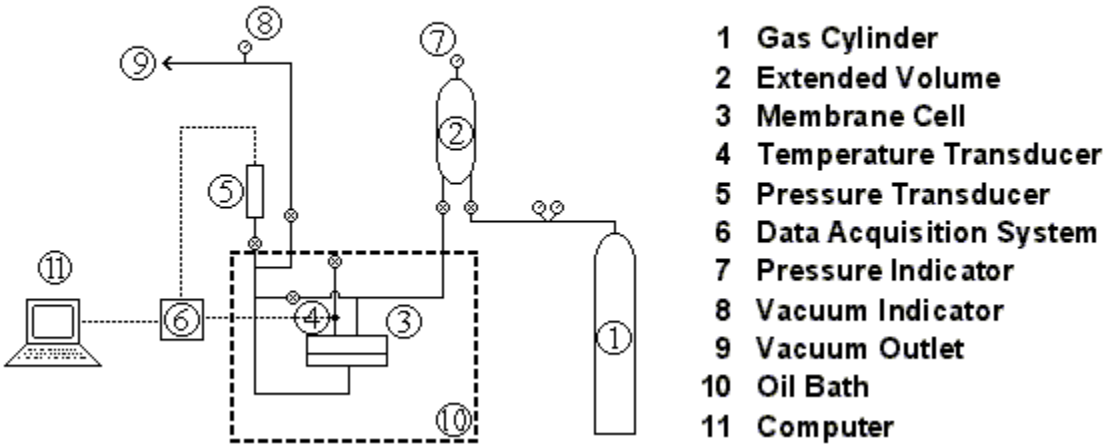

Figure 3.2: Gas permeation apparatus using constant volume/variable pressure method

The constant volume/variable pressure method has been described in detail by Pye et al. (1976). This method involved observing the pressure increase in a constant volume in which gas transport occurred, by employing a constant pressure difference between the two sides of a membrane. A schematic of a gas separation apparatus is shown in Figure 3.2. The membrane cell consists of two compartments separated by a membrane. A porous disk is placed in the bottom compartment of the cell to provide mechanical strength to the membrane such that the membrane can withstand the pressure difference employed during the experiments. The disk does not provide any resistance to the gas flow. An o-ring is placed in between the two compartments of the membrane cell to seal the cells.

Before experimentation takes place, the permeate side is kept under vacuum to remove residual air in the testing unit. During testing, the upstream pressure is kept constant, while an increase in downstream pressure of the permeate chamber is directly measured by the pressure transducer. Once steady state has been achieved, the pressure increase in the permeate chamber is

linear with time and the gas permeability coefficient can be calculated from the slope of the curve at steady state of pressure on the permeation side versus time.

In the continuous flow method, the permeant passes through the membrane under constant pressure differential, and into a flowing stream of inert carrier gas in the pressure compartment (Sridhar and Khan, 1999). Equipment setup from this method is very similar to that of the constant volume/variable pressure method, except that at the downstream side of the membrane cell, vacuum is replaced by a continuous gas carrier flow. By varying the carrier flow rate, the permeant gas partial pressure at the bottom membrane surface can be controlled, which also alters the driving force across the membrane. Helium or nitrogen are common carrier gases. This technique is advantageous in that the permeation rates can be easily adjusted by varying the carrier gas flow rate. This allows adjustment of the concentration of the permeant within the detectable range of the analyzer.

The vacuum time-lag method is currently a popular means to assess the permeability and diffusion coefficients of a gas through a polymer film for a given set of operating conditions (temperature and pressure). In this method, the permeate gas is allowed to accumulate in a pre-evacuated downstream volume. The mathematical analysis is based on the assumptions of a constant diffusion coefficient and constant membrane thickness (i.e. negligible swelling by permeant) throughout the entire permeation process.

Figure 3.3 illustrates a common plot obtained from time-lag method. The value of time-lag (θ) is determined from the x-intercept of the steady state tangent line. θ can be used to directly

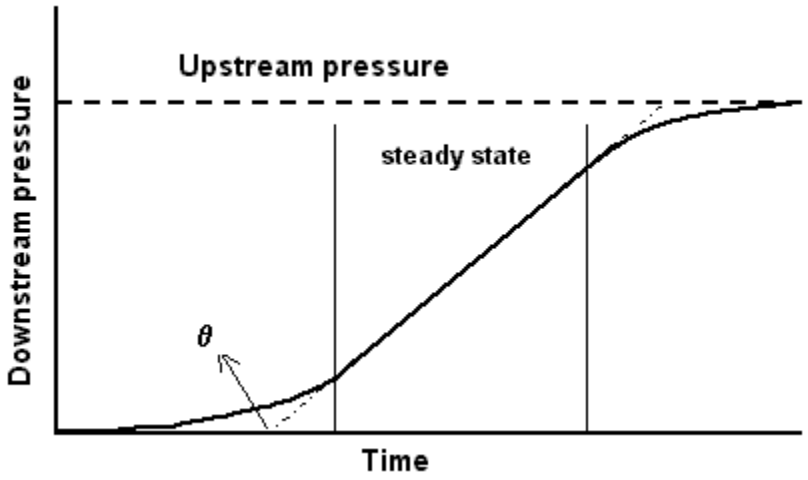

Figure 3.3: Determination of time-lag from a steady state permeation

calculate the permeate diffusion coefficient using the following expression:

$$\theta = \frac{L^2}{6D} \tag{3.1}$$

The variable L represents membrane thickness, and D is the diffusion coefficient. The framework and limitations of this technique, as well as some innovative attempts to apply to organic vapor, can be found in the recent studies of Yeom et al. (1999) and Favre et al. (2002).

In a recent review, Baker (2002) pointed out that data from the literature should be treated carefully. Some of the reported selectivities were based on the ratios from pure gas permeabilities, while others used a hard vacuum or sweep gas on the permeate side of the membrane. Both procedures yield high selectivities, but in an industrial plant, the feed gas will be at 100 to 150 psig and at a temperature sufficient to maintain the gas in the vapor phase. Furthermore, the permeate gas will be at a pressure of 10-20 psig. Under these operating conditions, plasticization and loss of selectivity occur with even the most rigid polymer membranes; therefore, under

industrial operating conditions, selectivities would usually be quite low.

Since the objective of this study could be achieved by collecting permeability data, a simple apparatus similar to that in Figure 3.1 was all that was required. A soap film bubble flow meter was connected at the downstream side of the membrane cell, and the permeate flow rate was determined using the bubble flow meter. Six readings were taken for each experiment to control for variability and ensure the flow had reached a steady state.

3.3 Permeation Tests

The experiments were performed at normal ambient lab temperature. Feed gas pressure came directly from a gas cylinder fitted with a pressure regulator and a test gauge. The downstream pressure was atmospheric, nominally assumed for all calculations to be 1 atm.

Stability of the membranes was determined by repeating tests over 24 hours, 72 hours, and a one week duration. These stability tests were preformed at two or three times the normal testing pressure. This is referred to as ”conditioning” of the membrane, and helps to increase gas flux once the membrane is stabilized. This stabilization is achieved when the interaction between the feed gas and the polymer chains reaches equilibrium.

Chapter 4

Poly(ethylene oxide) Membranes Containing $AgNO_3$

4.1 Introduction

Olefin and paraffin gas mixtures are often found in petrochemical process streams. Some are a by-product of Liquified Petroleum Gas production in crude oil refining. Olefins are a valuable feedstock for the production of commercial products such as polymers (polyesters, polyethylene, polypropylene, etc.), synthetic fluids, surfactants, additives, and specialty chemicals. Paraffins can be dehydrogenated to produce olefins of greater economic value.

Currently, the separation of ethylene and propylene from a light gas mixture is achieved by cryogenic distillation typical of the fractionation sequence used to recover olefins from ethylene reactor effluent streams and catalytic cracking reactors. The process is operated at a high pressure with a large number of trays and a high reflux ratio due to the close boiling points of the primary components. These systems are expensive to build and operate and are currently

only economically attractive for streams containing high quality olefins. Membrane technology may therefore be a very attractive alternative.

The objective of this section is to describe the development of an advanced membrane that exhibits high olefin permeability and olefin/paraffin selectivity. A further goal is to gain more knowledge regarding preparation and properties of poly(ethylene oxide) membranes containing a silver salt. The knowledge can then be further applied to advance the understanding of PEBAX® solid membranes (Chapter 5).

The basic transport mechanism of solution-diffusion has been illustrated in Chapter 2. Past studies of olefin/paraffin separation using facilitated transport membranes are reviewed in this chapter. An experimental design was used, and three main factors were considered. These factors are the weight-average molecular weight of PEO, the chemical form of silver salt, and the silver concentration in PEO.

4.2 Facilitated Transport

As described in Chapter 2, facilitated transport can dramatically improve membrane selectivity and permeability. In olefin/paraffin systems, it has been found that olefin transport can be facilitated by transition metal - most commonly cuprous and silver ions. Metal ions form a π-bond complexation with olefin molecules, which is described by the Dewar-Chatt model (see Figure 4.1 - Safarik and Eldridge 1998). The shaded areas in this diagram represent electron donor and acceptor interactions. Both the metal and alkene act as electron donors and acceptors in the complexation interaction. A sigma bond is formed between the overlap of the vacant outermost *s* atomic orbital of the metal and the full π molecular orbital of the olefin. A π component is formed by back-donation of electrons from the full outer d orbitals of the metal to the vacant

π*(antibonding) molecular orbital of the olefin.

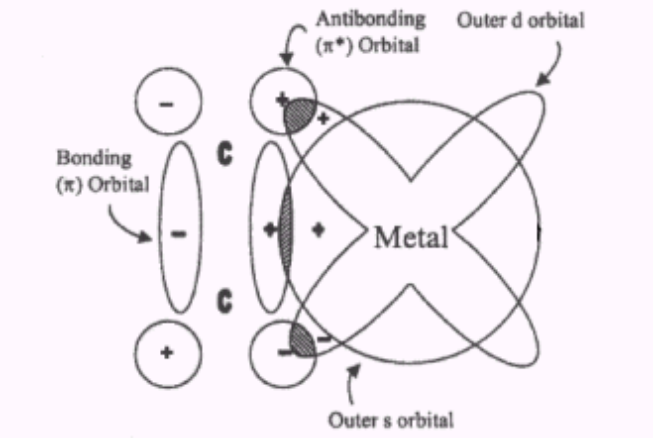

Figure 4.1: Dewar-Chatt model of π-bond complexation

The complexation reaction is fast enough to achieve high concentrations that drive the olefin fluxes. The reverse reaction should also be sufficiently fast to assure recovery of permeate molecules.

This separation process is based on the fact that complex-forming reactions enhance the permeation rate of olefin molecules. Paraffin molecules permeate through the membrane according to Fick's law of diffusion and at a lower rate than olefins, resulting in olefin/paraffin separations (Noble et al., 1989).

4.2.1 Background and Relevant Literature

Three configurations have been used to prepare membranes containing silver ions: supported liquid membranes, ion-exchange membranes, and salt/polymer membranes.

Gas separation using facilitated transport is most commonly carried out using "immobilized

liquid" membranes, prepared by dissolving the gas-carrier species in an appropriate solvent and using this solution to impregnate an electrically uncharged, rigid microporous matrix. The carrier species is then retained in the matrix by surface tension forces. Facilitated transport of gases via liquid membranes was first discussed in a review by Schultz et al. (1974). More work was done by Hughes et al. (1986) on silver-impregnated cellulose acetate membranes for both flat film and hollow fiber configurations. Teramoto et al. (1986; 1989) performed work on support and "flowing" membranes for ethane and ethylene separation. Several limitations of this membrane type were pointed out by those investigations:

* The tendency to degrade because the solution absorbed into the pores of the support membrane evaporates in the feed and sweep gas phase.

* The inability to tolerate poisons to Ag^+, such as acetylenes, H_2, or H_2S.

* A decline of performance due to water and/or Ag^+ loss.

* Minimum pressure differential across the fiber wall is necessary to maintain optimum performance and maximize permeator lifetime.

* The difficulty of making the membrane both thin and stable.

LeBlanc et al. (1980) introduced the ion-exchange type carrier membranes for olefin gas separations. With these membranes, silver ions are retained in the membrane by electrostatic interactions with the ion-exchange sites. They used a cation-exchange membrane of sulfonated polyphenylene oxide and obtained Ag^+ ions by soaking it in aqueous $AgNO_3$. This type of membrane has a better ability to retain the carrier gas under operating conditions and there is no problem with solvent condensing on the high pressure side of the membrane to wash out the carrier. Hydrated Nafion cation exchange membranes containing Ag^+ ions and Na^+ ions for c-2-butene/t-2-butene separation were studied by Funke et al. (1993). Ho and Dalrymple

(1994) reported separations using poly(vinyl alcohol)-containing silver nitrate membranes in the thin film composite structure. The silver salt is trapped in the crosslinked poly(vinyl alcohol) matrix, yet ions are mobile in the hydrated polymer. Yamaguchi et al. (1996) compared an ion-exchange membrane (silver form Nafion) with a silver salt/polymer blend membrane ($AgBF_4$/Nafion blend) on 1,3-butadiene/1-butene and 1,5-hexadiene/1-hexene systems.

Recent studies done by Yang and Hsiue (1998) reported gas transport properties of swollen complex membranes of linear low density polyethylene (LLDPE), silicone rubber (SR), and poly(1-trimethylsilyl-1-propyne) (PTMSP). The swollen complex membranes were constructed by dense matrix membranes, graft copolymers, metal ions, and the swelling agent. Low volatility glycerol impregnated in the membrane matrix served as the swelling agent of the film and as an activator of the Ag^+ complex.

The disadvantages of the above membranes include the need for addition of water, solvent, or swelling agent to the polymer matrix, and the need for some membranes to be operated with water-vapor-saturated feed and permeate streams. Downstream processing is still required to remove the extra component from the olefin-rich-permeate stream. Pinnau et al. (1997) was the first group to propose the use of solid polymeric membrane for olefin/paraffin separation. They report high pure-gas ethylene/ethane and propylene/propane selectivities using $AgBF_4$ in poly(ethylene oxide) or propylene oxide/allylglycidylether copolyer (PO-AGE) with a microporous poly(ether imide) membrane as the support material. With an increase in $AgBF_4$ loading, ethylene/ethane selectivity increases dramatically (from 160 to 2400 as $AgBF_4$ concentration increases from 50% to 80%). A similar increase is found for propylene/propane separation. The selectivities are significantly lower with mixed-gas permeation tests (2400 from pure-gas permeation vs. 120 from mixed-gas). The long term stability tests of this composite mem-

brane show a decrease in selectivity after 20 days. Pinnau and his group (Sunderrajan et al., 2001) recently compared four different silver salts ($AgBF_4$, $AgNO_3$, $AgCF_3SO_3$, $AgCF_3CO_2$) in poly(ethylene oxide) (PEO) and found $AgBF_4$ to be the most soluble salt in PEO. Also, PEO membranes containing $AgBF_4$ showed an high ethylene/ehane selectivity of 240 (Pinnau and Toy, 2001). Other solid polymer materials such as poly(2,6-dimethyl-1,4-phenylene-oxide), poly(2-ethyl-2-oxazoline) (POZ), cellulose acetate, and poly(ether-*b*-amide) copolymer have also been studied for olefin/paraffin separation using silver salts as olefin facilitated transport carriers (Bai et al., 2000; Hong et al., 2001; Ryu et al., 2001; Morisato et al., 2001).

4.3 Experimental

Poly(ethylene oxide) (PEO) is a highly hydrophillic polymer. Three types of PEO with molecular weights of 1 million, 4 million, and 7 million g/mol, were purchased from Sigma-Aldrich Canada. The physical properties of PEO are summarized in Appendix A in Table A.1.

The structure of the PEO repeating unit is:

$$(\text{-}CH_2CH_2O\text{-})_n$$

Flat films were prepared by the solution casting method as described in Chapter 3, and water was used as the solvent. Since high molecular weight PEO was used in the experiments, high solution viscosity could have resulted in uneven dispersion. To counteract this, the polymer solution was made with less than 2 % PEO solid by weight. For the samples with a molecular weight of 1 million and 4 million, 2% of polymer solution was prepared and for 7 million, the polymer solution only contained 1.5% PEO by weight. The polymer solutions were prepared at room temperature with vigorous stirring. After complete dissolution of the PEO in water, silver salt was added to the solution. In the mean time, the flask and rubber stopper was covered with foil to avoid light contact with the solution. The casting solution was then poured onto a glass

plate and left to air-dry for 3 days until the membrane was free of water.

$AgNO_3$ was selected as our source of silver salt in this study. Sunderrajan et al. (2001) suggested that silver salt ions can be solubilized by the polymer due to interaction of salt cations with electrons on a heteroatom in the polymer backbone such as the ether oxygens in PEO. The weight percentages of silver nitrate chosen are 50, 65, and 80, corresponding to 4:1, 2:1, and 1:1 molar ratios of oxygen atoms to silver atoms, respectively.

Due to difficulties in controlling the exact thickness of the membrane upon preparation, the thickness of the PEO membrane could not be pre-determined exactly. It was only possible to target a range of thickness. To control for this, thickness was measured after the membrane had been prepared.

4.4 Results and Discussion

Pure gas permeation tests were conducted using ethane and ethylene at room temperature, with a feed pressure of 100 psig. The thickness of the PEO membrane ranged from 70 to 90 μm. A full 2^3 factorial design with 3 centre point replications was set up for the experimental runs (see Appendix B Table B.1). Membrane thicknesses were represented as T1 (thickness 1) and T2 (thickness 2).

It was observed during the testing that membrane preparation was sensitive to light exposure. After adding silver salt to the polymer solution, the color of the solution gradually turned brown in color, indicating silver oxidation. The dried PEO membranes containing $AgNO_3$ became black and brittle after one day. Additionally, even when first formed/by this time, areas of uneven thickness could be seen on the surface of the membrane, which suggested membrane

defects. This was later confirmed by permeability tests.

Table 4.1 presents the result summary from the ethane and ethylene permeability tests. α_{AB} denotes pure gas selectivity of ethylene over ethane. Sample calculations on flux, permeability, and selectivity are included in Appendix C and raw data are in Appendix E. In some experimental runs, high selectivities of ethylene/ethane were observed; however, others showed almost no preferable selectivity over ethylene. Poor data reproducibility, even with the same membrane receipt, is apparent from the preliminary permeability results.

Table 4.1: Results from preliminary permeability tests of PEO membranes containing $AgNO_3$

no.	**mol. wt.**	**Ag wt.%**	**permeability (Barrer)**		**selectivity**
			ethane	**ethylene**	α_{AB}
1	1M	80	1562.48	1175.11	0.75
			21027.01	13602.94	0.65
			93.87	16272.78	173.35
2	1M	80	218784.28	184773.58	0.84
			164448.08	135412.52	0.82
3	4M	50	6945.50	65748.45	9.47
4	4M	50	209.07	6181.41	29.57
			3.64	6490.30	1782.39
			109.24	30.60	0.28
5	4M	50	553.06	327.83	0.59
6	7M	50	61.98	47.24	0.76
			19325.04	19706.40	1.02
			58.00	56.66	0.98
			1202.34	2152.18	0.56
			129.81	87.18	0.67

Pure PEO membranes were made during the course of experiments. Pinnau et al. (1997) reported in their study of PEO membranes containing $AgBF_4$ that pure PEO exhibits low ethylene/ethane selectivity of 1.2. However, our experiments were unable to obtain such a result from pure PEO membranes. All the pure PEO membranes, regardless of molecular weight,

showed extremely high gas flux, suggesting membrane defects. It is suspected that since PEO is a highly hydrophilic polymer, the relative humidity in the room may have affected the membrane structure during casting. This was verified by similar work which was later conducted by another member in the research group. A vacuum was installed to de-gas the dissolved air in the polymer solution, and the membranes were prepared in this vacuum rather than air-dried in a fume hood. The vacuum-dried PEO membranes were transparent, which stands in contrast to the translucent membrane the air-dried method produced. It is therefore likely that the membrane instability demonstrated in our trials was at least partly due to water and air trapped inside the polymer chain, which caused defects in the polymer structure.

Assuming that those of our membranes which did yield high ethylene/ethane selectivities were the ones that suffered the least from these defects, it is encouraging to note the relatively high selectivity that the PEO with $AgNO_3$ membrane showed. However, due to the fact that they appear to suffer structure damage from humidity and oxidation of silver salts, one must consider seriously the feasibility of employing this material in further testing. Since the preliminary results showed problems with membrane stability and inconsistent permeation data, the proposed experimental design was not carried out to completion. The experience and knowledge acquired from this investigation provided good groundwork in understanding membrane preparation and testing techniques, which we applied to the investigation of gas properties of PEBAX®2533 membranes (Chapter 5).

Chapter 5

Poly(ether-*b*-amide) Copolymer Membranes

5.1 Introduction

The history of polyether block amide (PEBA) resin can be dated to 1972 research initiatives by Atochem in which the goal was a ”soft” nylon material. The actual polyether block amide polymer was commercialized in 1981 (Dennis and O’Brien, 2000).

Polyether block amide (PEBA) resin is best known under the trademark PEBAX®, and is a thermoplastic elastomer combining linear chains of rigid polyamide segments interspaced with flexible polyether segments. It is produced by polycondensation of a dicarboxylic polyamide and a polyether diol in the presence of heat, vacuum, and a catalyst (Cen et al., 2002).

The structure of the PEBAX repeating unit is:

$$HO\ [\text{-C(=O)-PA-C(=O)-O-PE-}]_n\ H$$

where PA is an aliphatic polyamide ”hard segment” (i.e., Nylon-6 [PA6], or Nylon-12 [PA12]), and PE is an amorphous polyether ”soft segment”. The soft segment is either poly(ethylene oxide), or poly(tetramethylene oxide). This crystalline/amorphous structure creates a blend of properties of thermoplastics and rubbers. In application to permeation, the hard amide block provides the mechanical strength, whereas gas transport occurs primarily in the soft ether segments (Bondar et al., 2000).

Currently, the main commercial applications range from sporting goods (shoe soles), industrial equipment (conveyor belts), as well as functional films (breathable clothing, drying films) and various other materials.

5.2 Relevant Literature

Only in recent years have membranes based on PEBAX® polymer been investigated in separation processes. In the pulp and paper industry, recovery of methanol from water wet air streams is crucial to control hazardous air pollutant emissions. Rezac et al. (1997) evaluated the sorption and diffusion characteristics of water and methanol in a series of PEBAX® copolymers. Their results indicated that PEBAX® materials can be used to selectively separate methanol from air, but not methanol from water. The PEBAX® series in their study consist of Nylon-12 and polytetramethylene oxide of varying ratios. Among the four grades of PEBAX® (2533, 3533, 5533, and 6333), the 2533 grade was the most promising due to high permeation rates.

Djebbar et al. (1998) studied the pervaporation of three aqueous ethyl ester solutions with PEBAX® membranes of different polyamide composition ranging from 25 to 80 weight percent. PEBAX® was chosen as the material of interest due to its hydrophobicity and high se-

lectivity of aromatic organic compounds from water. The separation is considered to be an alternative for the extraction of volatile organic compounds (VOCs) from aqueous media. It was shown in this study that the use of PEBAX® membranes of high polyether content is most advantageous for VOCs extraction, as long as the polymer swelling from the penetrant is not excessive. PEBAX® grade 3533 was investigated for the pervaporation separation of isopropanol-water and ethyl butyrate-water mixtures (Sampranpiboon et al., 2000).

Bondar et al. (2000) found that in applications such as the removal of CO_2 from mixtures of hydrogen in syngas, PEBA was found to have high selectivity on polar or quadrupolar/nonpolar systems (e.g. CO_2/H_2 or CO_2/N_2). Bondar's group evaluated membranes made from four grades of PEBAX®, which range from 80 to 53 weight percent of polyether (PE) in the block copolymer. The PEBAX® grades are 2533, 4011, 1074, 4033 in desending PE weight percent. Their sorption and permeation results suggest strong interaction between the polar gas CO_2 and the PE blocks in the copolymer. They found that PE composition and CO_2 permeability were directly correlated. Kim et al. (2001) reported the particular selectivity of CO_2 over N_2 is 61 and that of SO_2 over N_2 is 500 . Strong affinity of polar species to the PE block is attributed to the high permeability and permselectivity of polarizable gases through PEBAX® copolymer.

Although PEBAX® copolymer has an excellent gas selectivity for organic gas separation in pervaporation and in polarizable/non polar gas mixture, there are almost no results regarding the permeation of hydrocarbons through PEBAX® membranes until a recent article by Morisato et al. (2001). This group utilized membranes based on PEBAX®2533 doped with $AgBF_4$ to separate ethylene and ethane. The group reported the value of mixed-gas ethylene/ethane selectivity to be less than 2 as the $AgBF_4$ concentration increased from 0 to 70%. The selectivity increased to 26 when the salt concentration was raised from 70 to 90%.

The objective of our study is to investigate the gas permeation process through a dry PEBAX® membrane from the view point of organic gas separation. Permeation experiments were conducted using pure gas feed. The effects of membrane preparation conditions and operating conditions on the separation performance of the PEBAX® membrane will be reported and compared with literature data.

5.3 Experimental

The hydrophobic PEBAX® (grade 2533) copolymer was supplied by ATOFINA Chemical, Inc. (Philadelphia, PA.). Physical property data for PEBAX®2533 are summarized in Table A.2 of Appendix A. PEBAX®2533 flat film was prepared by the solution casting method as previously mentioned in Section 3.1. Among choices of solvents, Kim et al. (2001) compared various solvents for the preparation of the PEBAX® polymer solution, and reported a 3:1 by weight mixture of 1-propanol and 1-butanol at 80^{o}C gave best solubility to the copolymer. In this study, only 2533 grade of PEBAX® is used. It was found that either pure 1-propanol or 1-butanol can completely dissolve the polymer at 90^{o}C while vigorously stirring over a 48-hour span. Therefore, 1-propanol, Certified ACS grade, was chosen to make a 3 weight percent PEBAX®2533 solution. The polymer solution was then poured into a Petri dish and dried at room temperature for 48 hours under the fume hood such that solvent can be completely removed.

Permeability tests of a single pure gas permeation through the membrane cells were performed in this study. The set-up of the permeation cell is shown in Figure 3.1. The permeation properties from six gases were studied. The six gases are nitrogen, carbon dioxide, ethane, ethylene, propane, and propylene. Gases were purchased from Praxair Inc., with at least 99% purity. The

studied pressures range from 25 psig to 200 psig and the temperatures of interest range from 25^{o}C to 75^{o}C. The permeation cell is placed in a 6-litre VWR circulation bath (Model 1167) with built-in temperature controller. Inside the bath, water was circulated to maintain constant temperature surrounding the permeation cell.

5.4 Results and Discussion

5.4.1 Effect of Permeation Time on Flux and Selectivity

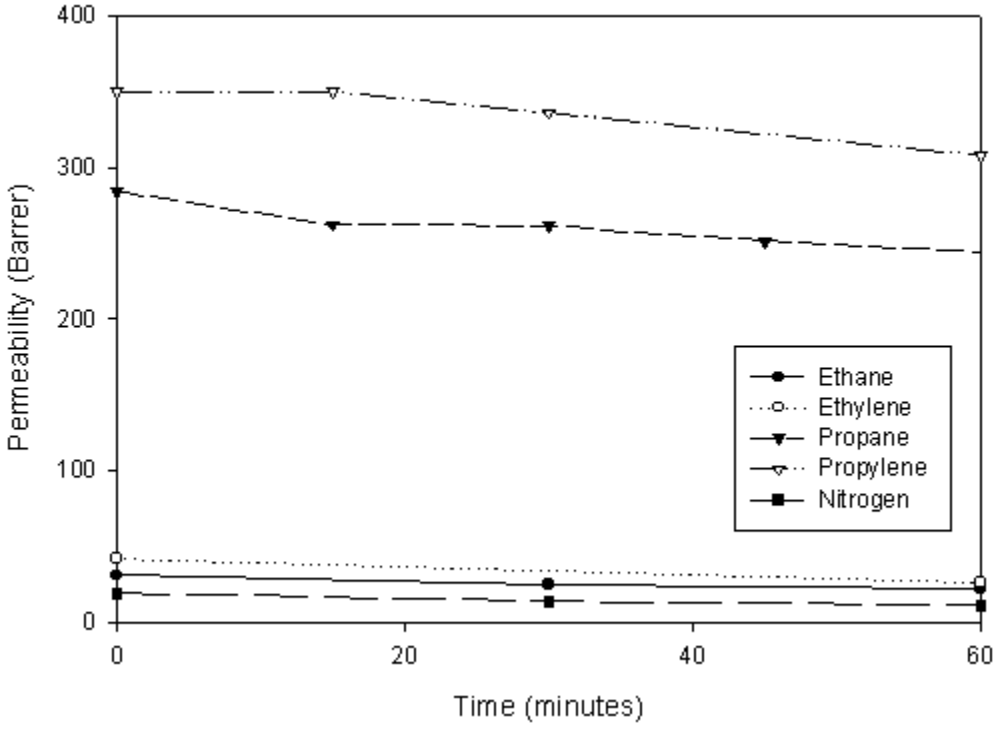

Figure 5.1: Time Dependency of permeability for PEBAX®2533(short term), P=75 psig.

The results of Figure 5.1 are from a series of short permeability tests, each lasting about one hour. A sample calculation is given in Appendix C, Section C.2 and raw data given in Ap-

pendix E. Each of the five gases (ethane, ethylene, propane, propylene, and nitrogen) was passed though a PEBAX membrane of 20 μm, with an upstream pressure of 75 psig. The results showed that C3 hydrocarbons (propane and propylene) have at least 7 times higher permeability than the C2 hydrocarbons (ethane and ethylene). Nitrogen was found to have the lowest permeability value of 10 Barrers after the first hour. These measurements reflect a fast check on the penetrant interaction with the membrane. It can be seen that the permeabilities of all five gases show a decreasing trend. This is an indication that interaction may occur between penetrant gas and the membrane material.

Permeability measurements were also taken for a much longer period of time to evaluate the time effect using another piece of 20 μm PEBAX membrane, as seen in Figure 5.2. Relative to other gases, permeabilities of propane and propylene took a longer time to stabilize. The results provide estimates for the conditioning period. It will take at least 24 hours of operation for ethane, ethylene or nitrogen and 72 hours for propane and propylene to give consistent results.

The extent of polymer-penetrant interaction can be seen in Figure 5.3. The values of the exponent in the power law model indicate that nitrogen has little interaction with PEBAX copolymer, whereas both ethylene and propylene have much stronger interaction with PEBAX. Similar trends are observed with ethane and propane permeation and the results are included in Appendix D, Figures D.1 and D.2.

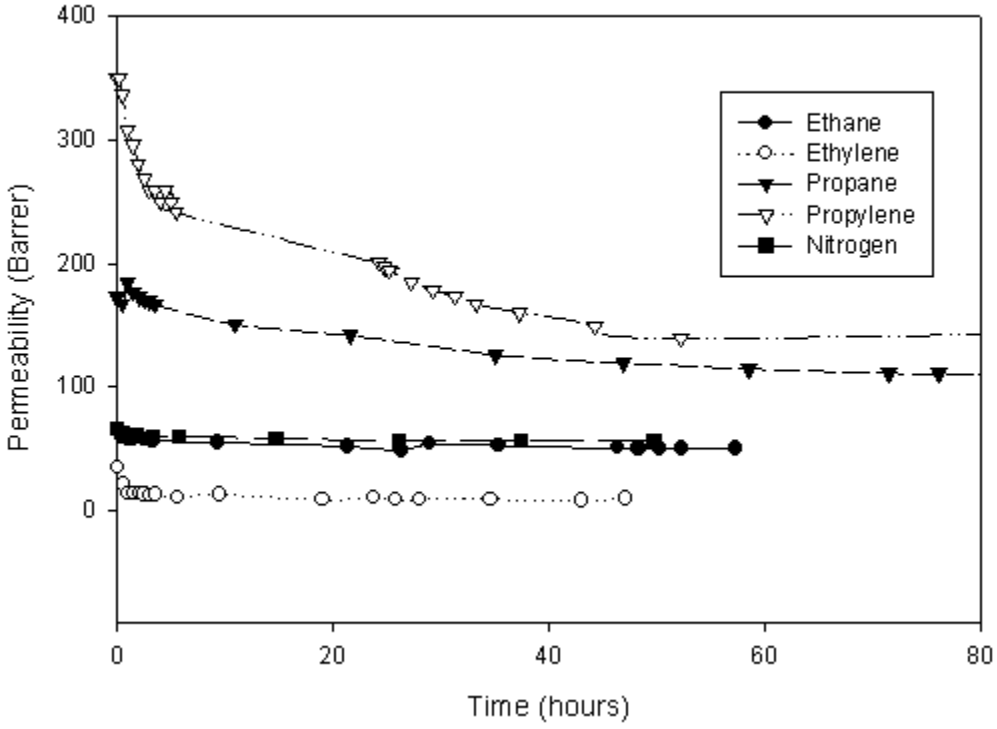

Figure 5.2: Time Dependency of permeability for PEBAX®2533 (long term)

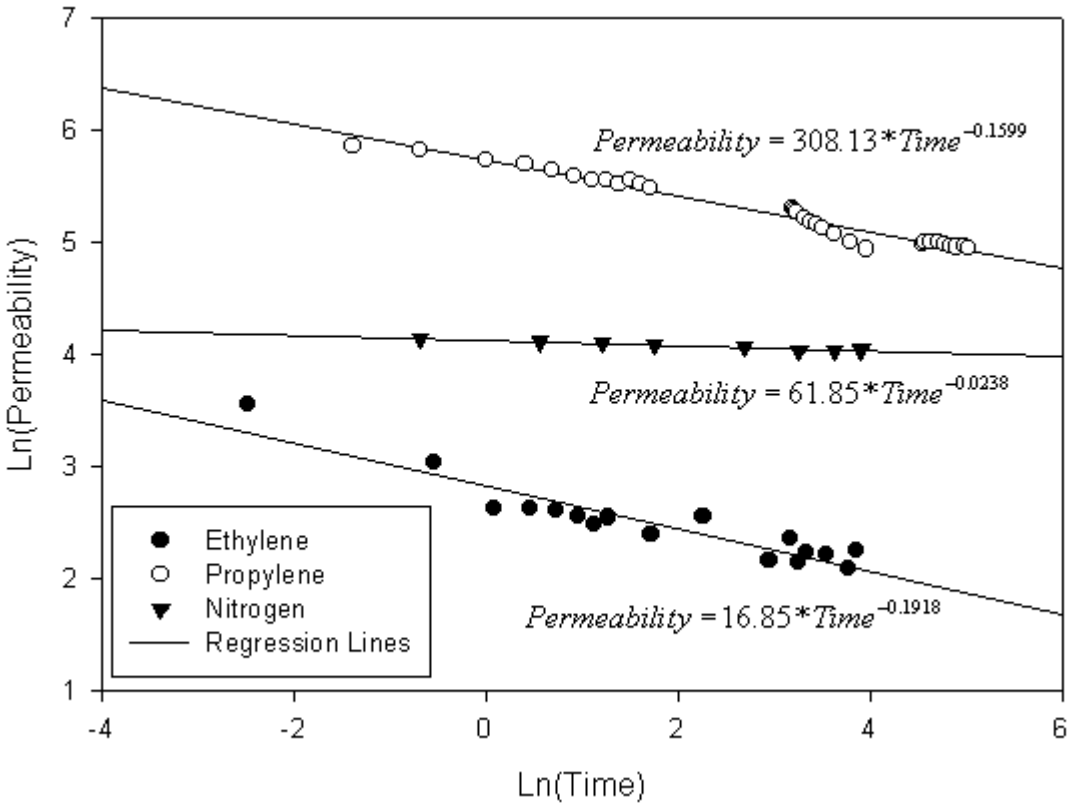

Figure 5.3: Log-log plot of permeability vs. time (Nitrogen, Ethylene, Propylene)

5.4.2 Effect of Pressure on Permeability and Selectivity

The permeabilities of PEBAX®2533 film were determined as a function of the feed pressure. The measurements were carried out at 25^{o}C and pressures up to 100 psig. After the membrane had been conditioned with testing gas for three days under high pressure (200 psig) and room temperature, permeation measurements were taken while varying the feed pressure.

The permeabilities of ethane and ethylene have an almost linear relationship to feed pressures, as shown in Figure 5.4. This confirms the linear and positive response induced by an organic gas that permeates across a rubbery membrane (see Figure 2.5 (c), Section 2.3.2). Figure 5.5 presents the results from the propane and propylene permeability tests. The curved nature of the responses from propane and propylene indicates that plasticization was present in our testing pressure range. The plasticization pressure is defined by the lowest value on a permeability versus pressure curve, as shown in Figure 2.5 (d) (see Sections 2.3.2 and 2.3.3). The plasticization pressure for propane and propylene is estimated to be around 20 psig. Responses from ethane, propane and nitrogen were plotted together in Figure 5.6. The permeability of nitrogen is independent of gas pressure under the experimental conditions, representing an ideal case.

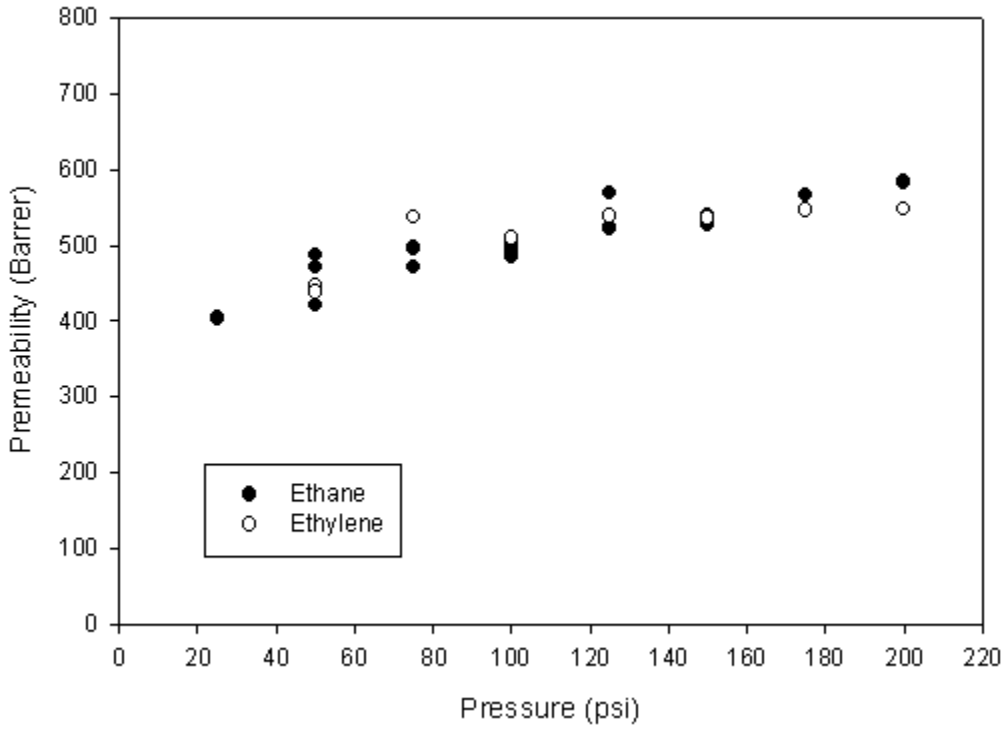

Figure 5.4: Permeability as a function of feed pressure (Ethane, Ethylene). Temperature: 25^{o}C.

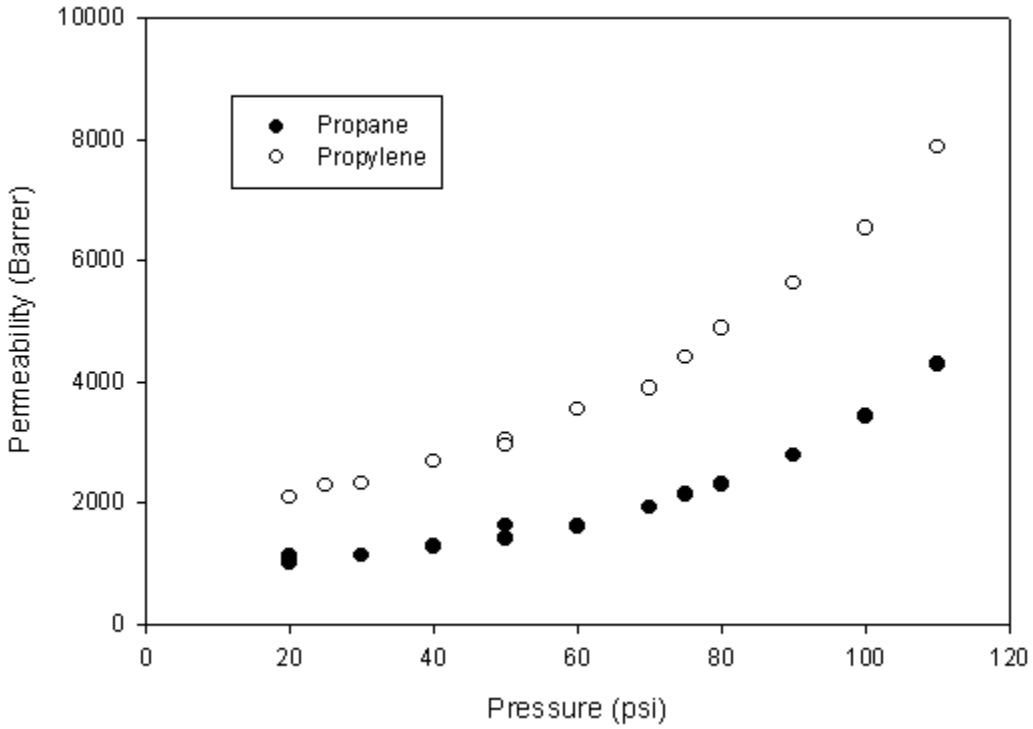

Figure 5.5: Permeability as a function of feed pressure (Propane, Propylene). Temperature: 25^{o}C.

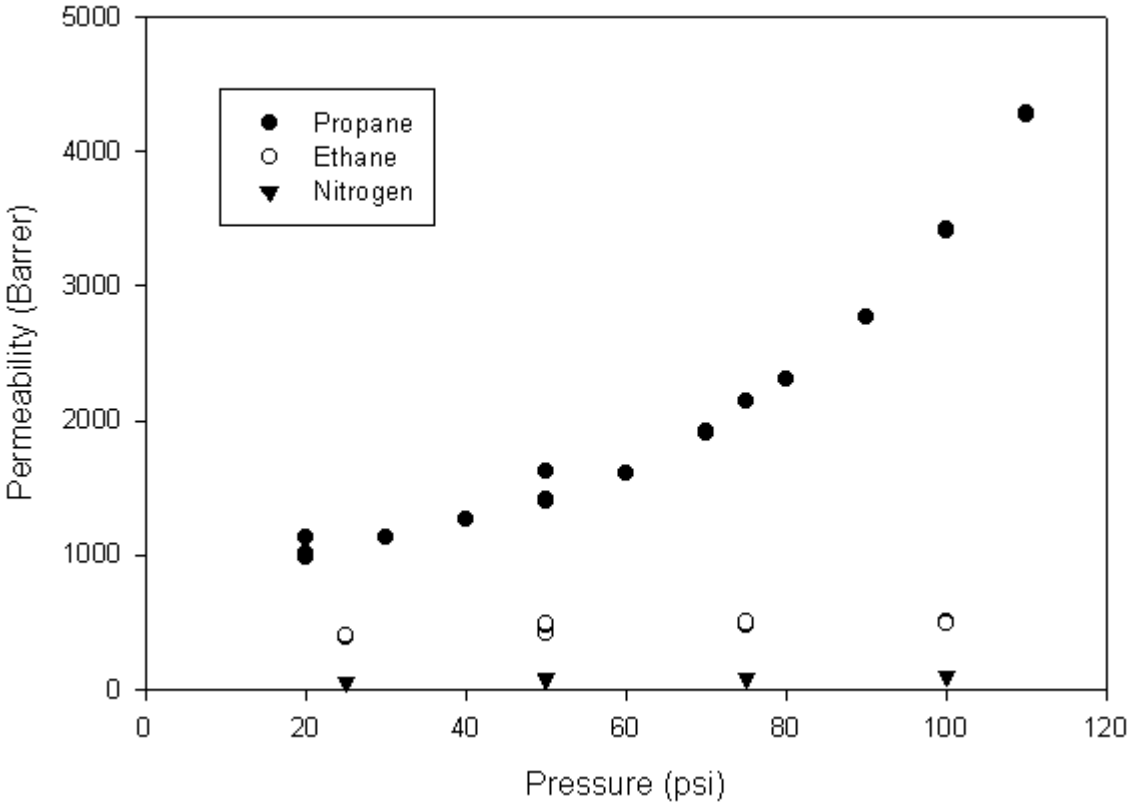

Figure 5.6: Permeability as a function of feed pressure (Nitrogen, Ethane, Propane). Temperature: 25^{o}C.

At higher pressure, the permeabilities of propane and propylene strongly affect the selectivities for gas pairs involving propane and propylene. Table 5.1 presents the calculated selectivities of different gas pairs in relationship with pressure changes. Increasing trends in selectivity with pressure can be observed for the pairs of propylene/ethylene, propane/ethane, propane/nitrogen, and propylene/nitrogen. For the ethane/nitrogen and ethylene/nitrogen pairs, there was a slight decrease in selecitivites when pressure was increased. This may be explained from Equation 2.8. Although gas diffusivity selectivity (*D*) increases as pressure (the driving force) increases, the solubility selectivity (*S*) of the gas into polymer decreases, causing a counter effect and thus reducing overall permselectivity. Selectivities remain constant for the ethane/ethylene and propane/propylene pairs, since pressure has similar effects on both components in the pairs.

Table 5.1: Pressure effect on selectivities of different gas pairs

pressure (psig)	**selectivity**			
	C_3H_8/C_3H_6	C_3H_8/C_2H_6	C_2H_6/C_2H_4	C_3H_6/C_2H_4
25	2.19	2.62	1.30	4.44
50	2.03	3.21	0.96	6.78
75	2.05	4.42	1.11	8.16
100	1.91	6.91	1.03	12.83
pressure (psig)	**selectivity**			
	C_3H_8/N_2	C_3H_6/N_2	C_2H_6/N_2	C_2H_4/N_2
25	20.89	45.85	7.96	10.32
50	19.40	39.46	6.05	5.82
75	24.74	50.78	5.59	6.22
100	36.31	69.45	5.25	5.41

5.4.3 ”Memory” of PEBAX®2533

To determine whether PEBAX has ”memory” of prior permeations, after a set of pressure tests were run under various temperatures, another set of pressure tests were preformed at 25^{o}C. For propane gas, the second set of tests showed lower permeability than the first time, as seen in Figure 5.7. This indicates that with temperature and pressure changes, the PEBAX structures

are altered. Similar results were observed with ethane, as seen in Figure 5.8.

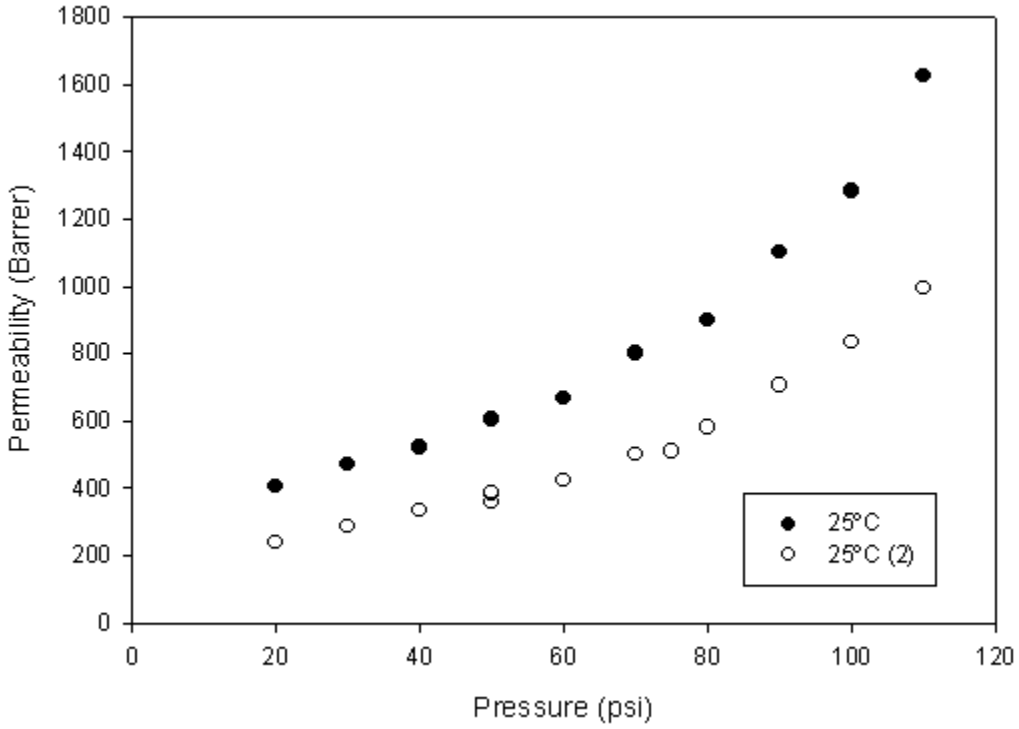

Figure 5.7: Permeability as a function of feed pressure. Propane through PEBAX® 2533

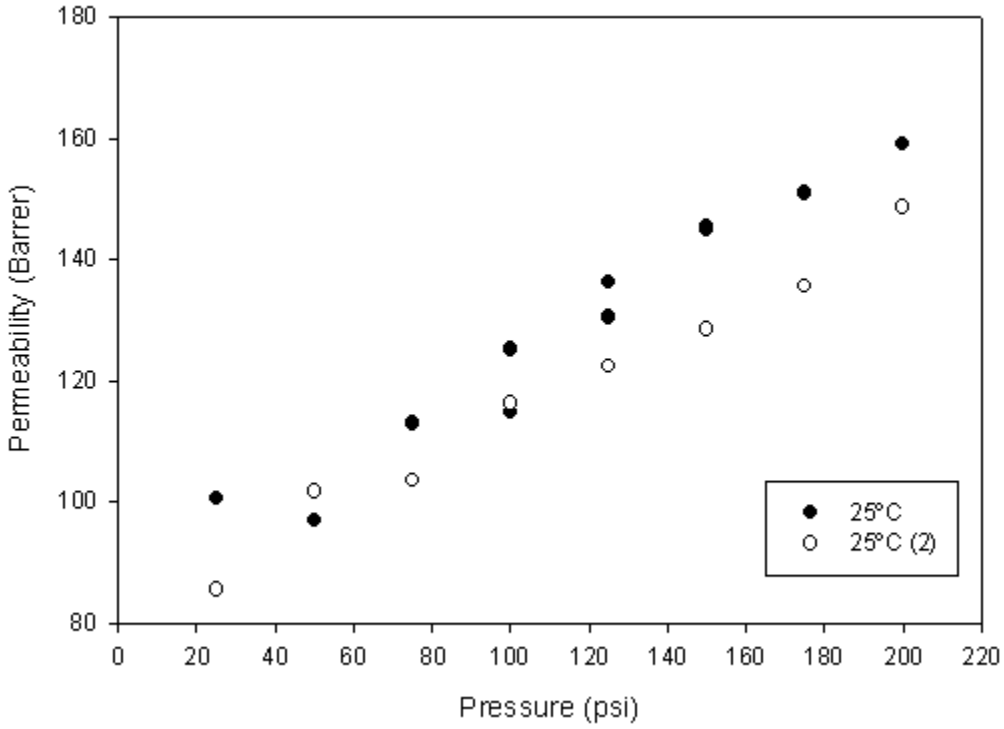

Figure 5.8: Permeability as a function of feed pressure. Ethane through PEBAX® 2533

5.4.4 Effect of Temperature

As discussed previously in Chapter 2, permeation is an activated process and the permeability coefficient can be approximated by an Arrehnius expression, as shown in Equation C.11. Figure 5.9 shows the temperature dependency of propane permeation. On a log-log graph, the relationship between permeability and inverse temperature is linear. Linear regression was applied to the permeability data and pre-exponential values and the activation energy of permeation were determined and are summarized in Table 5.2. Sample calculations on pre-exponential factor and activation energy values for permeation can be found in Appendix C. It can be seen clearly from Table 5.2 that as pressure increases, the activation energy of propane permeation decreases. Similar trends were observed for propylene, as seen in Figure 5.10.

Nitrogen shows a distinctly different trend from propane and propylene. Figure 5.11 shows that all regression lines are similar in slope and position. Comparing with results from the propane tests (same as in Table 5.2), nitrogen has both a higher pre-exponential value and activation energy (see Table 5.3). Ethane and ethylene exhibit similar behavior to nitrogen, but there is a slight decrease in activation energy as pressure increases (see Figure 5.12). This indicates that the permeability of nitrogen in PEBAX is not affected by the temperature changes and that C3 hydrocarbons are more affected by temperature than C2 hydrocarbons are.

Plots of temperature dependency of ethane, and ethylene permeability are included in Appendix D, Figures D.3 and D.4. Table D.1 compares calculated values of pre-exponential factors and activation energy for ethane and ethylene.

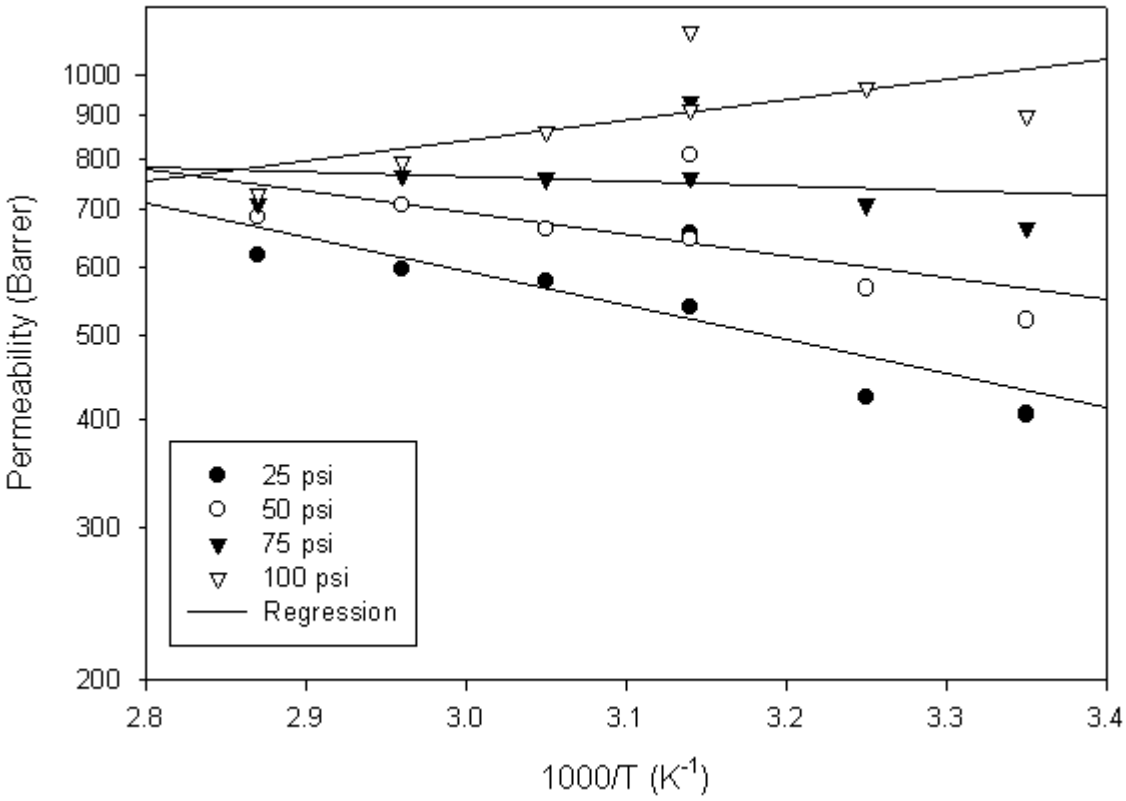

Figure 5.9: Temperature dependency of propane permeability in PEBAX® 2533

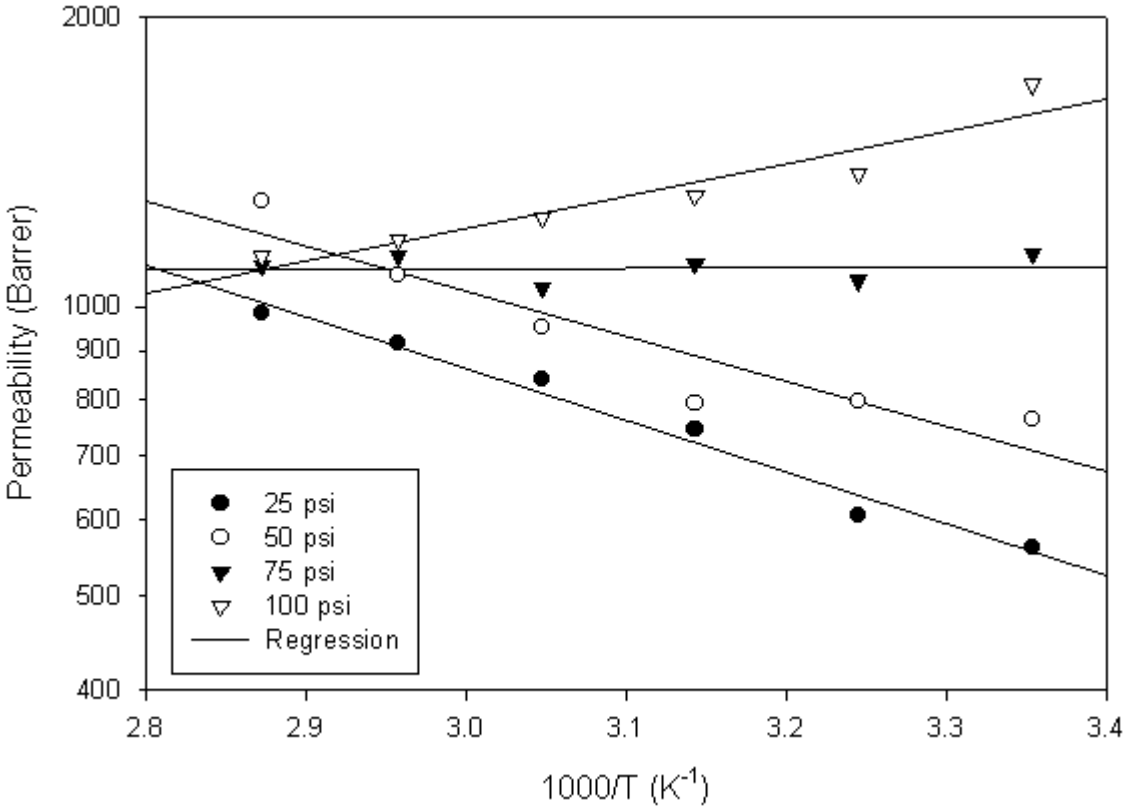

Figure 5.10: Temperature dependency of propylene permeability in PEBAX® 2533

Table 5.2: Calculated values of pre-exponential factors and activation energy for propane and propylene permeation

pressure (psig)	**propane**		**propylene**	
	P_0 (Barrer)	E_p (KJ/mol.K)	P_0 (Barrer)	E_p (KJ/mol.K)
25	10281.23	7.99	52950.46	11.39
50	4413.56	5.22	18960.75	8.08
75	1259.78	1.47	847.47	-0.66
100	187.63	-4.07	90.51	-7.09

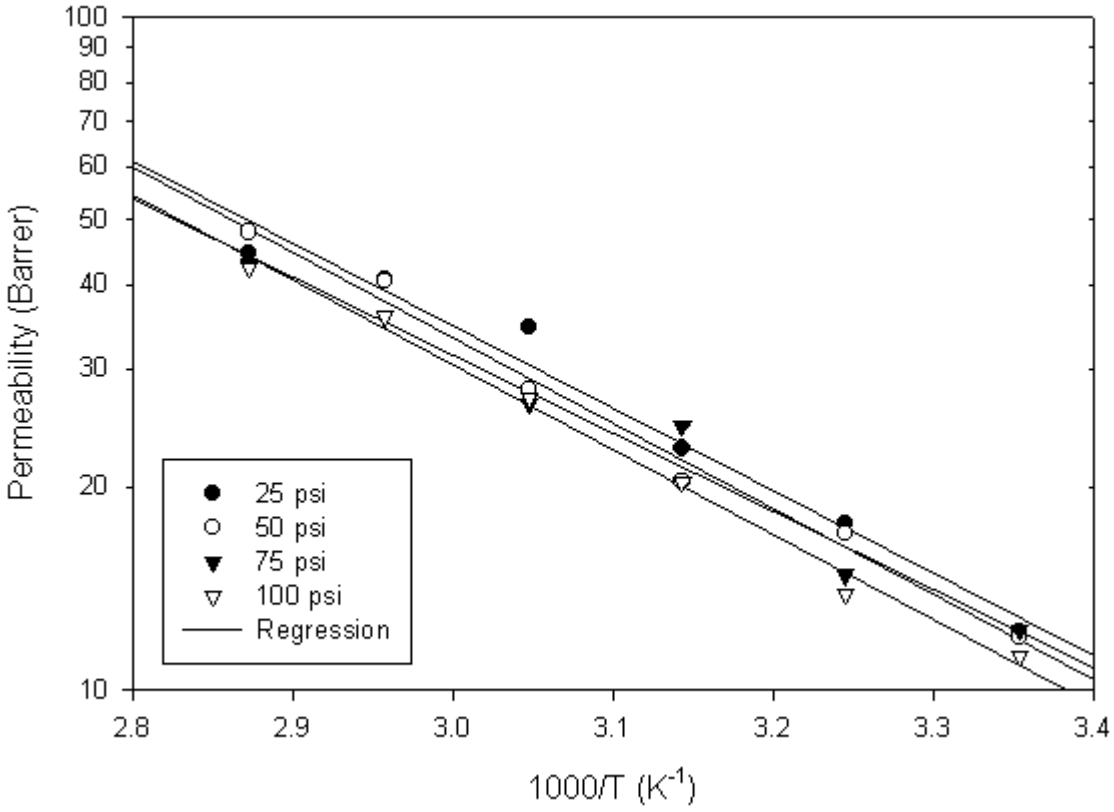

Figure 5.11: Temperature dependency of nitrogen permeability in PEBAX® 2533

Table 5.3: Calculated values of pre-exponential factors and activation energy for propane and nitrogen permeation

pressure (psig)	**propane**		**nitrogen**	
	P_0 (Barrer)	E_p (KJ/mol.K)	P_0 (Barrer)	E_p (KJ/mol.K)
25	10281.23	7.99	161337.91	23.40
50	4413.56	5.22	211336.77	24.26
75	1259.78	1.47	96566.12	22.26
100	187.63	-4.07	185817.33	24.16

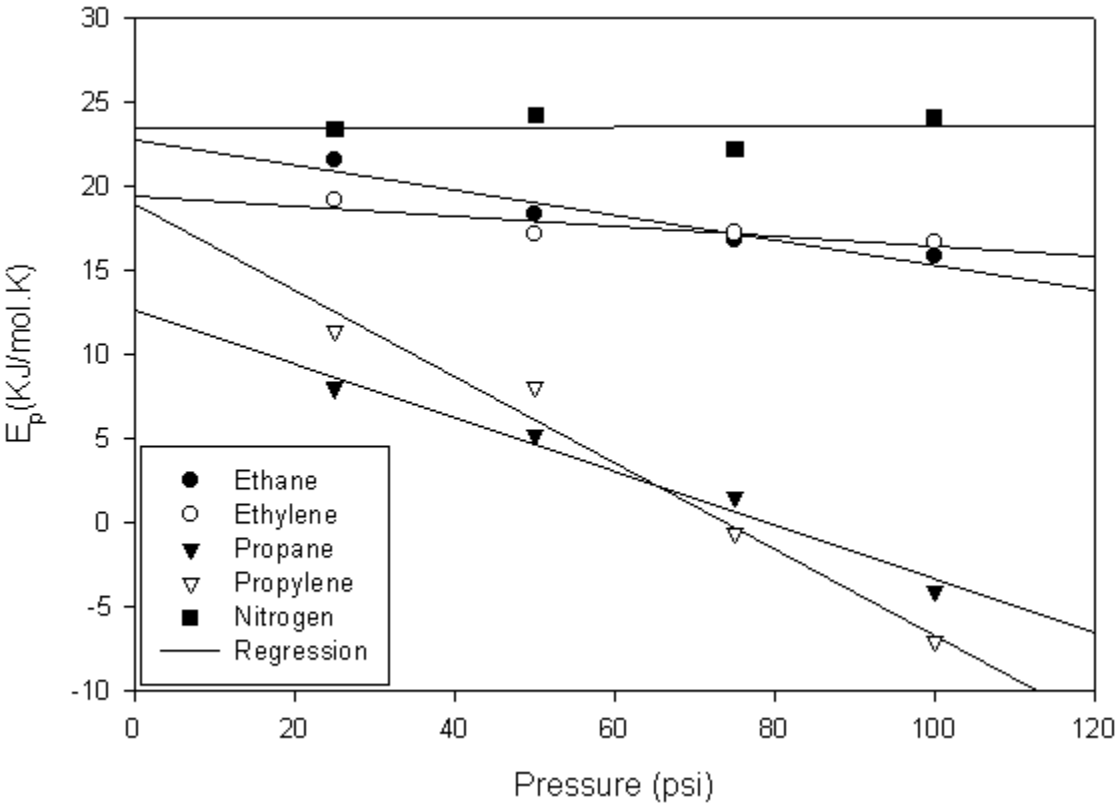

Figure 5.12: Pressure dependence of activation energy of permeation

5.4.5 Polar vs. Non-Polar Gases

In permeation studies done by Kim et al. (2001), Kim and Lee (2001), and Bondar et al. (2000), PEBAX® membranes have shown high selectivities for separations of CO_2/N_2. Kim et al. (2001) reported that as temperature increases, the selectivity of CO_2/N_2 decreases. To confirm the above findings, CO_2 and N_2 permeability tests were conducted at temperatures ranging from 25^{o}C to 75^{o}C at pressures of 25 and 50 psig. Selectivities of CO_2/N_2 were plotted against inverse temperature (1000/T), shown as Figure 5.13. Figure 5.14 is taken from Kim and Lee (2001), who used PEBAX®1657 at a pressure of 3 atm. Although a different grade of PEBAX® was used in our experiments, a similar trend is observed for the temperature dependency of CO_2/N_2 separation using this type of copolymer. Our study verified that selectivity of polar and non-polar gas pairs using PEBAX® membranes is high and it has an inverse temperature dependency.

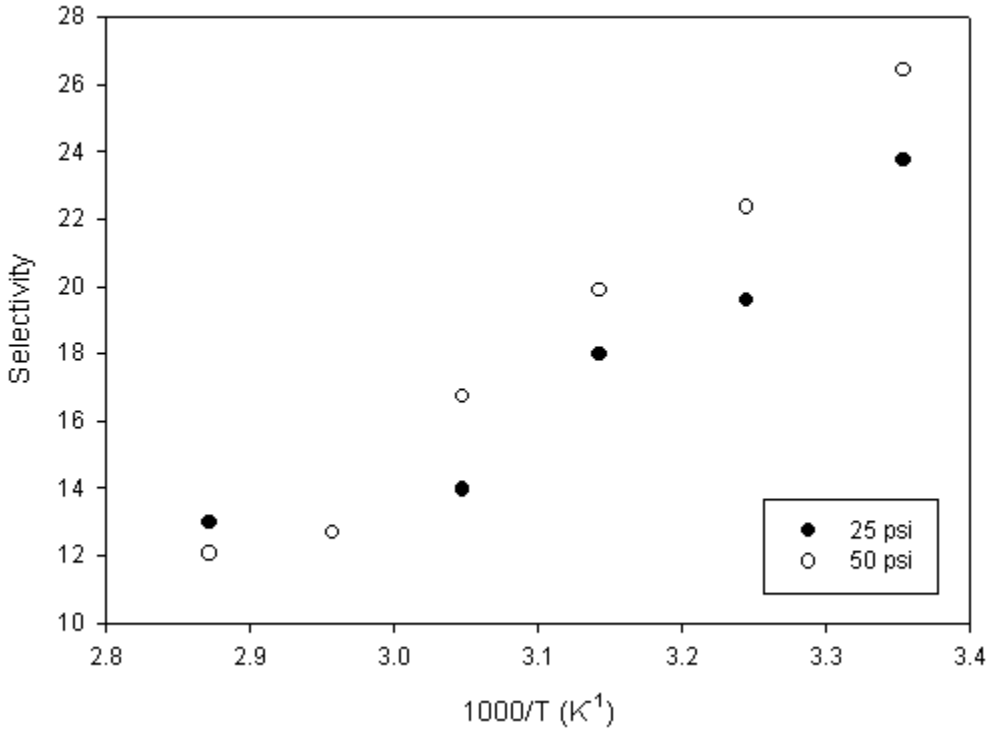

Figure 5.13: Temperature dependency of CO_2/N_2 selectivity for PEBAX®2533

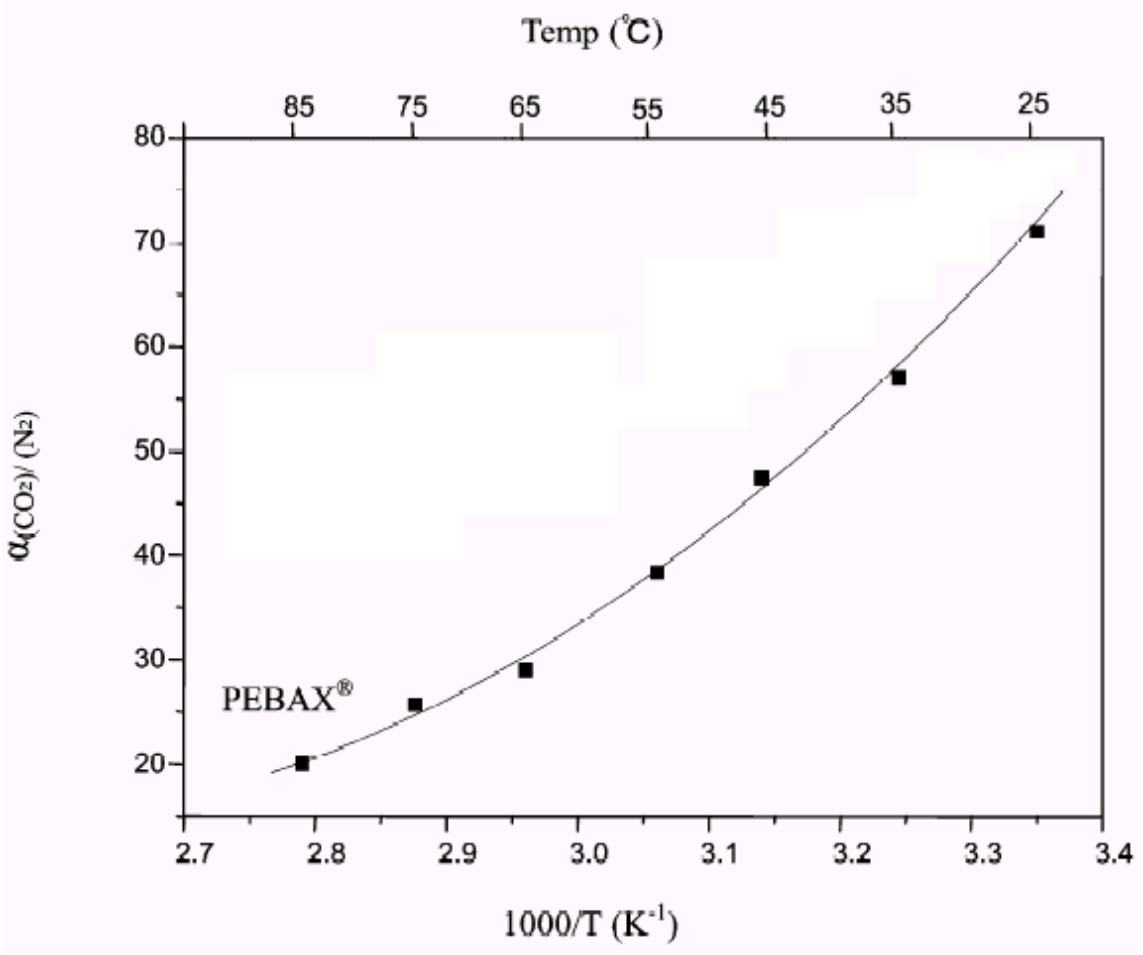

Figure 5.14: Selectivity of CO_2/N_2 versus Temperature from Kim and Lee (2001)

Chapter 6

Concluding Remarks and Recommendations

6.1 Concluding Remarks

The gas permeation properties on two types of polymeric membranes for hydrocarbon gas separations have been investigated. One is poly(ethylene oxide) containing $AgNO_3$ and the other is poly(ether-*b*-amide) PEBAX®2533 block copolymer.

The permeability results from PEO membranes containing $AgNO_3$ were compared with results from PEO membranes containing $AgBF_4$ from Pinnau et al. (1997). However, since the prepared PEO containing $AgNO_3$ membranes gave inconclusive permeability results for ethane and ethylene separations under operating conditions of 100 psig and room temperature, only pure PEO gas properties were discussed. The inconclusive results likely stem from membrane instability and defects due to flaws with the method of preparation and the oxidation of silver salts.

The second polymer material, PEBAX®2533 membranes showed high hydrocarbon permeation. The permeability of PEBAX®2533 film was determined as a function of feed pressures and operating temperatures. Permeation properties obtained from propane and propylene indicate plasticization effects on the PEBAX®2533 polymer matrix. Nitrogen showed no interaction with the membrane material, which is considered ideal. Premeabilities of propane and propylene are strongly affected by both temperature and pressure. This is consistent with observations in the literature. As pressure increases, the permeability of propane and propylene increases. Their temperature dependency of permeation can be approximated by Arrehnius expressions and it is found that the activation energy of permeation decreases as pressure increases. Due to the polar nature of this membrane material, it has been investigated for separating polar and non-polar gas pairs. CO_2/N_2 separation is temperature sensitive with PEBAX and higher selectivity is achieved at lower temperature.

6.2 Recommendations

Based on this work, some recommendations that may provide further insight into gas separation membranes are listed below.

First of all, systematic methods to investigate reasons for membrane defects should be pursued with PEO membranes containing silver salts. Different silver salts may be used for this investigation to validate literature data. In the literature, it has been noted that there is a lack of detailed preparation method. Since membrane preparation can greatly affect membrane properties, it is important to eliminate the possibility of causing defects due to improper membrane preparation.

Secondly, mixed gas permeability tests may be conducted using PEBAX®2533 membranes.

As mentioned in the background section, gas selectivities calculated from pure gas permeability can only give partial insight into the separation system. In order to account for effects of multicomponent cases, it is not sufficient to use pure gas permeation data only.

Thirdly, from collected permeation data on PEBAX membranes, optimal operating conditions can be determined for each gas pair to achieve highest permeability and selectivity.

Finally, silver-doped PEBAX may be prepared and tested, so the results can be compared against reported literature data by Morisato et al. (2001).

Bibliography

S. Bai, S. Sridhar, and A. Khan. Recovery of propylene from refinery off-gas using metal incorporated ethylcellulose membranes. *Journal of Membrane Science*, 174:67–79, 2000.

R. W. Baker. Future directions of membrane gas separation technology. *Industrial & Engineering Chemistry Research*, 41:1393–1411, 2002.

J. Bitter. *Transport Mechanisms in Membrane Separation Processes*. Plenum Press, New York and London, 1991.

V. Bondar, B. D. Freeman, and I. Pinnau. Gas transport properties of poly(ether-b-amide) segmented block copolymers. *Journal of Polymer Science Part B: Polymer Physics*, 38: 2051–2062, 2000.

A. Bos, I. Punt, H. Strathmann, and M. Wessling. Suppression of gas separation membrane plasticization by homogeneous polymer blending. *AIChE Journal*, 47:1088–1093, 2001.

Y. Cen, C. Staudt-Bickel, and R. Lichtenthaler. Sorption properties of organic solvents in PEBA membranes. *Journal of Membrane Science*, 206:341–349, 2002.

M. Cohen and D. Turnbull. Molecular transport in liquids and glasses. *Journal of Chemical Physics*, 31:1164–1169, 1959.

L. M. Costello and W. J. Koros. Effect of structure on the temperature dependence of gas transport and sorption in a series of polycarbonates. *Journal of Polymer Science: Part B: Polymer Physics*, 32:701–713, 1994.

G. M. Dennis and G. O'Brien. Polyether block amide resins: bridging the gap between thermoplastics and rubbers. American Chemical Society (ACS) Meeting, 2000. Ohio, USA.

M. Djebbar, Q. Nguyen, R. Clement, and Y. Germain. Pervaporation of aqueous ester solutions through hydrophobic poly(ether-block-amide) copolymer membranes. *Journal of Membrane Science*, 146:125–133, 1998.

R. Eldridge. Olefin/paraffin separation technology: a review. *Industrial & Engineering Chemistry Research*, 32:2208–2212, 1993.

E. Favre, N. Morliere, and D. Roizard. Experimental evidence and implications of an imperfect upstream pressure step for the time-lag technique. *Journal of Membrane Science*, 207:59–72, 2002.

B. D. Freeman and I. Pinnau. Separation of gases using solubility-selective polymers. *Trends in Polymer Science*, 5:167–173, 1997.

H. H. Funke, R. D. Noble, and C. A. Koval. Separation of gaseous olefin isomers using facilitated transport membranes. *Journal of Membrane Science*, 82:229–236, 1993.

S. George and S. Thomas. Transport phenomena through polymeric systems. *Progress in Polymer Science*, 26:985–1017, 2001.

K. Ghosal and B. D. Freeman. Gas separation using polymer membranes: an overview. *Polymers for Advanced Technologies*, 5:673–697, 1993.

W. Ho and D. Dalrymple. Facilitated transport of olefins in Ag^{+}-containing polymer membranes. *Journal of Membrane Science*, 91:13–25, 1994.

S. U. Hong, J. Y. Kim, and Y. S. Kang. Effect of water on the facilitated transport of olefins through solid polymer electrolyte membranes. *Journal of Membrane Science*, 181:289–293, 2001.

R. Hughes, J. Mahoney, and E. Steigelmann. *Recent Developments in Separation Science, Volume 9*. 1986.

A. Ismail and W. Lorna. Penetrant-induced plasticization phenomenon in glassy polymers for gas separation membrane. *Separation and Purification Technology*, 27:173–194, 2002.

H. D. Kamaruddin and W. J. Koros. Some observations about the application of Fick's first law for membrane separation of multicomponent mixtures. *Journal of Membrane Science*, 135: 147–159, 1997.

R. E. Kesting. *Synthetic polymeric membranes: a structural perspective*. John Wiley & Sons, Toronto, 2 edition, 1985.

J. H. Kim, S. Y. Ha, and Y. M. Lee. Gas permeation of poly(amide-6-b-ethylene oxide) copolymer. *Journal of Membrane Science*, 190:179–193, 2001.

J. H. Kim and Y. M. Lee. Gas permeation properties of poly(amide-6-b-ethylene oxide)-silica hybrid membranes. *Journal of Membrane Science*, 193:209–225, 2001.

W. Koros and R. Chern. *Handbook of separation process technology*. John Wiley & Sons, 1987.

W. Koros and G. Fleming. Membrane-based gas separation. *Journal of Membrane Science*, 83: 1–80, 1993.

W. Koros, G. Fleming, S. Jordan, T. Kim, and H. Hoehn. Polymeric membrane materials for solution-diffusion based permeation separations. *Progress in Polymer Science*, 13:339–401, 1988.

J. Krol, M. Boerrigter, and G. Koops. Polyimide hollow fiber gas separation membranes: preparation and the suppression of plasticization in propane/propylene environments. *Journal of Membrane Science*, 184:275–286, 2001.

O. H. J. LeBlanc, W. J. Ward, S. L. Matson, and S. G. Kimura. Facilitated transport in ion-exchange membranes. *Journal of Membrane science*, 6:339–343, 1980.

A. Morisato, Z. He, I. Pinnau, and T. Merkel. Transport properties of PA12-PTMO/$AgBF_4$ solid polymer electrolyte membranes for olefin/paraffin separation. *Polymeric Materials: Science and Engineering*, 85:96–99, 2001.

M. Mulder. *Basic Principles of Membrane Technology*. Kluwer Academic Publishers, Dordrecht, The Netherlands, 1991.

R. Noble and S. Stern, editors. *Membrane Separations Technology, Principles and Applications*. Elsevier Science B.V., Amsterdam, The Netherlands, 1995.

R. D. Noble, C. A. Koval, and J. J. Pellegrino. Facilitated transport membrane systems. *Chemical Engineering Progress*, 85:58–70, 1989.

S. Pauly, J. Brandrup, and E. Immergut, editors. *Polymer Handbook*. John Wiley & Sons, New York, 3rd edition, 1989.

J. Petropoulos. Plasticization effects on the gas permeability and permselectivity of polymer membranes. *Journal of Membrane Science*, 75:47–59, 1992.

J. Petropoulos. *Polymeric gas separation membranes*, chapter 2. CRC Press, Inc., Boca Raton, Florida, 1994.

I. Pinnau and B. Freeman, editors. *Membrane Formation and Modification*, chapter 1. American Chemical Society, Washington, DC, 2000.

I. Pinnau and L. Toy. Solid polymer electrolyte composite membranes for olefin/paraffin separation. *Journal of Membrane Science*, 184:39–48, 2001.

I. Pinnau, L. Toy, S. Sunderrajan, and B. D. Freeman. Solid polymer electrolyte membranes for olefin/paraffin separation. *Polymeric Materials: Science and Engineering*, 77:269–270, 1997.

D. Pye, H. Hoehn, and M. Panar. Measurement of gas permeability of polymers. I. permeabilities in constant volume/variable pressure apparatus. *Journal of Applied Polymer Science*, 20: 1921–1931, 1976.

M. E. Rezac, T. John, and P. H. Pfromm. Effect of copolymer composition on the solubility and diffusivity of water and methanol in a series of polyether amides. *Journal of Applied Polymer Science*, 65:1983–1993, 1997.

J. H. Ryu, H. Lee, Y. J. Kim, Y. S. Kang, and H. S. Kim. Facilitated olefin transport by reversible olefin coordination to silver ions in dry cellulose acetate membrane. *Chemistry-A European Journal*, 7:1525–1529, 2001.

D. J. Safarik and R. Eldridge. Olefin/paraffin separations by reactive absorption: a review. *Industrial & Engineering Chemistry Research*, 37:2571–2581, 1998.

P. Sampranpiboon, R. Jiraratananon, D. Uttapap, X. Feng, and R. Huang. Pervaporation separation of ethyl butyrate and isopropanol with polyether block amide (PEBA) membranes. *Journal of Membrane Science*, 173:53–59, 2000.

J. Schultz, J. Goddard, and S. Suchdeo. Facilitated transport via carrier-mediated diffusion in membranes. Part I. mechanistic aspects, experimental systems and characteristic regimes. *AIChE Journal*, 20:417–445, 1974.

R. W. Spillman. Economics of gas separation membranes. *Chemical Engineering Progress*, 85: 41–62, 1989.

S. Sridhar and A. Khan. Simulation studies for the separation of propylene and propane by ethylcellulose membrane. *Journal of Membrane Science*, 159:209–219, 1999.

S. Stern. Polymers for gas separations: the next decade. *Journal of Membrane Science*, 94: 1–65, 1994.

H. Strathmann. Membrane separation processes: current relevance and future opportunities. *AIChE Journal*, 4:1077–1087, 2001.

S. Sunderrajan, B. D. Freeman, C. Hall, and I. Pinnau. Propane and propylene sorption in solid polymer electrolytes based on poly(ethylene oxide) and silver salts. *Journal of Membrane Science*, 182:1–12, 2001.

M. Teramoto, H. Matsuyama, T. Yamshiro, and Y. Katayama. Separation of ethylene from ethane by supported liquid membranes containing silver nitrate as a carrier. *Journal of Chemical Engineering of Japan*, 19:419–424, 1986.

M. Teramoto, H. Matsuyama, T. Yamshiro, and S. Koamoto. Separation of ethylene from ethane by a flowing liquid membrane using silver nitrate as a carrier. *Journal of Membrane Science*, 45:115–136, 1989.

T. Yamaguchi, C. Baertsch, C. A. Koval, R. D. Noble, and C. N. Bowman. Olefin separation using silver impregnated ion-exchange membranes and silver salt/polymer blend membranes. *Journal of Membrane Science*, 117:151–161, 1996.

J.-S. Yang and G.-H. Hsiue. Swollen polymeric complex membranes for olefin/paraffin separation. *Journal of Membrane Science*, 138:203–211, 1998.

C. Yeom, B. Kim, and J. Lee. Precise on-line measurements of permeation transients through dense polymeric membranes using a new permeation apparatus. *Journal of Membrane Science*, 161:55–66, 1999.

Appendix A

Physical Properties of Polymers

All data are from manufacturer's information unless otherwise noted. T_g: Glass transition temperature; T_m: melting point.

A.1 Poly(ethylene oxide)

Table A.1: Selected Properties of Poly(ethylene oxide)

density	1.111 g/cm^3
T_m	60-63 ^{o}C
flash point	270 ^{o}C
percent volatile	0.15 %
T_g	-60 ^{o}C
Inhibitor	200 - 500 ppm BHT

A.2 PEBAX®2533

Results from characterization study done by Bondar et al. (2000) are based on elemental analysis, differential scanning calorimetry (DSC) and wide-angle X-ray diffraction spectroscopy (WAXD). PE: Poly(tetramethylene oxide); PA: Polyamide 12 (Nylon-12).

Table A.2: Selected Properties of PEBAX®2533

density	1.01 g/cm^3
melting point (ASTM D3418)	147.78 ^{o}C
hardness (D2240)	25 Shore D
ultimate tensile strength (D638)	4950 psi
ultimate enlongation (D638)	640 %
weight percent PE	80
T_g	-77 ^{o}C
T_m(PE)	9 ^{o}C
T_m(PA)	126 ^{o}C
crystallinity in PA block	14 % by weight

Appendix B

Preliminary Design Data

Table B.1: Factorial design on PEO permeability tests

	Coded Value			Operating Conditions		
Trial	A	C	D	PEO Mwt	Ag (wt.%)	Thickness
1	1	1	1	7.00E+06	80	T1
2	1	1	-1	7.00E+06	80	T2
3	1	-1	1	7.00E+06	50	T1
4	1	-1	-1	7.00E+06	50	T2
5	-1	1	1	1.00E+06	80	T1
6	-1	1	-1	1.00E+06	80	T2
7	-1	-1	1	1.00E+06	50	T1
8	-1	-1	-1	1.00E+06	50	T2
center 1	0	0	1	4.00E+06	65	T1
center 2	0	0	1	4.00E+06	65	T1
center 3	0	0	1	4.00E+06	65	T1
center 4	0	0	-1	4.00E+06	65	T2
center 5	0	0	-1	4.00E+06	65	T2
center 6	0	0	-1	4.00E+06	65	T2

Appendix C

Sample Calculations

C.1 PEO Tests

Results in Table 4.1 were obtained from the calculations detailed below.

In experiment no. 1, PEO molecular weight of 1 million g/mol containing 80% silver, a flat film membrane with an average of 80 μm in thickness was prepared. The diameter of the membrane cross section was 3.5 cm. When pure ethane gas was fed at 100 psig, the measured downstream flow of 1 mL takes an average of 9.49 seconds. Assuming temperature of 23^{o}C and pressure of 1 atm, the flow rate can be corrected to standard temperature and pressure (STP):

$$PV = nRT \tag{C.1}$$

$$\frac{V_1}{V_2} = \frac{T_1}{T_2} * \frac{P_2}{P_1} \tag{C.2}$$

$$P_1 = P_2 = 1atm \tag{C.3}$$

$$flow\,rate\,(\dot{V}) = \frac{V}{time} \tag{C.4}$$

$$\dot{V}_{STP} = \frac{T_{273K}}{T_{296K}} * \dot{V}_{296K} \tag{C.5}$$

Ethane flux is, therefore,

$$\text{Flux} = \frac{\dot{V}_{STP}}{\text{membrane area}}$$

$$= \frac{1\text{ mL}}{9.49\text{ sec}} \left| \frac{273.15\text{ K}}{296.15\text{ K}} \right| \frac{}{1/4*\pi*(3.5)^2\text{ cm}^2} \left| \frac{1\text{ cm}^3}{1\text{ mL}} \right.$$

$$= 0.0101\text{ cm}^3\text{ (STP) / cm}^2\text{ sec}$$

According to Equation 2.4, the ethane permeability can be calculated,

$$P_A = \frac{N_A}{(p_1 - p_2)/l} = \frac{N_A}{(\Delta p/l)} \tag{C.6}$$

$$\text{P}_{ethane} = \frac{0.0101\text{ cm}^3}{\text{cm}^2\text{ sec}} \left| \frac{80\ \mu\text{m}}{100\text{ psi}} \right| \frac{1\text{ cm}}{10^4\ \mu\text{m}} \left| \frac{14.696\text{ psi}}{760\text{ mmHg}} \right| \frac{10\text{ mmHg}}{1\text{ cmHg}}$$

$$= 1.562*10^{-7}\text{ cm}^3\text{ cm / cm}^2\text{ sec cmHg}$$

Since 1 Barrer = $1*10^{-10}$ cm^3 (STP) cm / cm^2 sec cmHg,

$$\text{P}_{ethane} = 1562\text{ Barrer}$$

Similarly, ethylene permeability can be calculated as 1175 Barrer. α_{AB} denotes the pure gas selectivity of ethylene over ethane and can be calculated as the ratio of ethylene permeability to ethane permeability.

$$\alpha_{AB} = \frac{P_{ethylene}}{P_{ethane}} = \frac{1175\ Barrer}{1562\ Barrer} = 0.75 \tag{C.7}$$

C.2 PEBAX Tests

Permeabilities were calculated in the same manner as in the previous section. For clarity, another example from PEBAX®2533 tests is taken to show the detailed calculation. The raw data for this section can be found in Appendix E.

Referring to Figure 5.1, the permeability for PEBAX®2533 at 30 minutes, using propane gas:

$$\begin{aligned} \text{membrane thickness} &= 20\ \mu\text{m} \\ \text{pressure} &= 75\ \text{psig} \\ \text{membrane diameter} &= 3.5\ \text{cm} \\ \text{temperature} &= 23^{o}\text{C} \\ \text{pressure} &= 1\ \text{atm} \end{aligned}$$

The measured downstream propane flow of 1 mL takes an average of 18.88 seconds. The propane flux at standard temperature and pressure (STP) is:

$$\text{Flux} = \frac{\dot{V}_{STP}}{\text{membrane area}}$$

$$= \frac{1\ \text{mL} \mid 273.15\ \text{K} \mid \mid 1\ \text{cm}^3}{18.88\ \text{sec} \mid 296.15\ \text{K} \mid 1/4*\pi*(3.5)^2\ \text{cm}^2 \mid 1\ \text{mL}}$$

$$= 0.005\ \text{cm}^3\ (\text{STP}) / \text{cm}^2\ \text{sec}$$

Propane permeability is:

$$P_{propane} = \frac{0.005\ cm^3}{cm^2\ sec} \left| \frac{20\ \mu m}{100\ psi} \right| \frac{1\ cm}{10^4\ \mu m} \left| \frac{14.696\ psi}{760\ mmHg} \right| \frac{10\ mmHg}{1\ cmHg}$$

$$= 2.619*10^{-8}\ cm^3\ cm\ /\ cm^2\ sec\ cmHg$$

1 Barrer = $1*10^{-10}$ cm^3 (STP) cm / cm^2 sec cmHg

$P_{propane}$ = 261.9 Barrer

Permeability vs. Time, Figure 5.3

Relationship between permeabilities and the permeation time can be fitted to power law models. Using nitrogen permeability as an example, the coefficient and exponent of the model are calculated as follows:

time (hour)	**N_2 permeability (Barrer)**	**Ln(time)**	**Ln(permeability)**
0.000	66.669	N/A	4.200
0.500	62.655	-0.693	4.138
1.750	60.943	0.560	4.110
3.333	60.304	1.204	4.099
5.750	59.663	1.749	4.089
14.750	58.630	2.691	4.071
26.083	56.112	3.261	4.027
37.417	56.661	3.622	4.037
49.750	56.711	3.907	4.038

$$Permeability \ = \ a * Time^{b} \tag{C.8}$$

$$Ln(permeability) \ = \ b * Ln(time) + Ln(a) \tag{C.9}$$

The slope and y-intercept of the regression line were estimated using least squares, and they are -0.0238 and 4.125, respectively.

$$\begin{aligned} exponent &= -0.0238 \\ coefficient &= e^{y-intercept} \\ &= 61.85 \end{aligned}$$

Thus, for nitrogen,

$$Permeability \ = \ 61.85 * Time^{-0.0238} \tag{C.10}$$

Temperature Dependency of Permeability

As mentioned in Chapter 2, Section 2.3.1, temperature dependence of permeability can be expressed by an Arrhenius relationship:

$$P_0 \ = \ P_0 * e^{-E_p/RT} \tag{C.11}$$

where P_0 is the pre-exponential factor and E_p is the activation energy of permeation. Conventionally, 1000/T is used in calculations instead of 1/T to simplify the unit conversion.

$$Ln(P) \ = \ \frac{-E_p}{R} * Ln\frac{1000}{T} + Ln(P_0) \tag{C.12}$$

Example: Propane at 25 psig

temperature T (^oC)	**1000/T (K^{-1})**	**permability P Barrer**	**Ln(P)**
25	3.35	405.33	6.0047
35	3.25	424.90	6.0518
45	3.14	540.40	6.2923
55	3.05	577.18	6.3581
65	2.96	596.60	6.3912
75	2.87	620.00	6.4297

Results from linear regression:

Slope = -0.961

Intercept = 9.238

$$\begin{aligned} Ep &= -0.961 * -1 * R \\ &= 0.961 * 8.314 \quad (KJ/mol\ K) \\ &= 7.99 \quad (KJ/mol\ K) \\ P_0 &= e^{9.238} \\ &= 10281.23 \quad (Barrer) \end{aligned}$$

Appendix D

Experimental Data for PEBAX®2533 Permeability Study

D.1 Relationship between Permeability and Time

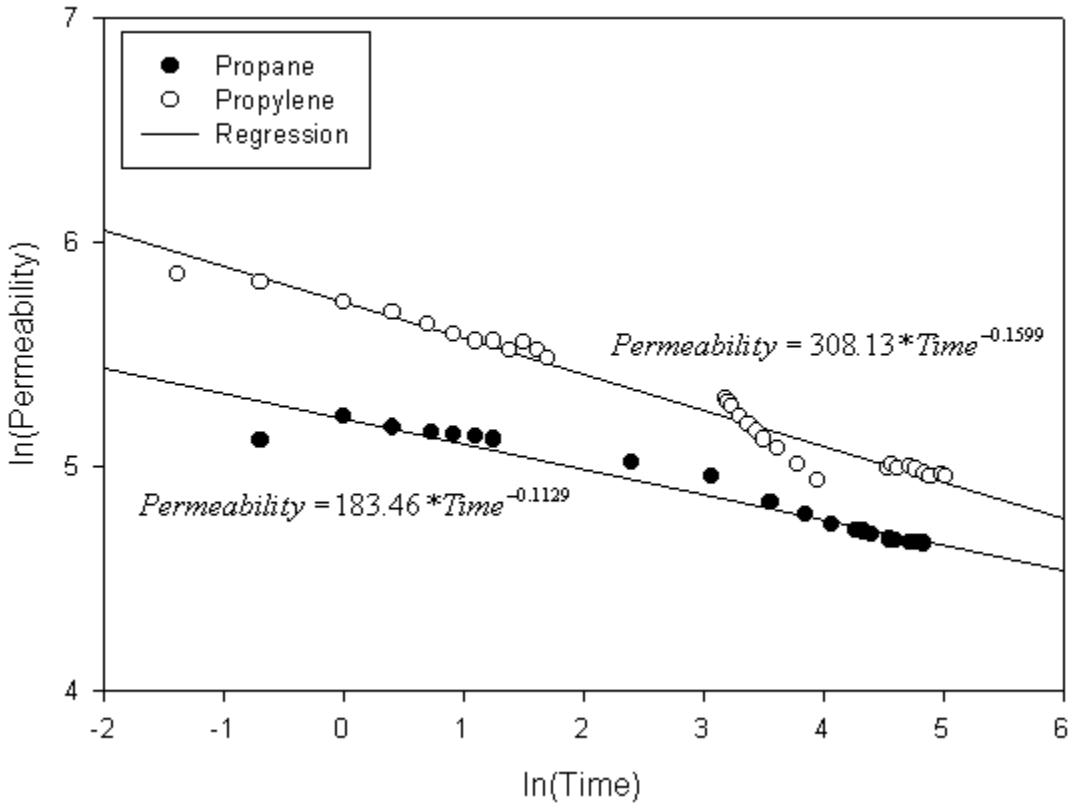

Figure D.1: Ln(Permeability) versus Ln(Time) - Propane and Propylene

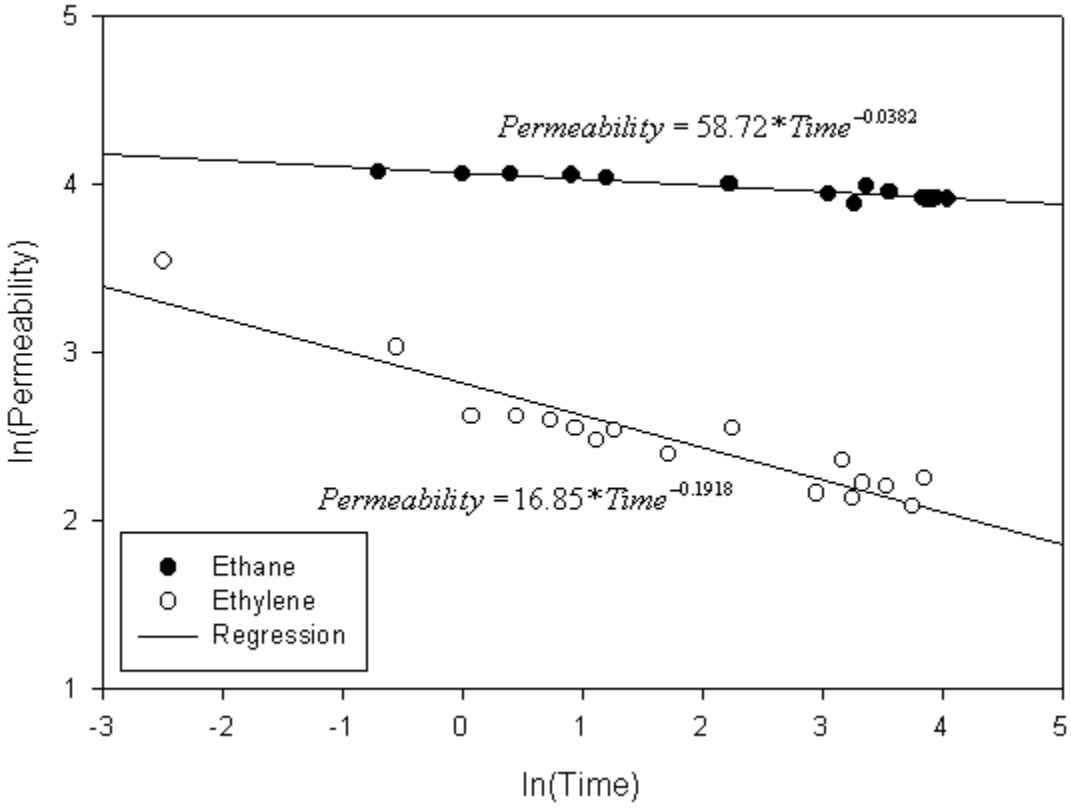

Figure D.2: Ln(Permeability) versus Ln(Time) - Ethane and Ethylene

D.2 Temperature Effects

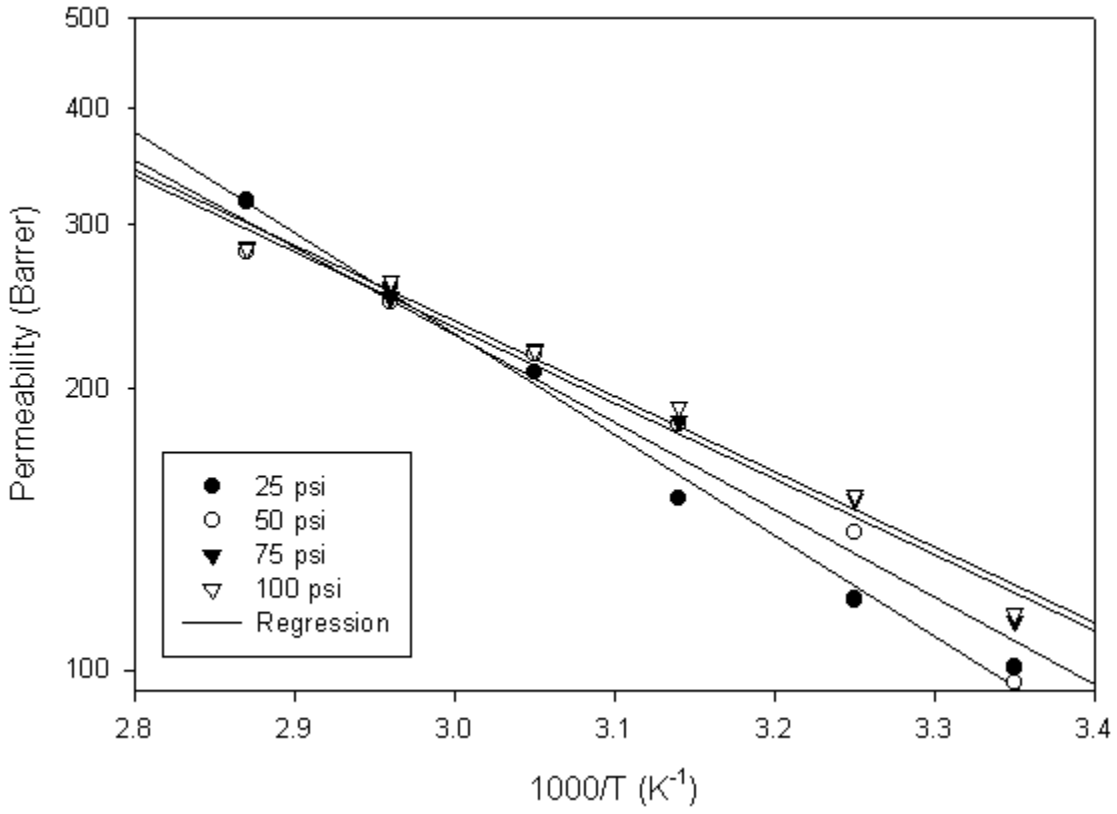

Figure D.3: Temperature dependency of ethane permeability in PEBAX® 2533

Table D.1: Calculated values of pre-exponential factors and activation energy for ethane and ethylene permeation

pressure (psig)	**ethane**		**ethylene**	
	P_0 (Barrer)	E_p (KJ/mol.K)	P_0 (Barrer)	E_p (KJ/mol.K)
25	435592.16	21.56	296013.09	19.16
50	18650.06	18.33	144837.80	17.17
75	19253.87	16.78	152724.93	17.19
100	15862.38	15.88	128378.85	16.72

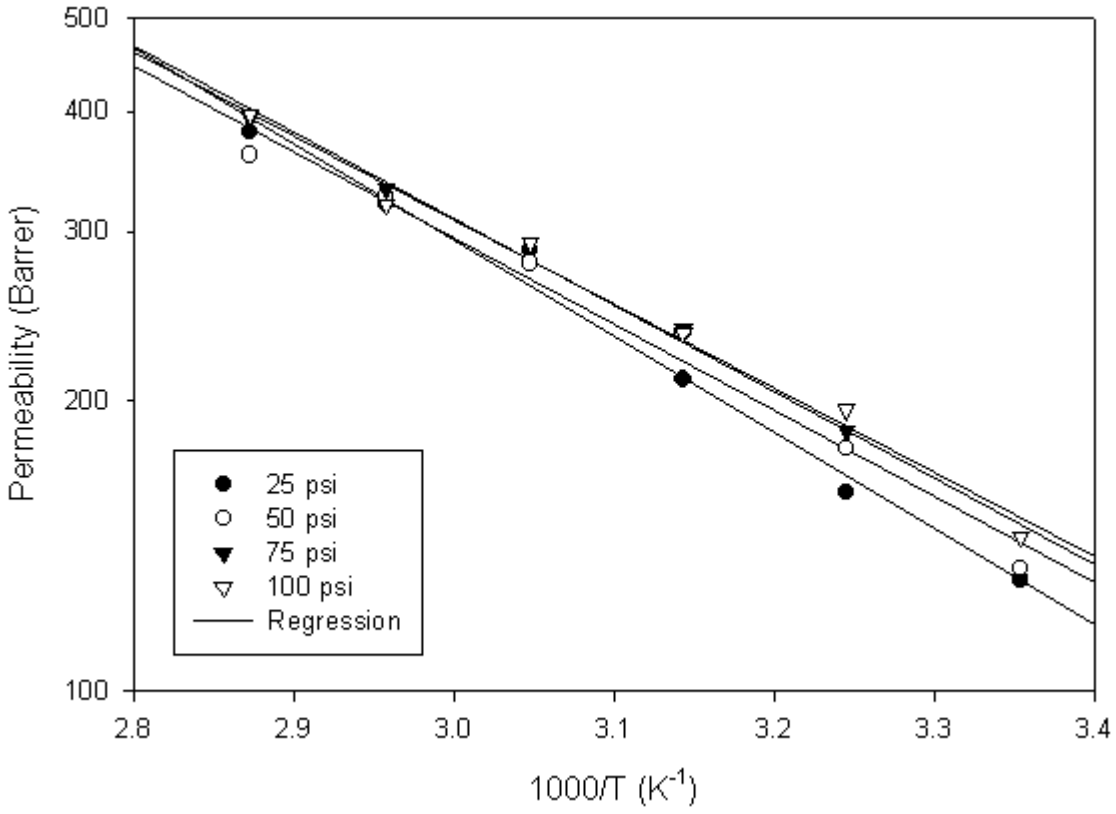

Figure D.4: Temperature dependency of ethylene permeability in PEBAX® 2533

Appendix E

Raw data

E.1 PEO Tests

No. 1 (This and subsequent numbers correspond to Table 4.1.)

Mol. Wt	1M
Silver	AgNO3
Ag %	80
Membrane Thickness	8.00E-03 cm
Test Date	Oct. 22, 2001

Gas	Ethane	Ethylene	Ethane	Ethylene	Ethane	Ethylene
Pressure (psi)	100	100	100	100	100	100
Volume (ml)	1	1	25	25	10	25
Average Time (sec)	9.491	12.620	17.632	27.255	1579.794	22.783
Flow rate (ml/s)	0.097	0.073	1.308	0.846	0.006	1.012
Flux (cm3/cm2.s)	1.010E-02	7.596E-03	1.359E-01	8.793E-02	6.068E-04	1.052E-01
Permeability (cm^3.cm/cm^2.s.cmHg)	1.562E-07	1.175E-07	2.103E-06	1.360E-06	9.387E-09	1.627E-06
Permeability (barrer)	1562.48	1175.11	21027.01	13602.94	93.87	16272.78
Ethylene/Ethane α_{AB}		0.752		0.647		173.350

No. 2

Mol. Wt	1M
Silver	AgNO3
Ag %	50
Membrane Thickness	8.00E-03 cm
Test Date	Nov. 13, 2001

Gas	Ethane	Ethylene
Pressure (psi)	50	50
Volume (ml)	9	9
Average Time (sec)	38.433	4.060
Flow rate (ml/s)	0.216	2.045
Flux (cm3/cm2.s)	2.245E-02	2.125E-01
Permeability (cm^3.cm/cm^2.s.cmHg)	6.945E-07	6.575E-06
Permeability (barrer)	6,945.5	65,748.4
Ethylene/Ethane α_{AB}		9.466

No. 3

Mol. Wt	4M
Silver	AgNO3
Ag %	80
Membrane Thickness	8.00E-03 cm
Test Date	Nov. 5, 2001

Gas	Ethane	Ethylene	Ethane	Ethylene
Pressure (psi)	30	28	24	23
Volume (ml)	9	9	1	1
Average Time (sec)	6.778	8.026	9.018	10.952
Flow rate (ml/s)	1.225	1.034	0.102	0.084
Flux (cm3/cm2.s)	1.273E-01	1.075E-01	1.063E-02	8.754E-03
Permeability (cm^3.cm/cm^2.s.cmHg)	2.188E-05	1.848E-05	1.644E-05	1.354E-05
Permeability (barrer)	218784.28	184773.58	164448.08	135412.52
Ethylene/Ethane α_{AB}		0.845		0.823

No. 4

Mol. Wt	7M
Silver	AgNO3
Ag %	50
Membrane Thickness	8.00E-03 cm
Test Date	Nov. 18, 2001

Gas	Ethane	Ethylene	Ethane	Ethylene	Ethane	Ethylene
Pressure (psi)	98.5	102	49	51.5	98.5	98.5
Volume (ml)	1	1	9	9	1	1
Average Time (sec)	242.908	307.760	14.095	13.151	146.012	149.468
Flow rate (ml/s)	0.004	0.003	0.589	0.631	0.006	0.006
Flux (cm3/cm2.s)	3.947E-04	3.115E-04	6.121E-02	6.561E-02	6.566E-04	6.414E-04
Permeability (cm^3.cm/cm^2.s.cmHg)	6.198E-09	4.724E-09	1.933E-06	1.971E-06	5.800E-09	5.666E-09
Permeability (barrer)	61.98	47.24	19325.04	19706.40	58.00	56.66
Ethylene/Ethane α_{AB}		0.762		1.020		0.977

Gas	Ethane	Ethylene	Ethane	Ethylene
Pressure (psi)	95	100	100	97
Volume (ml)	1	1	1	1
Average Time (sec)	4.080	6.938	114.245	175.377
Flow rate (ml/s)	0.226	0.133	0.008	0.005
Flux (cm3/cm2.s)	2.350E-02	1.382E-02	8.391E-04	5.466E-04
Permeability (cm^3.cm/cm^2.s.cmHg)	2.152E-07	1.202E-07	1.298E-08	8.718E-09
Permeability (barrer)	2152.18	1202.34	129.81	87.18
Ethylene/Ethane α_{AB}		0.559		0.672

No. 5

Mol. Wt	4M
Silver	AgNO3
Ag %	50
Membrane Thickness	7.00E-03 cm
Test Date	Nov. 21, 2001

Gas	Ethane	Ethylene	Ethane	Ethylene	Ethane	Ethylene
Pressure (psi)	101	101	151	101	150	145
Volume (ml)	1	9	1	9	1	1
Average Time (sec)	61.453	18.706	2359.980	17.816	79.188	292.480
Flow rate (ml/s)	0.015	0.444	0.000	0.466	0.012	0.003
Flux (cm3/cm2.s)	1.560E-03	4.612E-02	4.062E-05	4.843E-02	1.211E-03	3.278E-04
Permeability (cm^3.cm/cm^2.s.cmHg)	2.091E-08	6.181E-07	3.641E-10	6.490E-07	1.092E-08	3.060E-09
Permeability (barrer)	209.07	6181.41	3.64	6490.30	109.24	30.60
Ethylene/Ethane α_{AB}		29.567		1782.392		0.280

No. 6

Mol. Wt	4M
Silver	AgNO3
Ag %	50
Membrane Thickness	5.00E-03 cm
Test Date	Nov. 14, 2001

Gas	Ethane	Ethylene
Pressure (psi)	54	126.5
Volume (ml)	1	1
Average Time (sec)	31.035	22.350
Flow rate (ml/s)	0.030	0.041
Flux (cm3/cm2.s)	3.089E-03	4.289E-03
Permeability (cm^3.cm/cm^2.s.cmHg)	5.531E-08	3.278E-08
Permeability (barrer)	553.06	327.83
Ethylene/Ethane α_{AB}		0.593

E.2 PEBAX Tests

PEBAX(2533) membrane with support

Corresponds to Figure 5.1 to 5.3, Figure D.1 and D.2 in Appendix D

0.002 cm

Gas	**Nitrogen**		
Pressure (psi)	75		
Volume (mL)	1		
Duration (min)	0	30	60
Average	259.84	364.655	452.02
Flow rate (mL/s)	0.003549633	0.00252934	0.002040478
Flux (cm3/cm2.s)	0.000368941	0.00026289	0.000212083
Permeability (cm3.cm/cm2.s.cmHg)	1.902E-09	1.356E-09	1.094E-09
Permeability (barrer)	19.02	13.56	10.94

Gas	**Ethylene**	
Pressure (psi)	75	
Volume (mL)	1	
Duration (min)	0	60
Average	119.44	192.23
Flow rate (mL/s)	0.007722176	0.00479809
Flux (cm3/cm2.s)	0.000802627	0.0004987
Permeability (cm3.cm/cm2.s.cmHg)	4.139E-09	2.572E-09
Permeability (barrer)	41.39	25.72

Gas	**Ethane**		
Pressure (psi)	75		
Volume (mL)	1		
Duration (min)	0	30	60
Average	161.935	201.88	224.21
Flow rate (mL/s)	0.005695721	0.00456874	0.004113718
Flux (cm3/cm2.s)	0.000592001	0.00047487	0.000427571
Permeability (cm3.cm/cm2.s.cmHg)	3.053E-09	2.449E-09	2.205E-09
Permeability (barrer)	30.53	24.49	22.05

Gas	**Propane**											
Pressure (psi)	75											
Volume (mL)	1											
Duration (min)	0	15	30	45	70	80	95	110	125	140	155	190
Duration (hr)	0.0	0.3	0.5	0.8	1.2	1.3	1.6	1.8	2.1	2.3	2.6	3.2
Average	17.37	18.8325	18.8775	19.635	20.615	21.4125	21.8925	22.3975	23.2125	22.725	23.45833333	25.072
Flow rate (mL/s)	0.053099404	0.04897579	0.048859047	0.04697411	0.04474105	0.04307468	0.042130257	0.04118034	0.03973448	0.04058687	0.039318081	0.036787518
Flux (cm3/cm2.s)	0.005519042	0.00509044	0.005078308	0.004882391	0.00465029	0.00447709	0.004378931	0.0042802	0.00412992	0.00421852	0.00408664	0.003823618
Permeability (cm3.cm/cm2.s.cmHg)	2.846E-08	2.625E-08	2.619E-08	2.518E-08	2.398E-08	2.309E-08	2.258E-08	2.207E-08	2.130E-08	2.175E-08	2.107E-08	1.972E-08
Permeability (barrer)	284.59	262.49	261.86	251.76	239.79	230.86	225.80	220.71	212.96	217.53	210.73	197.16

Gas	**Propylene**											
Pressure (psi)	75											
Volume (mL)	1											
Duration (min)	0	15	30	60	90	120	150	180	210	240	270	300
Duration (hr)	0	0.25	0.5	1	1.5	2	2.5	3	3.5	4	4.5	5
Average	14.11333333	14.12	14.68833333	16.02166667	16.7133333	17.6166667	18.40666667	19.065	19.0533333	19.8183333	19.10166667	19.80833333
Flow rate (mL/s)	0.065352148	0.06532129	0.062793826	0.057568084	0.05518568	0.05235591	0.050108837	0.04837853	0.04840815	0.04653957	0.048285664	0.046563062
Flux (cm3/cm2.s)	0.006792566	0.00678936	0.00652666	0.005983507	0.00573588	0.00544176	0.005208208	0.00502836	0.00503144	0.00483723	0.005018712	0.004839668
Permeability (cm3.cm/cm2.s.cmHg)	3.503E-08	3.501E-08	3.365E-08	3.085E-08	2.958E-08	2.806E-08	2.686E-08	2.593E-08	2.594E-08	2.494E-08	2.588E-08	2.496E-08
Permeability (barrer)	350.26	350.09	336.55	308.54	295.77	280.60	268.56	259.29	259.45	249.43	258.79	249.56

Gas	**Propylene**											
Pressure (psi)	75											
Volume (mL)	1		leave overnight									
Duration (min)	330	605	1395	1425	1455	1485	1515	1635	1755	1875	1995	2235
Duration (hr)	5.5	10.0833333	23.25	23.75	24.25	24.75	25.25	27.25	29.25	31.25	33.25	37.25
Average	20.49	25.075	22.20833333	23.78666667	24.615	25.035	25.40166667	26.7433333	27.6516667	28.5033333	29.57	30.87166667
Flow rate (mL/s)	0.04501399	0.03678312	0.041531106	0.038775364	0.03747051	0.03684189	0.036310084	0.03448847	0.03335555	0.0323589	0.031191635	0.029876477
Flux (cm3/cm2.s)	0.004678661	0.00382316	0.004316657	0.004030231	0.00389461	0.00382927	0.003773995	0.00358466	0.00346691	0.00336332	0.003241994	0.003105299
Permeability (cm3.cm/cm2.s.cmHg)	2.413E-08	1.971E-08	2.226E-08	2.078E-08	2.008E-08	1.975E-08	1.946E-08	1.848E-08	1.788E-08	1.734E-08	1.672E-08	1.601E-08
Permeability (barrer)	241.25	197.14	222.59	207.82	200.83	197.46	194.61	184.84	178.77	173.43	167.17	160.12

Gas	**Propylene**											
Pressure (psi)	75											
Volume (mL)	1											
Duration (min)	2655	3135	3615	4185	4365	4545	4905	5625	5805	6105	6680	7085
Duration (hr)	44.25	52.25	60.25	69.75	72.75	75.75	81.75	93.75	96.75	101.75	111.3333333	118.0833333
Average	33.1	35.4866667	37.06333333	27.88333333	28.9733333	29.6633333	30.46666667	33.7283333	33.065	33.515	33.45666667	33.76833333
Flow rate (mL/s)	0.027865156	0.02599108	0.024885421	0.033078422	0.03183398	0.03109349	0.030273632	0.02734605	0.02789465	0.02752011	0.027568098	0.027313656
Flux (cm3/cm2.s)	0.002896246	0.00270146	0.002586539	0.003438102	0.00330876	0.00323179	0.003146578	0.00284229	0.00289931	0.00286038	0.002865371	0.002838925
Permeability (cm3.cm/cm2.s.cmHg)	1.493E-08	1.393E-08	1.334E-08	1.773E-08	1.706E-08	1.666E-08	1.623E-08	1.466E-08	1.495E-08	1.475E-08	1.478E-08	1.464E-08
Permeability (barrer)	149.34	139.30	133.37	177.29	170.62	166.65	162.25	146.56	149.50	147.50	147.75	146.39

Gas	**Ethylene**											
Pressure (psi)	150											
Volume (mL)	1											
Duration (min)	5	35	65	95	125	155	185	215	335	575	1145	1430
Duration (hr)	0.1	0.6	1.1	1.6	2.1	2.6	3.1	3.6	5.6	9.6	19.1	23.8
Average	71.215	118.965	180.225	180.06	183.0325	193.4725	206.07	194.5475	224.8625	193.54	283.7975	234.39
Flow rate (mL/s)	0.012951438	0.00775301	0.005117695	0.005122385	0.0050392	0.00476728	0.004475841	0.00474093	0.00410178	0.00476561	0.003249982	0.003935051
Flux (cm3/cm2.s)	0.001346146	0.00080583	0.000531923	0.00053241	0.00052376	0.0004955	0.00046521	0.00049276	0.00042633	0.00049533	0.000337796	0.000409001
Permeability (cm3.cm/cm2.s.cmHg)	3.471E-09	2.078E-09	1.371E-09	1.373E-09	1.350E-09	1.278E-09	1.199E-09	1.270E-09	1.099E-09	1.277E-09	8.709E-10	1.055E-09
Permeability (barrer)	34.71	20.78	13.71	13.73	13.50	12.78	11.99	12.70	10.99	12.77	8.71	10.55

Gas	**Ethylene**				
Pressure (psi)	150				
Volume (mL)	1				
Duration (min)	1550	1685	2075	2585	2825
Duration (hr)	25.8	28.1	34.6	43.1	47.1
Average	292.255	267.59	271.8925	305.72	260.3425
Flow rate (mL/s)	0.003155931	0.00344683	0.003392284	0.003016933	0.00354278
Flux (cm3/cm2.s)	0.000328021	0.00035826	0.000352587	0.000313574	0.00036823
Permeability (cm3.cm/cm2.s.cmHg)	8.457E-10	9.237E-10	9.091E-10	8.085E-10	9.494E-10
Permeability (barrer)	8.46	9.24	9.09	8.08	9.49

Propylene

Time	Permeability	lnP	lnx
0	350.2580957	5.8586703	
0.250	350.0927236	5.85819804	-1.386294361
0.500	336.5466418	5.81873675	-0.693147181
1.000	308.5390153	5.7318483	0
1.500	295.7703983	5.68958347	0.405465108
2.000	280.6041206	5.63694485	0.693147181
2.500	268.5608072	5.59307736	0.916290732
3.000	259.2871365	5.55793608	1.098612289
3.500	259.4459022	5.55854821	1.252762968
4.000	249.4311289	5.51918284	1.386294361
4.500	258.789421	5.55601468	1.504077397
5.000	249.5570513	5.51968755	1.609437912
5.500	241.2547222	5.48585331	1.704748092
24.250	200.8250765	5.30243426	3.188416617
24.750	197.455932	5.28551543	3.208825489
25.250	194.6057053	5.27097549	3.228826156
27.250	184.8426745	5.21950505	3.305053521
29.250	178.7707525	5.18610427	3.375879574
31.250	173.4291635	5.15576924	3.442019376
33.250	167.1731233	5.11902994	3.504054767
37.250	160.1244698	5.07595145	3.617651945
44.250	149.3446905	5.00625699	3.789855371
52.250	139.3004675	4.93663324	3.956039891
93.750	146.5625119	4.98745204	4.540631665
96.750	149.5027751	5.00731495	4.572130332
101.750	147.4954276	4.99379718	4.622518824
111.333	147.7525931	4.99553921	4.712528704
118.083	146.3889025	4.9862668	4.77139059
126.667	143.7844461	4.96831528	4.841558964
133.167	141.7097733	4.95378112	4.891601477
145.083	143.0217742	4.96299689	4.97730829
151.083	141.2979636	4.95087088	5.017831561

y=x^a*exp(b)

slope	intercept	exp(b)
-0.15985617	5.730536341	308.134489

Ethylene

Time	ln(T)	Permeability	lnP
0.083	-2.48490665	34.7069385	3.54693963
0.583	-0.538996501	20.7763176	3.03381376
1.083	0.080042708	13.7142718	2.61843703
1.583	0.459532329	13.726839	2.61935297
2.083	0.733969175	13.5039112	2.60297936
2.583	0.949080555	12.7752245	2.54750771
3.083	1.126011263	11.9942477	2.48442718
3.583	1.276293466	12.7046332	2.54196675
5.583	1.71978597	10.9918489	2.39715399
9.583	2.260025479	12.770769	2.54715889
19.083	2.948815354	8.70921917	2.16438214
23.833	3.171085161	10.5450515	2.3556567
25.833	3.251665648	8.45718509	2.13501639
28.083	3.335176281	9.2367227	2.22318714
34.583	3.54337187	9.09055832	2.20723633
43.083	3.763136225	8.08470047	2.08997345
47.083	3.851919081	9.49385762	2.25064502

y=x^a*exp(b)

slope	intercept	exp(b)
-0.1917719	2.824279433	16.8487999

PEBAX(2533) membrane with support Second Set 0.002 cm

Gas	**Nitrogen**										
Pressure (psi)	150										
Volume (mL)	1										
Duration (min)	0	30	105	200	345	885	1565	2245	2985		
Duration (hr)	0.0	0.5	1.8	3.3	5.8	14.8	26.1	37.4	49.8		
Average	37.07333333	39.44833333	40.55666667	40.98666667	41.42666667	42.15666667	44.04833333	43.62166667	43.58333333		
Flow rate (mL/s)	0.024878709	0.023380878	0.022741925	0.022503334	0.022264322	0.021878785	0.020939195	0.021144003	0.0211626		
Flux (cm3/cm2.s)	0.002585841	0.00243016	0.002363748	0.00233895	0.002314107	0.002274035	0.002176376	0.002197664	0.002199597		
Permeability (cm3.cm/cm2.s.cmHg)	6.667E-09	6.266E-09	6.094E-09	6.030E-09	5.966E-09	5.863E-09	5.611E-09	5.666E-09	5.671E-09		
Permeability (barrer)	66.67	62.66	60.94	60.30	59.66	58.63	56.11	56.66	56.71		

Gas	**Ethane**									
Pressure (psi)	150									
Volume (mL)	1									
Duration (min)	30	60	90	150	200	560	1280	1580	1740	2120
Duration (hr)	0.5	1.0	1.5	2.5	3.3	9.3	21.3	26.3	29.0	35.3
Average	41.95833333	42.26166667	42.6175	42.71333333	43.54833333	44.93833333	47.745	50.77	45.75333333	47.02833333
Flow rate (mL/s)	0.021982204	0.021824427	0.021642205	0.021593647	0.021179609	0.020524496	0.019317974	0.018166962	0.020158895	0.019612361
Flux (cm3/cm2.s)	0.002284785	0.002268386	0.002249446	0.002244399	0.002201365	0.002133273	0.00200787	0.001888236	0.002095274	0.002038468
Permeability (cm3.cm/cm2.s.cmHg)	5.891E-09	5.848E-09	5.800E-09	5.787E-09	5.676E-09	5.500E-09	5.177E-09	4.868E-09	5.402E-09	5.256E-09
Permeability (barrer)	58.91	58.48	58.00	57.87	56.76	55.00	51.77	48.68	54.02	52.56

Gas	**Ethane**				
Pressure (psi)	150				
Volume (mL)	1				
Duration (min)	2780	2900	3020	3140	3440
Duration (hr)	46.3	48.3	50.3	52.3	57.3
Average	48.91666667	49.30833333	49.23666667	49.17666667	49.21166667
Flow rate (mL/s)	0.018855264	0.018705492	0.018732719	0.018755575	0.018742236
Flux (cm3/cm2.s)	0.001959777	0.00194421	0.00194704	0.001949415	0.001948029
Permeability (cm3.cm/cm2.s.cmHg)	5.053E-09	5.013E-09	5.020E-09	5.026E-09	5.022E-09
Permeability (barrer)	50.53	50.13	50.20	50.26	50.22

Gas	**Propane**										
Pressure (psi)	75										
Volume (mL)	1										
Duration (min)	0	30	60	90	125	150	180	210	660	1295	2105
Duration (hr)	0.0	0.5	1.0	1.5	2.1	2.5	3.0	3.5	11.0	21.6	35.1
Average	28.62333333	29.59	26.67333333	28.01333333	28.63	28.94333333	29.195	29.575	32.78833333	34.88333333	39.2
Flow rate (mL/s)	0.032223244	0.031170553	0.03457898	0.032924916	0.032215741	0.031866981	0.031592281	0.031186362	0.028130026	0.026440611	0.023528996
Flux (cm3/cm2.s)	0.003349217	0.003239802	0.003594067	0.003422147	0.003348437	0.003312188	0.003283636	0.003241446	0.002923776	0.002748182	0.002445555
Permeability (cm3.cm/cm2.s.cmHg)	1.727E-08	1.671E-08	1.853E-08	1.765E-08	1.727E-08	1.708E-08	1.693E-08	1.671E-08	1.508E-08	1.417E-08	1.261E-08
Permeability (barrer)	172.70	167.06	185.33	176.46	172.66	170.79	169.32	167.14	150.76	141.71	126.10

Gas	**Propane**										
Pressure (psi)	75										
Volume (mL)	1										
Duration (min)	2815	3510	4290	4565	4915	5640	5875	6000	6750	7140	7550
Duration (hr)	46.9	58.5	71.5	76.1	81.9	94.0	97.9	100.0	112.5	119.0	125.8
Average	41.36666667	43.175	44.48666667	44.59166667	45.08833333	46.195	46.37166667	46.44	46.82	46.955	46.99333333
Flow rate (mL/s)	0.022296615	0.021362748	0.020732878	0.020684059	0.020456215	0.019966158	0.019890091	0.019860824	0.01969963	0.019642991	0.019626968
Flux (cm3/cm2.s)	0.002317464	0.0022204	0.002154932	0.002149858	0.002126177	0.002075241	0.002067335	0.002064293	0.002047539	0.002041652	0.002039986
Permeability (cm3.cm/cm2.s.cmHg)	1.195E-08	1.145E-08	1.111E-08	1.109E-08	1.096E-08	1.070E-08	1.066E-08	1.064E-08	1.056E-08	1.053E-08	1.052E-08
Permeability (barrer)	119.50	114.49	111.12	110.86	109.64	107.01	106.60	106.45	105.58	105.28	105.19

Gas	**Ethylene**									
Pressure (psi)	150									
Volume (mL)	1									
Duration (min)	25	55	85	115	145	190	235	280	325	370
Duration (hr)	0.4	0.9	1.4	1.9	2.4	3.2	3.9	4.7	5.4	6.2
Average	56.08	57.26166667	59.55166667	60.54833333	61.66833333	60.15	60.24166667	60.265	60.36666667	60.50833333
Flow rate (mL/s)	0.016446802	0.016107401	0.015488007	0.015233064	0.014956406	0.015333943	0.01531061	0.015304682	0.015278906	0.015243134
Flux (cm3/cm2.s)	0.001709446	0.00167417	0.001609791	0.001583293	0.001554538	0.001593778	0.001591353	0.001590737	0.001588058	0.00158434
Permeability (cm3.cm/cm2.s.cmHg)	4.407E-09	4.316E-09	4.150E-09	4.082E-09	4.008E-09	4.109E-09	4.103E-09	4.101E-09	4.094E-09	4.085E-09
Permeability (barrer)	44.07	43.16	41.50	40.82	40.08	41.09	41.03	41.01	40.94	40.85

Gas	**Ethylene**								
Pressure (psi)	150								
Volume (mL)	1								
Duration (min)	610	985	1525	1810	2185	2605	3415	4170	5105
Duration (hr)	10.2	16.4	25.4	30.2	36.4	43.4	56.9	69.5	85.1
Average	61.52166667	63.43833333	64.60333333	64.46666667	66.38	65.06	67.52333333	65.81	64.15833333
Flow rate (mL/s)	0.014992062	0.014539106	0.01427692	0.014307187	0.013894797	0.014176708	0.013659525	0.014015144	0.014375945
Flux (cm3/cm2.s)	0.001558244	0.001511164	0.001483913	0.001487059	0.001444196	0.001473498	0.001419743	0.001456705	0.001494206
Permeability (cm3.cm/cm2.s.cmHg)	4.018E-09	3.896E-09	3.826E-09	3.834E-09	3.723E-09	3.799E-09	3.660E-09	3.756E-09	3.852E-09
Permeability (barrer)	40.18	38.96	38.26	38.34	37.23	37.99	36.60	37.56	38.52

Gas	**Propylene**														
Pressure (psi)	75														
Volume (mL)	1														
Duration (min)	10	40	70	100	145	190	285	585	1260	10	130				
Duration (hr)	0.2	0.7	1.2	1.7	2.4	3.2	4.8	9.8	21.0	0.2	2.2				
Average	19.77	19.30166667	19.38666667	19.48333333	19.80833333	20.105	20.665	21.82833333	32.10833333	18.5	22.29166667				
Flow rate (mL/s)	0.046653346	0.047785337	0.047575825	0.047339777	0.046563062	0.045875984	0.044632792	0.042254103	0.028725772	0.049856035	0.04137585				
Flux (cm3/cm2.s)	0.004849052	0.004966709	0.004944932	0.004920398	0.004839668	0.004768254	0.00463904	0.004391804	0.002985697	0.005181933	0.00430052				
Permeability (cm3.cm/cm2.s.cmHg)	2.500E-08	2.561E-08	2.550E-08	2.537E-08	2.496E-08	2.459E-08	2.392E-08	2.265E-08	1.540E-08	2.672E-08	2.218E-08				
Permeability (barrer)	250.04	256.11	254.99	253.72	249.56	245.87	239.21	226.46	153.96	267.21	221.76				
Gas	**Propylene**														
Pressure (psi)	75														
Volume (mL)	1														
Duration (min)	250	370	550	640	1145	1350	1540	2045	2610	2765					
Duration (hr)	4.2	6.2	9.2	10.7	19.1	22.5	25.7	34.1	43.5	46.1					
Average	23.77166667	24.53833333	25.52333333	26	27.56166667	27.68166667	27.63666667	28.55833333	29.99666667	29.95833333					
Flow rate (mL/s)	0.038799831	0.037587584	0.036136998	0.035474487	0.033464473	0.033319405	0.033373658	0.032296585	0.030747972	0.030787315					
Flux (cm3/cm2.s)	0.004032774	0.003906775	0.003756005	0.003687144	0.003478228	0.00346315	0.003468789	0.00335684	0.00319588	0.00319997					
Permeability (cm3.cm/cm2.s.cmHg)	2.079E-08	2.015E-08	1.937E-08	1.901E-08	1.794E-08	1.786E-08	1.789E-08	1.731E-08	1.648E-08	1.650E-08					
Permeability (barrer)	207.95	201.45	193.68	190.13	179.35	178.58	178.87	173.10	164.80	165.01					

Nitrogen

Time	Permeability	ln(Time)	ln(P)
0.0	66.6693	#NUM!	4.1997
0.5	62.6555	-0.6931	4.1377
1.8	60.9432	0.5596	4.1099
3.3	60.3039	1.2040	4.0994
5.8	59.6634	1.7492	4.0887
14.8	58.6302	2.6912	4.0713
26.1	56.1123	3.2613	4.0274
37.4	56.6612	3.6221	4.0371
49.8	56.7110	3.9070	4.0380

y=x^a*exp(b)

slope	intercept	exp(b)
-0.023819352	4.124707328	61.84970495

Ethane

Time	Permeability	ln(Time)	ln(P)
0.5	58.9074	-0.6931	4.0760
1.0	58.4846	0.0000	4.0688
1.5	57.9962	0.4055	4.0604
2.5	57.8661	0.9163	4.0581
3.3	56.7566	1.2040	4.0388
9.3	55.0010	2.2336	4.0074
21.3	51.7678	3.0603	3.9468
26.3	48.6834	3.2708	3.8853
29.0	54.0213	3.3673	3.9894
35.3	52.5567	3.5648	3.9619
46.3	50.5279	3.8359	3.9225
48.3	50.1265	3.8781	3.9145
50.3	50.1995	3.9187	3.9160
52.3	50.2607	3.9576	3.9172
57.3	50.2250	4.0489	3.9165

y=x^a*exp(b)

slope	intercept	exp(b)
-0.038200318	4.072784437	58.72023799

Propane

Time	Permeability	ln(Time)	ln(P)
0.0	172.7021	#NUM!	5.1516
0.5	167.0601	-0.6931	5.1184
1.0	185.3278	0.0000	5.2221
1.5	176.4627	0.4055	5.1731
2.1	172.6619	0.7340	5.1513
2.5	170.7927	0.9163	5.1405
3.0	169.3204	1.0986	5.1318
3.5	167.1449	1.2528	5.1189
11.0	150.7643	2.3979	5.0157
21.6	141.7098	3.0719	4.9538
35.1	126.1048	3.5577	4.8371
46.9	119.4998	3.8484	4.7833
58.5	114.4947	4.0690	4.7405
71.5	111.1189	4.2697	4.7106
76.1	110.8572	4.3318	4.7082
81.9	109.6361	4.4057	4.6972
94.0	107.0096	4.5433	4.6729
97.9	106.6019	4.5841	4.6691
100.0	106.4451	4.6052	4.6676
112.5	105.5811	4.7230	4.6595
119.0	105.2776	4.7791	4.6566
125.8	105.1917	4.8350	4.6558

y=x^a*exp(b)		
slope	intercept	exp(b)
-0.112872531	5.212013282	183.4630495

Ethylene

Time	Permeability	ln(Time)	ln(P)
0.4	44.0737	-0.8755	3.7859
0.9	43.1642	-0.0870	3.7650
1.4	41.5044	0.3483	3.7258
1.9	40.8212	0.6506	3.7092
2.4	40.0798	0.8824	3.6909
3.2	41.0915	1.1527	3.7158
3.9	41.0290	1.3652	3.7143
4.7	41.0131	1.5404	3.7139
5.4	40.9440	1.6895	3.7122
6.2	40.8482	1.8192	3.7099
10.2	40.1754	2.3191	3.6933
16.4	38.9615	2.7983	3.6626
25.4	38.2589	3.2354	3.6444
30.2	38.3400	3.4067	3.6465
36.4	37.2349	3.5950	3.6172
43.4	37.9904	3.7708	3.6373
56.9	36.6045	4.0416	3.6002
69.5	37.5574	4.2413	3.6259
85.1	38.5243	4.4436	3.6513

y=x^a*exp(b)		
slope	intercept	exp(b)
-0.029888645	3.748791621	42.46973144

Propylene

Time	Permeability	ln(Time)	ln(P)
0.2	250.0409	-1.7918	5.5216
0.7	256.1079	-0.4055	5.5456
1.2	254.9850	0.1542	5.5412
1.7	253.7199	0.5108	5.5362
2.4	249.5571	0.8824	5.5197
3.2	245.8746	1.1527	5.5048
4.8	239.2117	1.5581	5.4773
9.8	226.4630	2.2773	5.4226
21.0	153.9572	3.0445	5.0367
0.2	267.2059	-1.7918	5.5880
2.2	221.7559	0.7732	5.4016
4.2	207.9496	1.4271	5.3373
6.2	201.4525	1.8192	5.3056
9.2	193.6780	2.2156	5.2662
10.7	190.1273	2.3671	5.2477
19.1	179.3545	2.9488	5.1894
22.5	178.5770	3.1135	5.1850
25.7	178.8678	3.2452	5.1866
34.1	173.0952	3.5288	5.1538
43.5	164.7953	3.7728	5.1047
46.1	165.0062	3.8305	5.1060

y=x^a*exp(b)		
slope	intercept	exp(b)
-0.094147058	5.497058916	243.97333

Corresponds to Figure 5.4 to 5.13, Table 5.1 to 5.3,
Figure D.3 and D.4, Table D1 in Appendix D

2-May-02 Cell 1	0.015492857 cm										
Gas	**Propane**										
Pressure (psi)	125	125	125	125	125	125	120	115			
Volume (mL)	1	1	1	1	1	1	1	1			
Duration	10	25	55	100	170	470	1190	1730			
hr	0.167	0.417	0.917	1.667	2.833	7.833	19.833	28.833			
Average	1.490E+01	1.561E+01	1.621E+01	1.699E+01	1.769E+01	1.561E+01	1.314E+01	1.364E+01			
Flow rate (mL/s)	6.190E-02	5.910E-02	5.689E-02	5.430E-02	5.213E-02	5.910E-02	7.021E-02	6.762E-02			
Flux (cm3/cm2.s)	6.434E-03	6.143E-03	5.913E-03	5.644E-03	5.419E-03	6.143E-03	7.298E-03	7.028E-03			
Permeability (cm3.cm/cm2.s.cmHg)	1.542E-07	1.472E-07	1.417E-07	1.353E-07	1.299E-07	1.472E-07	1.822E-07	1.831E-07			
Permeability (Barrer)	1542.00	1472.18	1417.09	1352.58	1298.68	1472.18	1821.86	1830.92			
Gas	**Propane**										
Pressure (psi)	120	117.5	115	115	115						
Volume (mL)	1	1	1	1	1						
Duration	2750	3230	4105	4755	4840						
hr	45.833	53.833	68.417	79.250	80.667						
Average	1.194E+01	1.242E+01	1.233E+01	1.255E+01	1.239E+01						
Flow rate (mL/s)	7.727E-02	7.429E-02	7.478E-02	7.351E-02	7.444E-02						
Flux (cm3/cm2.s)	8.031E-03	7.722E-03	7.773E-03	7.641E-03	7.737E-03						
Permeability (cm3.cm/cm2.s.cmHg)	2.005E-07	1.969E-07	2.025E-07	1.990E-07	2.016E-07						
Permeability (Barrer)	2005.01	1968.77	2024.89	1990.46	2015.63						
Gas	25										
Pressure (psi)	20	40	60	80	100	110	90	70	50	30	
Volume (ml)	0.1	0.1	0.2	0.5	0.5	0.5	0.5	0.5	0.2	0.1	
Average Time (sec)	3.519E+01	1.370E+01	1.429E+01	1.984E+01	1.112E+01	7.985E+00	1.438E+01	2.543E+01	1.890E+01	2.023E+01	
Flow rate (ml/s)	2.603E-03	6.690E-03	1.282E-02	2.308E-02	4.121E-02	5.737E-02	3.185E-02	1.802E-02	9.696E-03	4.529E-03	
Flux (cm3/cm2.s)	2.706E-04	6.953E-04	1.332E-03	2.399E-03	4.284E-03	5.963E-03	3.311E-03	1.872E-03	1.008E-03	4.708E-04	
Permeability (cm^3.cm/cm^2.s.cmHg)	4.053E-08	5.208E-08	6.653E-08	8.985E-08	1.283E-07	1.624E-07	1.102E-07	8.014E-08	6.039E-08	4.701E-08	
Permeability (barrer)	405.33	520.76	665.28	898.51	1283.27	1623.90	1101.99	801.38	603.85	470.12	
Gas	35C				45C				55C		
Pressure (psi)	20	50	75	100	20	50	75	100	20	50	75
Volume (ml)	0.1	0.2	0.2	0.5	0.1	0.2	0.2	0.5	0.1	0.2	0.2
Average Time (sec)	3.248E+01	1.947E+01	1.039E+01	1.427E+01	2.545E+01	1.652E+01	9.558E+00	1.489E+01	2.245E+01	1.559E+01	9.098E+00
Flow rate (ml/s)	2.729E-03	9.108E-03	1.706E-02	3.106E-02	4.221E-03	1.301E-02	2.248E-02	3.608E-02	3.707E-03	1.068E-02	1.830E-02
Flux (cm3/cm2.s)	2.837E-04	9.466E-04	1.773E-03	3.228E-03	4.387E-04	1.352E-03	2.336E-03	3.750E-03	3.853E-04	1.110E-03	1.902E-03
Permeability (cm^3.cm/cm^2.s.cmHg)	4.249E-08	5.672E-08	7.083E-08	9.670E-08	6.571E-08	8.101E-08	9.332E-08	1.124E-07	5.772E-08	6.652E-08	7.597E-08
Permeability (barrer)	424.90	567.20	708.29	967.00	657.11	810.12	933.25	1123.53	577.18	665.23	759.67

Propane	cell 1								
Gas	55C	65C				75C			
Pressure (psi)	100	20	50	75	100	20	50	75	100
Volume (ml)	0.5	0.1	0.2	0.2	0.5	0.1	0.2	0.2	0.5
Average Time (sec)	1.506E+01	2.108E+01	1.419E+01	8.763E+00	1.580E+01	1.970E+01	1.423E+01	9.172E+00	1.676E+01
Flow rate (ml/s)	2.763E-02	3.832E-03	1.139E-02	1.844E-02	2.556E-02	3.982E-03	1.103E-02	1.711E-02	2.341E-02
Flux (cm3/cm2.s)	2.872E-03	3.983E-04	1.184E-03	1.916E-03	2.657E-03	4.139E-04	1.146E-03	1.778E-03	2.433E-03
Permeability ($cm^3.cm/cm^2.s.cmHg$)	8.604E-08	5.966E-08	7.092E-08	7.654E-08	7.960E-08	6.200E-08	6.868E-08	7.103E-08	7.288E-08
Permeability (barrer)	860.43	596.60	709.19	765.39	795.97	620.00	686.80	710.31	728.82

Gas	25								
Pressure (psi)	20	50	75	100	110	90	70	50	50
Volume (ml)	0.1	0.1	0.1	0.5	0.5	0.5	0.2	0.1	0.1
Average Time (sec)	6.027E+01	1.597E+01	7.460E+00	1.710E+01	1.304E+01	2.243E+01	1.628E+01	1.499E+01	1.471E+01
Flow rate (ml/s)	1.520E-03	5.737E-03	1.228E-02	2.679E-02	3.512E-02	2.042E-02	1.125E-02	6.112E-03	6.229E-03
Flux (cm3/cm2.s)	1.580E-04	5.963E-04	1.276E-03	2.785E-03	3.651E-03	2.123E-03	1.170E-03	6.353E-04	6.475E-04
Permeability ($cm^3.cm/cm^2.s.cmHg$)	2.367E-08	3.573E-08	5.099E-08	8.342E-08	9.943E-08	7.066E-08	5.007E-08	3.807E-08	3.879E-08
Permeability (barrer)	236.67	357.26	509.87	834.21	994.26	706.57	500.65	380.66	387.95

Gas				
Pressure (psi)	30	40	60	80
Volume (ml)	0.1	0.1	0.1	0.2
Average Time (sec)	3.307E+01	2.132E+01	1.122E+01	1.226E+01
Flow rate (ml/s)	2.771E-03	4.297E-03	8.168E-03	1.494E-02
Flux (cm3/cm2.s)	2.880E-04	4.466E-04	8.489E-04	1.553E-03
Permeability ($cm^3.cm/cm^2.s.cmHg$)	2.876E-08	3.345E-08	4.239E-08	5.816E-08
Permeability (barrer)	287.59	334.51	423.88	581.63

Pressure			25	50	75	100		20	50	75	100
Temperature (ºC)		1000/T (K)	P	P	P	P		ln(P)	ln(P)	ln(P)	ln(P)
	25	3.35	405.33	520.76	665.28	898.51		6.0047	6.2553	6.5002	6.8007
	45	3.14	540.40	645.09	760.70	912.31		6.2923	6.4694	6.6342	6.8160
	35	3.25	424.90	567.20	708.29	967.00		6.0518	6.3407	6.5629	6.8742
	45	3.14	657.11	810.12	933.25	1123.53					
	55	3.05	577.18	665.23	759.67	860.43		6.3581	6.5001	6.6329	6.7574
	65	2.96	596.60	709.19	765.39	795.97		6.3912	6.5641	6.6404	6.6796
	75	2.87	620.00	686.80	710.31	728.82		6.4297	6.5320	6.5657	6.5914
	25	3.35	236.67	357.26	509.87	834.21					

Pressure	Slope	Intercept	Po	Ep (KJ/mol.K)
25	-0.961391354	9.238075637	10281.23	7.99
50	-0.627998784	8.392436723	4413.56	5.22
75	-0.177013283	7.138690169	1259.78	1.47
100	0.489412449	5.234467369	187.63	-4.07

$\ln P = \ln Po + (-Ep/R)*(1/T)$

1-Jun-02 Cell 1		0.015492857 cm								
Gas	**Propylene**		25ºC							
Pressure (psi)	117.5	117.5	25	50	75	20	40	60	80	100
Volume (ml)	1	2	0.1	0.5	0.5	0.1	0.1	0.5	0.5	0.5
Average Time (sec)	1.118E+01	2.211E+01	2.030E+01	3.731E+01	1.673E+01	2.852E+01	1.055E+01	2.552E+01	1.425E+01	8.387E+00
Flow rate (ml/s)	8.197E-02	8.286E-02	4.513E-03	1.228E-02	2.737E-02	3.213E-03	8.688E-03	1.795E-02	3.214E-02	5.462E-02
Flux (cm3/cm2.s)	8.520E-03	8.612E-03	4.691E-04	1.276E-03	2.845E-03	3.339E-04	9.030E-04	1.866E-03	3.341E-03	5.677E-03
Permeability ($cm^3.cm/cm^2.s.cmHg$)	2.172E-07	2.196E-07	5.622E-08	7.647E-08	1.137E-07	5.002E-08	6.763E-08	9.316E-08	1.251E-07	1.701E-07
Permeability (barrer)	2172.24	2195.81	562.16	764.66	1136.54	500.18	676.32	931.59	1251.04	1700.74

Gas	25C					35ºC				
Pressure (psi)	110	90	70	50	30	25	50	75	100	
Volume (ml)	1	0.5	0.5	0.1	0.1	0.1	0.1	0.5	0.5	
Average Time (sec)	1.292E+01	1.079E+01	2.001E+01	7.642E+00	1.645E+01	1.817E+01	6.918E+00	1.729E+01	1.003E+01	
Flow rate (ml/s)	7.091E-02	4.245E-02	2.289E-02	1.199E-02	5.568E-03	4.880E-03	1.281E-02	2.564E-02	4.417E-02	
Flux (cm3/cm2.s)	7.370E-03	4.412E-03	2.379E-03	1.246E-03	5.787E-04	5.072E-04	1.332E-03	2.665E-03	4.591E-03	
Permeability ($cm^3.cm/cm^2.s.cmHg$)	2.007E-07	1.469E-07	1.018E-07	7.466E-08	5.779E-08	6.078E-08	7.979E-08	1.064E-07	1.375E-07	
Permeability (barrer)	2007.25	1468.58	1018.23	746.62	577.94	607.79	797.92	1064.46	1375.48	

Gas	45ºC							55ºC			
Pressure (psi)	25	50	75	100	75	50	25	25	50	75	100
Volume (ml)	0.1	0.5	0.5	0.5	0.5	0.5	0.1	0.1	0.5	0.5	0.5
Average Time (sec)	1.437E+01	3.364E+01	1.611E+01	1.025E+01	1.640E+01	3.144E+01	1.403E+01	1.232E+01	2.725E+01	1.650E+01	1.049E+01
Flow rate (ml/s)	5.973E-03	1.276E-02	2.665E-02	4.187E-02	2.617E-02	1.365E-02	6.122E-03	6.757E-03	1.528E-02	2.523E-02	3.966E-02
Flux (cm3/cm2.s)	6.208E-04	1.326E-03	2.770E-03	4.352E-03	2.720E-03	1.419E-03	6.363E-04	7.023E-04	1.588E-03	2.622E-03	4.122E-03
Permeability ($cm^3.cm/cm^2.s.cmHg$)	7.440E-08	7.947E-08	1.106E-07	1.304E-07	1.087E-07	8.502E-08	7.625E-08	8.416E-08	9.513E-08	1.047E-07	1.235E-07
Permeability (barrer)	743.98	794.70	1106.30	1303.66	1086.63	850.22	762.46	841.64	951.28	1047.34	1235.03

Gas	65ºC				75ºC			
Pressure (psi)	25	50	75	100	25	50	75	100
Volume (ml)	0.1	0.5	0.5	1	0.1	0.5	0.5	1
Average Time (sec)	1.099E+01	2.337E+01	1.482E+01	2.142E+01	9.942E+00	2.418E+01	1.478E+01	2.169E+01
Flow rate (ml/s)	7.352E-03	1.728E-02	2.725E-02	3.771E-02	7.892E-03	2.068E-02	2.654E-02	3.618E-02
Flux (cm3/cm2.s)	7.642E-04	1.796E-03	2.832E-03	3.920E-03	8.203E-04	2.149E-03	2.759E-03	3.761E-03
Permeability ($cm^3.cm/cm^2.s.cmHg$)	9.158E-08	1.076E-07	1.131E-07	1.174E-07	9.829E-08	1.288E-07	1.102E-07	1.127E-07
Permeability (barrer)	915.75	1076.28	1131.34	1174.26	982.94	1287.76	1102.07	1126.59

Pressure			25	50	75	100
Temperature (°C)		1000/T (K)	P	P	P	P
	25	3.354016435	562.16	764.66	1136.54	1700.74
	35	3.245172805	607.79	797.92	1064.46	1375.48
	45	3.14317146	743.98	794.70	1106.30	1303.66
	55	3.047386866	841.64	951.28	1047.34	1235.03
	65	2.957267485	915.75	1076.28	1131.34	1174.26
	75	2.872325147	982.94	1287.76	1102.07	1126.59
	45	3.14317146	762.46	841.64	951.28	1047.34
	25	3.354016435	486.33	788.77	1181.25	1720.23

	25	50	75	100
ln(P)	ln(P)	ln(P)	ln(P)	ln(P)
	6.3318	6.6394	7.0357	7.4388
	6.4098	6.6820	6.9702	7.2266
	6.6120	6.6780	7.0088	7.1729
	6.7354	6.8578	6.9540	7.1188
	6.8197	6.9813	7.0312	7.0684
	6.8905	7.1607	7.0049	7.0270
	6.6366	6.7354	6.8578	6.9540
	6.1869	6.6705	7.0743	7.4502

Pressure	Slope	Intercept	Po	Ep (KJ/mol.K)
25	-1.369384663	10.87711199	52950.45767	11.38506409
50	-0.971314385	9.850126379	18960.7509	8.075507795
75	0.079585373	6.742259669	847.4735835	-0.661672788
100	0.852554923	4.505438242	90.50799973	-7.088141626

$\ln P = \ln Po + (-Ep/R)*(1/T)$

Selectivity (Propylene/Propane)				
	25 psi	50 psi	75 psi	100 psi
25°C	1.39	1.47	1.71	1.89
35°C	1.43	1.41	1.50	1.42
45°C	1.13	0.98	1.19	1.16
55°C	1.46	1.43	1.38	1.44
65°C	1.53	1.52	1.48	1.48
75°C	1.59	1.88	1.55	1.55

7-May-02 Cell 1	0.01549286 cm												
Gas	**Ethane**												
Pressure (psi)	200	200	200	200	200	200	200	200	200	200	200		
Volume (ml)	0.2	0.2	0.2	0.2	0.2	0.2	0.2	0.2	0.2	0.2	0.2		
Duration	15	45	75	105	870	1190	1820	2470	2625	2925	3220		
hr	0.250	0.750	1.250	1.750	14.500	19.833	30.333	41.167	43.750	48.750	53.667		
Average Time (sec)	1.810E+01	1.832E+01	1.824E+01	1.774E+01	2.098E+01	2.118E+01	2.175E+01	2.168E+01	2.159E+01	2.163E+01	2.214E+01		
Flow rate (ml/s)	1.019E-02	1.007E-02	1.011E-02	1.040E-02	8.795E-03	8.710E-03	8.481E-03	8.509E-03	8.543E-03	8.530E-03	8.331E-03		
Flux (cm3/cm2.s)	1.059E-03	1.047E-03	1.051E-03	1.081E-03	9.141E-04	9.053E-04	8.815E-04	8.844E-04	8.880E-04	8.866E-04	8.659E-04		
Permeability ($cm^3.cm/cm^2.s.cmHg$)	1.587E-08	1.568E-08	1.575E-08	1.619E-08	1.369E-08	1.356E-08	1.320E-08	1.325E-08	1.330E-08	1.328E-08	1.297E-08		
Permeability (barrer)	158.69	156.81	157.47	161.92	136.92	135.61	132.04	132.47	133.01	132.81	129.71		
Gas	25C												
Pressure (psi)	25	50	75	100	125	150	175	200	150	100	125	50	
Volume (ml)	0.01	0.05	0.05	0.05	0.1	0.1	0.1	0.1	0.1	0.05	0.05	0.05	
Average Time (sec)	1.136E+01	2.942E+01	1.685E+01	1.243E+01	1.676E+01	1.313E+01	1.080E+01	8.972E+00	1.307E+01	1.140E+01	8.745E+00	2.446E+01	
Flow rate (ml/s)	8.068E-04	1.557E-03	2.719E-03	3.687E-03	5.466E-03	6.976E-03	8.487E-03	1.021E-02	7.011E-03	4.019E-03	5.238E-03	1.872E-03	
Flux (cm3/cm2.s)	8.386E-05	1.618E-04	2.826E-04	3.832E-04	5.681E-04	7.250E-04	8.821E-04	1.061E-03	7.287E-04	4.177E-04	5.444E-04	1.946E-04	
Permeability ($cm^3.cm/cm^2.s.cmHg$)	1.005E-08	9.695E-09	1.129E-08	1.148E-08	1.362E-08	1.448E-08	1.510E-08	1.590E-08	1.455E-08	1.251E-08	1.305E-08	1.166E-08	
Permeability (barrer)	100.49	96.95	112.87	114.80	136.15	144.81	151.01	158.98	145.55	125.14	130.48	116.61	
Gas	35C				45C				55C				
Pressure (psi)	25	50	75	100	25	50	75	100	25	50	75	100	
Volume (ml)	0.05	0.05	0.05	0.1	0.05	0.05	0.05	0.1	0.05	0.05	0.05	0.1	
Average Time (sec)	4.645E+01	1.970E+01	1.205E+01	1.791E+01	3.497E+01	1.456E+01	9.643E+00	1.397E+01	2.489E+01	1.189E+01	7.818E+00	1.180E+01	
Flow rate (ml/s)	9.543E-04	2.249E-03	3.679E-03	4.950E-03	1.228E-03	2.948E-03	4.452E-03	6.147E-03	1.672E-03	3.500E-03	5.323E-03	7.055E-03	
Flux (cm3/cm2.s)	9.918E-05	2.338E-04	3.824E-04	5.145E-04	1.276E-04	3.064E-04	4.627E-04	6.389E-04	1.738E-04	3.638E-04	5.533E-04	7.333E-04	
Permeability ($cm^3.cm/cm^2.s.cmHg$)	1.189E-08	1.401E-08	1.527E-08	1.541E-08	1.529E-08	1.836E-08	1.848E-08	1.914E-08	2.083E-08	2.180E-08	2.210E-08	2.197E-08	
Permeability (barrer)	118.86	140.08	152.75	154.13	152.90	183.59	184.82	191.41	208.30	217.96	221.01	219.68	
Gas	65C				75C				25C				
Pressure (psi)	25	50	75	100	25	50	75	100	25	25	50	75	100
Volume (ml)	0.05	0.05	0.05	0.1	0.05	0.05	0.1	0.1	0.05	0.05	0.05	0.05	0.1
Average Time (sec)	1.950E+01	1.012E+01	6.693E+00	9.632E+00	1.535E+01	8.708E+00	1.149E+01	8.643E+00	1.854E+01	6.676E+01	2.808E+01	1.836E+01	2.455E+01
Flow rate (ml/s)	2.071E-03	3.990E-03	6.034E-03	8.387E-03	2.555E-03	4.505E-03	6.830E-03	9.077E-03	2.116E-03	6.862E-04	1.632E-03	2.495E-03	3.732E-03
Flux (cm3/cm2.s)	2.153E-04	4.147E-04	6.272E-04	8.717E-04	2.656E-04	4.682E-04	7.099E-04	9.435E-04	2.199E-04	7.132E-05	1.696E-04	2.593E-04	3.879E-04
Permeability ($cm^3.cm/cm^2.s.cmHg$)	2.580E-08	2.485E-08	2.505E-08	2.611E-08	3.182E-08	2.805E-08	2.836E-08	2.826E-08	2.635E-08	8.547E-09	1.016E-08	1.036E-08	1.162E-08
Permeability (barrer)	257.95	248.46	250.52	261.14	318.24	280.54	283.58	282.65	263.54	85.47	101.61	103.57	116.20

Gas	25C			
Pressure (psi)	125	150	175	200
Volume (ml)	0.1	0.1	0.1	0.1
Average Time (sec)	1.865E+01	1.480E+01	1.202E+01	9.593E+00
Flow rate (ml/s)	4.914E-03	6.190E-03	7.622E-03	9.550E-03
Flux (cm3/cm2.s)	5.107E-04	6.434E-04	7.922E-04	9.926E-04
Permeability ($cm^3.cm/cm^2.s.cmHg$)	1.224E-08	1.285E-08	1.356E-08	1.487E-08
Permeability (barrer)	122.40	128.50	135.62	148.68

Pressure			25	50	75	100		25	50	75	100
Temperature (ºC)		1000/T (K)	P	P	P	P		ln(P)	ln(P)	ln(P)	ln(P)
	25	3.354016435	1.005E+02	9.695E+01	1.129E+02	1.148E+02		4.6101	4.5742	4.7262	4.7432
	35	3.245172805	1.189E+02	1.401E+02	1.527E+02	1.541E+02		4.7779	4.9422	5.0288	5.0378
	45	3.14317146	1.529E+02	1.836E+02	1.848E+02	1.914E+02		5.0298	5.2127	5.2194	5.2544
	55	3.047386866	2.083E+02	2.180E+02	2.210E+02	2.197E+02		5.3390	5.3843	5.3982	5.3922
	65	2.957267485	2.580E+02	2.485E+02	2.505E+02	2.611E+02		5.5528	5.5153	5.5236	5.5651
	75	2.872325147	318.24	280.54	283.58	282.65		5.7628	5.6367	5.6475	5.6442
	25	3.354016435	8.547E+01	1.016E+02	1.036E+02	1.162E+02		4.4481	4.6211	4.6402	4.7553
	75	2.872325147	2.635E+02								

Pressure	Slope	Intercept	Po	Ep (KJ/mol.K)
25	-2.59334189	12.9844617	435592.16	21.56
50	-2.20511352	9.83360473	18650.06	18.33
75	-2.0186716	9.86546732	19253.87	16.78
100	-1.91063106	9.6717055	15862.38	15.88

$\ln P = \ln Po + (-Ep/R)*(1/T)$

15-May-02 Cell 1		0.01549286 cm													
Gas	**Ethylene**	25°C									35°C				
Pressure (psi)	200	25	50	75	100	125	150	175	200	50	25	50	75	100	
Volume (ml)	0.1	0.05	0.05	0.1	0.1	0.1	0.1	0.1	0.1	0.05	0.01	0.05	0.1	0.1	
Average Time (sec)	8.547E+00	4.374E+01	2.127E+01	2.631E+01	1.977E+01	1.442E+01	1.165E+01	9.733E+00	7.957E+00	1.982E+01	6.865E+00	1.545E+01	1.980E+01	1.411E+01	
Flow rate (ml/s)	1.072E-02	1.047E-03	2.154E-03	3.483E-03	4.635E-03	6.353E-03	7.867E-03	9.412E-03	1.151E-02	2.311E-03	1.291E-03	2.868E-03	4.477E-03	6.284E-03	
Flux (cm3/cm2.s)	1.114E-03	1.089E-04	2.238E-04	3.620E-04	4.817E-04	6.603E-04	8.177E-04	9.783E-04	1.197E-03	2.402E-04	1.342E-04	2.981E-04	4.653E-04	6.531E-04	
Permeability															
(cm^3.cm/cm^2.s.cmHg)	1.669E-08	1.304E-08	1.341E-08	1.446E-08	1.443E-08	1.582E-08	1.633E-08	1.675E-08	1.793E-08	1.439E-08	1.608E-08	1.786E-08	1.859E-08	1.957E-08	
Permeability (barrer)	166.89	130.44	134.12	144.60	144.32	158.25	163.32	167.48	179.27	143.92	160.82	178.63	185.87	195.66	
Selectivity (Ethylene/Ethane)		1.29806044	1.3833255	1.28112526	1.25716695	1.16225587	1.12780879	1.10907534	1.12756598	0.98881695					

Gas	45°C				55°C					
Pressure (psi)	25	50	75	100	25	50	75	100	50	25
Volume (ml)	0.05	0.05	0.1	0.1	0.05	0.05	0.1	0.1	0.05	0.05
Average Time (sec)	2.539E+01	1.133E+01	1.502E+01	1.134E+01	1.807E+01	9.322E+00	1.185E+01	8.858E+00	9.017E+00	1.712E+01
Flow rate (ml/s)	1.691E-03	3.789E-03	5.716E-03	7.569E-03	2.303E-03	4.465E-03	7.023E-03	9.397E-03	4.616E-03	2.431E-03
Flux (cm3/cm2.s)	1.757E-04	3.939E-04	5.941E-04	7.867E-04	2.394E-04	4.641E-04	7.300E-04	9.767E-04	4.798E-04	2.527E-04
Permeability										
(cm^3.cm/cm^2.s.cmHg)	2.106E-08	2.360E-08	2.373E-08	2.357E-08	2.868E-08	2.781E-08	2.916E-08	2.926E-08	2.875E-08	3.028E-08
Permeability (barrer)	210.60	235.99	237.32	235.68	286.85	278.05	291.59	292.60	287.46	302.76

Gas	65°C				75°C			
Pressure (psi)	25	50	75	100	25	50	75	100
Volume (ml)	0.05	0.1	0.1	0.5	0.1	0.1	0.5	0.5
Average Time (sec)	1.567E+01	1.542E+01	1.010E+01	3.938E+01	2.563E+01	1.357E+01	4.148E+01	3.074E+01
Flow rate (ml/s)	2.578E-03	5.240E-03	7.998E-03	1.026E-02	3.061E-03	5.783E-03	9.457E-03	1.276E-02
Flux (cm3/cm2.s)	2.679E-04	5.447E-04	8.313E-04	1.066E-03	3.182E-04	6.011E-04	9.830E-04	1.326E-03
Permeability								
(cm^3.cm/cm^2.s.cmHg)	3.211E-08	3.263E-08	3.320E-08	3.194E-08	3.812E-08	3.601E-08	3.926E-08	3.974E-08
Permeability (barrer)	321.06	326.34	332.05	319.36	381.25	360.15	392.64	397.39

Pressure			25	50	75	100		25	50	75	100
Temperature (°C)		1000/T (K)	P	P	P	P		ln(P)	ln(P)	ln(P)	ln(P)
	25	3.35401643	130.444344	134.118905	144.596546	144.319179		4.8709	4.8987	4.9739	4.9720
	35	3.24517281	160.823526	178.630165	185.867594	195.661656		5.0803	5.1853	5.2250	5.2764
	45	3.14317146	210.598939	235.99041	237.31718	235.678345		5.3500	5.4638	5.4694	5.4625
	55	3.04738687	286.847905	278.052193	291.594415	292.595657		5.6590	5.6278	5.6754	5.6788
	65	2.95726748	321.062885	326.3393	332.047545	319.357561		5.7716	5.7879	5.8053	5.7663
	75	2.87232515	381.249293	360.14944	392.641225	397.388771		5.9435	5.8865	5.9729	5.9849

	Selectivity (Ethylene/Ethane)			
	25 psi	50 psi	75 psi	100 psi
25°C	1.30	1.38	1.28	1.26
35°C	1.35	1.28	1.22	1.27
45°C	1.38	1.29	1.28	1.23
55°C	1.38	1.28	1.32	1.33
65°C	1.24	1.31	1.33	1.22
75°C	1.20	1.28	1.38	1.41

Pressure	Slope	Intercept	Po	Ep (KJ/mol.K)
25	-2.3047917	12.5981589	296013.09	19.16
50	-2.0650634	11.8833698	144837.80	17.17
75	-2.0675515	11.9363937	152724.93	17.19
100	-2.0105731	11.7627409	128378.85	16.72

$\ln P = \ln Po + (-Ep/R)*(1/T)$

21-May-02 Cell 1 0.015492857 cm

Gas	**Nitrogen**	25ºC			35ºC				45ºC			
Pressure (psi)	25	50	75	100	25	50	75	100	25	50	75	100
Volume (ml)	0.01	0.01	0.01	0.01	0.01	0.01	0.01	0.01	0.01	0.01	0.01	0.01
Average Time (sec)	9.379E+01	5.216E+01	3.391E+01	2.777E+01	6.273E+01	3.229E+01	2.486E+01	1.994E+01	4.684E+01	2.617E+01	1.443E+01	1.316E+01
Flow rate (ml/s)	9.768E-05	1.917E-04	2.949E-04	3.601E-04	1.413E-04	2.745E-04	3.565E-04	4.445E-04	1.833E-04	3.280E-04	5.949E-04	6.524E-04
Flux (cm3/cm2.s)	1.015E-05	1.993E-05	3.065E-05	3.743E-05	1.469E-05	2.853E-05	3.706E-05	4.620E-05	1.905E-05	3.410E-05	6.183E-05	6.781E-05
Permeability ($cm^3.cm/cm^2.s.cmHg$)	1.217E-09	1.194E-09	1.224E-09	1.121E-09	1.760E-09	1.710E-09	1.480E-09	1.384E-09	2.283E-09	2.043E-09	2.470E-09	2.031E-09
Permeability (barrer)	12.17	11.94	12.24	11.21	17.60	17.10	14.80	13.84	22.83	20.43	24.70	20.31

Gas	45C			55ºC				65ºC			
Pressure (psi)	50	75	100	25	50	75	100	25	50	75	100
Volume (ml)	0.01	0.01	0.01	0.01	0.01	0.01	0.01	0.01	0.01	0.05	0.05
Average Time (sec)	2.547E+01	1.945E+01	1.341E+01	3.007E+01	1.862E+01	1.297E+01	9.542E+00	2.465E+01	1.241E+01	4.673E+01	3.510E+01
Flow rate (ml/s)	3.370E-04	4.414E-04	6.403E-04	2.768E-04	4.471E-04	6.419E-04	8.724E-04	3.277E-04	6.510E-04	8.642E-04	1.151E-03
Flux (cm3/cm2.s)	3.503E-05	4.588E-05	6.655E-05	2.877E-05	4.647E-05	6.672E-05	9.067E-05	3.406E-05	6.766E-05	8.983E-05	1.196E-04
Permeability ($cm^3.cm/cm^2.s.cmHg$)	2.099E-09	1.832E-09	1.994E-09	3.448E-09	2.784E-09	2.665E-09	2.716E-09	4.082E-09	4.054E-09	3.588E-09	3.583E-09
Permeability (barrer)	20.99	18.32	19.94	34.48	27.84	26.65	27.16	40.82	40.54	35.88	35.83

Gas	75ºC			
Pressure (psi)	25	50	75	100
Volume (ml)	0.02	0.05	0.05	0.05
Average Time (sec)	4.386E+01	5.105E+01	3.801E+01	2.887E+01
Flow rate (ml/s)	3.578E-04	7.684E-04	1.032E-03	1.359E-03
Flux (cm3/cm2.s)	3.719E-05	7.987E-05	1.073E-04	1.412E-04
Permeability ($cm^3.cm/cm^2.s.cmHg$)	4.456E-09	4.786E-09	4.285E-09	4.231E-09
Permeability (barrer)	44.56	47.86	42.85	42.31

Pressure			25	50	75	100		25	50	75	100
Temperature (ºC)		1000/T (K)	P	P	P	P		ln (P)	ln (P)	ln (P)	ln (P)
	25	3.354016435	1.217E+01	1.194E+01	1.224E+01	1.121E+01		2.4987	2.4799	2.5049	2.4172
	35	3.245172805	1.760E+01	1.710E+01	1.480E+01	1.384E+01		2.8679	2.8388	2.6948	2.6276
	45	3.14317146	2.283E+01	2.043E+01	2.470E+01	2.031E+01		3.1281	3.0170	3.2068	3.0113
	55	3.047386866	3.448E+01	2.784E+01	2.665E+01	2.716E+01		3.5403	3.3266	3.2829	3.3019
	65	2.957267485	4.082E+01	4.054E+01	3.588E+01	3.583E+01		3.7091	3.7023	3.5802	3.5788
	75	2.872325147	4.456E+01	4.786E+01	4.285E+01	4.231E+01		3.7968	3.8682	3.7577	3.7449

Pressure	Slope	Intercept	Po	Ep (KJ/mol.K)
25	-2.814634019	11.99125626	161337.91	23.40
50	-2.918174106	12.26120823	211336.77	24.26
75	-2.676818599	11.47798328	96566.12	22.26
100	-2.906303299	12.13251938	185817.33	24.16

ln P = ln Po + (-Ep/R)*(1/T)

22-May-02 Cell 1		0.015492857 cm						
Gas	**CO2**							
Pressure (psi)	50	50	50	50	48.5	48.5	48.5	48.5
Volume (ml)	0.01	0.01	0.05	0.05	0.1	0.1	0.1	0.1
Duration	10	40	235	310	1430	1820	2995	5010
hr	0.167	0.667	3.917	5.167	23.833	30.333	49.917	83.500
Average Time (sec)	1.069E+01	7.903E+00	1.927E+01	1.458E+01	2.481E+01	2.079E+01	2.385E+01	1.955E+01
Flow rate (ml/s)	8.625E-04	1.167E-03	2.393E-03	3.164E-03	3.718E-03	4.437E-03	3.868E-03	4.719E-03
Flux (cm3/cm2.s)	8.965E-05	1.213E-04	2.487E-04	3.289E-04	3.865E-04	4.612E-04	4.020E-04	4.905E-04
Permeability ($cm^3.cm/cm^2.s.cmHg$)	5.372E-09	7.268E-09	1.490E-08	1.970E-08	2.387E-08	2.849E-08	2.483E-08	3.030E-08
Permeability (barrer)	53.7152	72.6775	149.0257	197.0480	238.7099	284.8519	248.3197	302.9725

Gas	25ºC			35ºC			45ºC	
Pressure (psi)	25	45	35	15	25	45	25	45
Volume (ml)	0.1	0.1	0.1	0.1	0.1	0.1	0.1	0.1
Average Time (sec)	3.949E+01	2.009E+01	2.686E+01	5.896E+01	3.203E+01	1.605E+01	2.602E+01	1.462E+01
Flow rate (ml/s)	2.320E-03	4.560E-03	3.411E-03	1.554E-03	2.767E-03	5.522E-03	3.300E-03	5.874E-03
Flux (cm3/cm2.s)	2.411E-04	4.739E-04	3.546E-04	1.615E-04	2.876E-04	5.739E-04	3.430E-04	6.105E-04
Permeability ($cm^3.cm/cm^2.s.cmHg$)	2.890E-08	3.155E-08	3.035E-08	3.226E-08	3.447E-08	3.821E-08	4.110E-08	4.064E-08
Permeability (barrer)	288.9673	315.5215	303.4851	322.5678	344.6936	382.0783	410.9728	406.4429

Gas	55ºC		65ºC		75ºC	
Pressure (psi)	25	45	25	45	25	45
Volume (ml)	0.1	0.1	0.1	0.1	0.1	0.1
Average Time (sec)	2.156E+01	1.238E+01	1.947E+01	1.086E+01	1.690E+01	9.412E+00
Flow rate (ml/s)	3.861E-03	6.724E-03	4.149E-03	7.442E-03	4.643E-03	8.336E-03
Flux (cm3/cm2.s)	4.013E-04	6.988E-04	4.312E-04	7.735E-04	4.826E-04	8.664E-04
Permeability ($cm^3.cm/cm^2.s.cmHg$)	4.809E-08	4.653E-08	5.167E-08	5.149E-08	5.783E-08	5.768E-08
Permeability (barrer)	480.9110	465.2504	516.7458	514.9210	578.3422	576.8287

Pressure			25	45		25	45	Selectivity (CO2/N2) 25 psi	50 psi
Temperature (ºC)		1000/T (K)	P	P		ln(P)	ln (P)	25ºC	23.75	26.43
	25	3.354016435	2.890E+02	3.155E+02		5.6663	5.7542	35ºC	19.59	22.35
	35	3.245172805	3.447E+02	3.821E+02		5.8427	5.9456	45ºC	18.00	19.89
	45	3.14317146	4.110E+02	4.064E+02		6.0185	6.0074	55ºC	13.95	16.71
	55	3.047386866	4.809E+02	4.653E+02		6.1757	6.1426	65ºC	12.66	12.70
	65	2.957267485	516.7458	514.9210		6.2476	6.2440	75ºC	12.98	12.05
	75	2.872325147	578.3422	576.8287		6.3602	6.3575			

Pressure	Slope	Intercept	Po	Ep (KJ/mol.K)
25	-1.44344951	10.53116212	37464.98807	12.00083923
45	-1.202087532	9.805584517	18134.73641	9.994155743

ln P = ln Po + (-Ep/R)*(1/T)